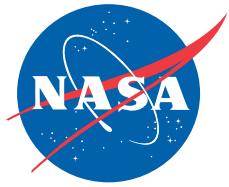# 2007 Research & Engineering Annual Report

*Patrick Stoliker, Albion Bowers, and Everlyn Cruciani*
*NASA Dryden Flight Research Center*
*Edwards, California*

**September 2008**

# NASA STI Program ... in Profile

Since its founding, NASA has been dedicated to the advancement of aeronautics and space science. The NASA scientific and technical information (STI) program plays a key part in helping NASA maintain this important role.

The NASA STI program is operated under the auspices of the Agency Chief Information Officer. It collects, organizes, provides for archiving, and disseminates NASA's STI. The NASA STI program provides access to the NASA Aeronautics and Space Database and its public interface, the NASA Technical Report Server, thus providing one of the largest collections of aeronautical and space science STI in the world. Results are published in both non-NASA channels and by NASA in the NASA STI Report Series, which includes the following report types:

- TECHNICAL PUBLICATION.
  Reports of completed research or a major significant phase of research that present the results of NASA programs and include extensive data or theoretical analysis. Includes compilations of significant scientific and technical data and information deemed to be of continuing reference value. NASA counterpart of peer-reviewed formal professional papers but has less stringent limitations on manuscript length and extent of graphic presentations.

- TECHNICAL MEMORANDUM.
  Scientific and technical findings that are preliminary or of specialized interest, e.g., quick release reports, working papers, and bibliographies that contain minimal annotation. Does not contain extensive analysis.

- CONTRACTOR REPORT.
  Scientific and technical findings by NASA-sponsored contractors and grantees.

- CONFERENCE PUBLICATION.
  Collected papers from scientific and technical conferences, symposia, seminars, or other meetings sponsored or cosponsored by NASA.

- SPECIAL PUBLICATION.
  Scientific, technical, or historical information from NASA programs, projects, and missions, often concerned with subjects having substantial public interest.

- TECHNICAL TRANSLATION.
  English-language translations of foreign scientific and technical material pertinent to NASA's mission.

Specialized services also include creating custom thesauri, building customized databases, and organizing and publishing research results.
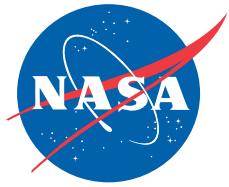
For more information about the NASA STI program, see the following:

Access the NASA STI program home page at http://www.sti.nasa.gov

- E-mail your question via the Internet to help@sti.nasa.gov

- Fax your question to the NASA STI Help Desk at (301) 621-0134

- Phone the NASA STI Help Desk at (301) 621-0390

- Write to:
  NASA STI Help Desk
  NASA Center for AeroSpace Information
  7115 Standard Drive
  Hanover, MD 21076-1320

NASA/TM-2008-214638

# 2007 Research & Engineering Annual Report

*Patrick Stoliker, Albion Bowers, and Everlyn Cruciani*
*NASA Dryden Flight Research Center*
*Edwards, California*

Available from:

NASA Center for AeroSpace Information
7115 Standard Drive
Hanover, MD 21076-1320
(301) 621-0390

# 2007 RESEARCH & ENGINEERING ANNUAL REPORT

## TABLE OF CONTENTS

| **\* Branch Codes** | **Branch Chief** |
|---|---|
| RA – Aerodynamics & Propulsion | Jennifer Cole |
| RC – Control and Dynamics | Tim Cox (Acting) |
| RF – Flight Systems | Glenn Bever |
| RI – Flight Instrumentation | John McGrath (Acting) |
| RS – Aerostructures | Tom Horn |

**Research & Engineering Directorate**

Director – Patrick Stoliker
Deputy Director – Al Bowers (Acting)
Associate Director – Ron Young
Administrative Officer – Everlyn Cruciani

# DEVELOPING A REQUIREMENTS DEVELOPMENT GUIDE FOR AN AUTOMATIC GROUND COLLISION AVOIDANCE SYSTEM

## Summary

An Automatic Ground Collision Avoidance System (Auto-GCAS) is designed to predict an impending collision with terrain and engage an autopilot to automatically perform a collision avoidance maneuver. The main goal is for the system to provide mishap protection for pilots that have either lost situational awareness, have become disoriented or misoriented, or that are experiencing g-induced loss of consciousness (GLOC).

A guide for developing core requirements and basic capabilities that are inherently common to various platform-specific implementations of an Auto-GCAS was developed. The guide is a document based upon the experience acquired during the development and flight test of the Advanced Fighter Technology Integration (AFTI)/F-16 (Lockheed Martin Corporation, Bethesda, Maryland) Auto-GCAS project aircraft from 1984 to 2007. Recommendations from the AFTI/F-16 Auto-GCAS system evaluation technical report were reviewed and refined for inclusion in this document.

## Objective

The objective was to provide a guide to assist in the development of core common requirements for an Auto-GCAS across multiple military and commercial aircraft platforms. An Auto-GCAS, as defined by the U.S. Department of Defense, engages an autopilot at the last moment to prevent controlled flight into terrain (CFIT). In some instances, previous ground proximity warning systems have failed to prevent CFIT primarily because the warnings were given prior to the last moment and pilots had come to consider the warnings as a nuisance. An Auto-GCAS is not a warning system, nor is it a situational awareness system that will allow a "line-in-the-sky" floor altitude to be dialed-in by the pilot. An Auto-GCAS system serves one primary purpose: to engage an autopilot to recover from an impending collision with terrain at that last possible moment.

## Approach

The recommendations in the guide were developed for the Automatic Collision Avoidance Technology/Fighter Risk Reduction Project (ACAT/FRRP) by a team that had many years of collective experience developing and flight-testing automatic collision avoidance technology. The team identified three top-level requirements and a fourth recommended requirement, which should be of primary consideration for any Auto-GCAS system. The four requirements that form the framework of the guide are:

1. Do not cause a mishap.
2. Avoid impeding operations.
3. Avoid collisions with terrain.
4. Integrate with existing platform systems.

The most important requirement for implementing an Auto-GCAS is to ensure that the system does not inadvertently cause a mishap. This requirement is accomplished by implementing a vigorous system-wide integrity monitor (SWIM) to ensure that the system does not engage when the system is either failed or significantly degraded. The second most important requirement is to not impede the normal mission and cause the system to become deemed a "nuisance," in which case it would not provide the proper level of military or commercial utility. The third requirement is to avoid collisions with terrain. The fourth requirement is aimed at mitigating the risk of implementing the system on large numbers of aircraft. This requirement is

supported by the functionally partitioned, modular software architecture being developed by the ACAT/FRRP program. The modular architecture is shown in figure 1.
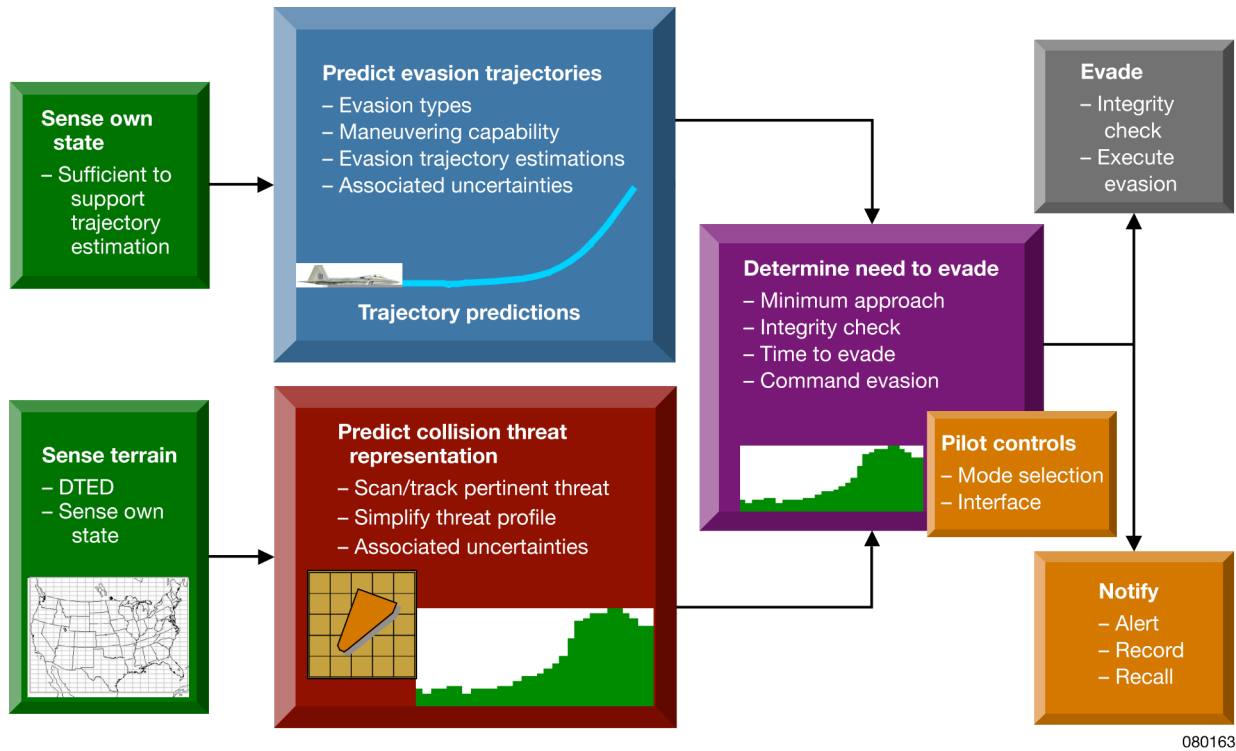


Figure 1. Functional diagram of an Auto-GCAS.

The Auto-GCAS ultimately compares predicted fly-up trajectories against a predicted terrain profile to predict impending terrain collisions. If an impending collision is detected, the flight control system performs an automatic evasion maneuver, such as a roll and pull, to avoid terrain. The evasion maneuvers must be performed in a timely and aggressive manner to avoid interfering with a pilot performing a mission (fig. 2).

5 g aggressive
but not timely

2 g timely but
not aggressive

Recovery
initiation

5 g optimum

080164
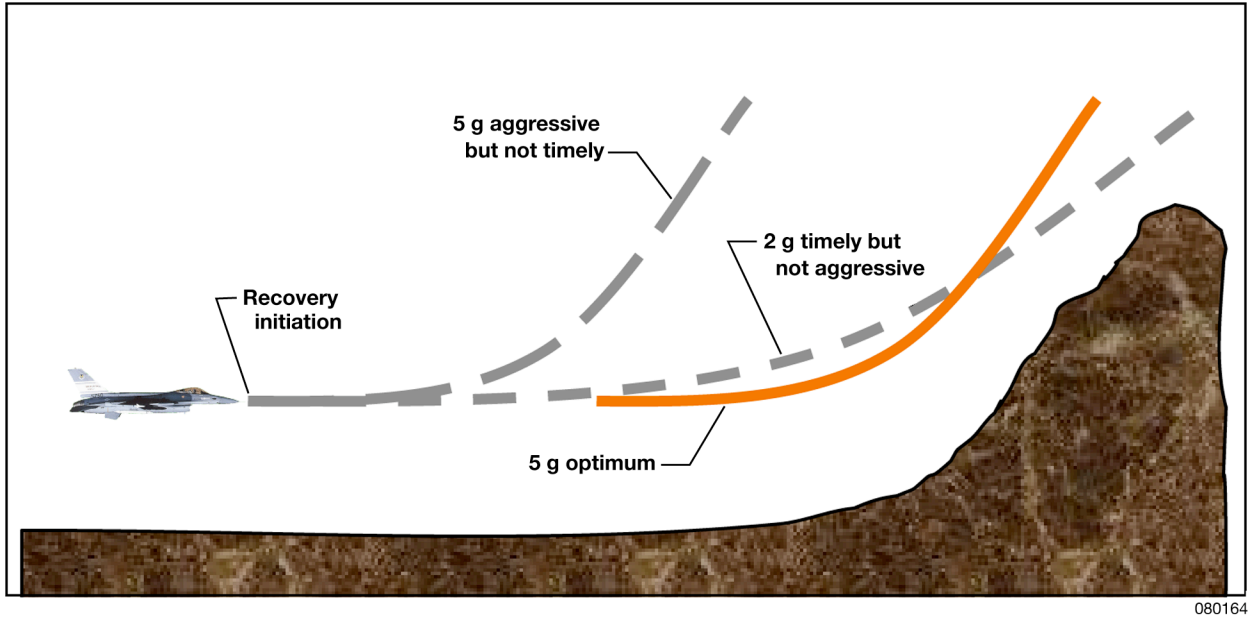
Figure 2. Auto-GCAS recovery maneuvers.

**Status**

The first draft of the guide has been completed and reviewed.

**Contacts**

Mark Skoog, Dryden Flight Research Center (DFRC), Code RF, (661) 276-5774
Loyd Hook, DFRC, Code RF, (661) 276-5714
Shaun C. McWherter, DFRC, Code RC, (661) 276-2530
Jamie Willhite, DFRC, Code RF, (661) 276-2198

# DIGITAL TERRAIN DATA COMPRESSION AND RENDERING FOR AUTOMATIC GROUND COLLISION AVOIDANCE SYSTEMS

## Summary

The Automatic Ground Collision Avoidance System (Auto-GCAS), Automatic Air Collision Avoidance System (Auto-ACAS), and Automatic Integrated Air-and-Ground Collision Avoidance System (Auto-ICAS) all rely on sensors to detect a collision threat, algorithms to determine the potential and imminence of a collision, and an autopilot to evade the potential collision. The Auto-GCAS uses a digital terrain map (DTM) as a primary input to determine ground proximity. Generally, the more accurately a DTM represents the actual terrain, the larger the DTM file size. Current fighter ground collision avoidance systems utilize a DTM that must be loaded on a flight-by-flight basis increasing the potential for procedural errors. Infrequent loading of the DTM would require that the map cover a much larger area than is typically used on aircraft ground collision avoidance systems, such as the F-16 (Lockheed Martin Corporation, Bethesda, Maryland) GCAS, if Auto-GCAS is to provide regular protection from controlled flight into terrain (CFIT). Methods to compress and subsequently decompress and render DTM data were explored, and software tools were developed to facilitate the installation of large region DTMs on any aircraft platform. This required compression and rendering methods that could tailor DTMs to the memory and computational performance made available to an Auto-GCAS on any particular platform.

## Objective

The study objective was to determine the feasibility and process required to incorporate a compressed DTM and complementary rendering algorithms into an Auto-GCAS.

## Approach

Among a wide variety of digital terrain data compression schemes evaluated as part of the study, surface facet approximation methods embedded in irregular, regular and semi-regular mathematical tree network structures were chosen. Among the irregular triangular, regular triangular, and semi-regular quad-tree and binary-tree structures, the last two semi-regular methods showed the most promise in delivering high compression ratios per specified error and rendering requirements. The ultimate compression approach recommended in the study consisted of subdividing the global (U.S.) terrain data into a regular cell network, followed by fitting free-edge biased linear regression surfaces or maximum elevation surfaces to the regular cell data and recursively subdividing the surfaces by way of semi-regular binary-tree or quad-tree structures until error tolerances are satisfied. In this study compression ratios as high as 8000:1 were achieved. These results are considered outstanding for the given rendering throughput and error tolerance requirements and compared to the 4:1 compression ratios implemented in current fighter digital terrain systems. Figure 1 shows the compression results for a quad-tree linear regression biased facet approach.

4
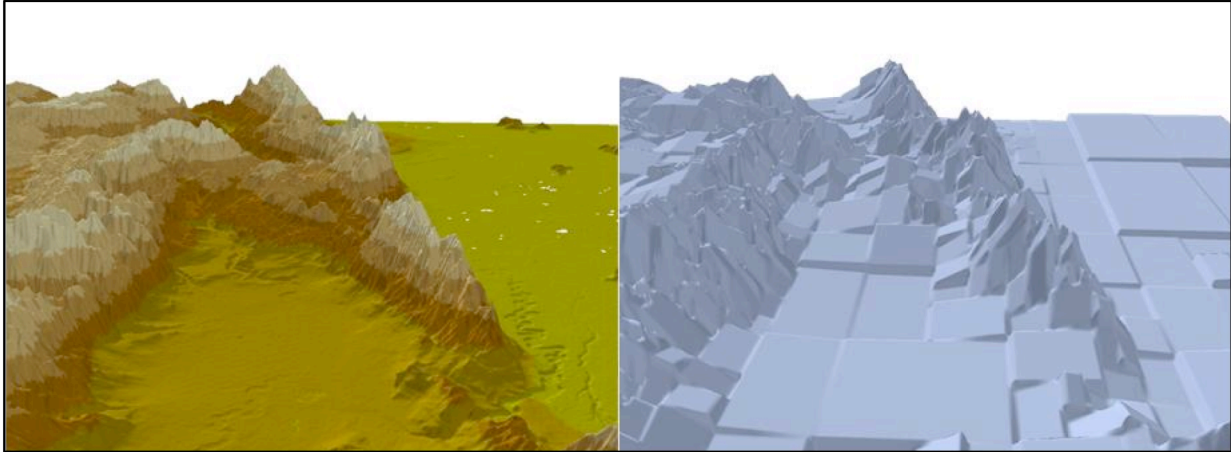
080165

Figure 1. Compression results for a quad-tree linear regression biased facet approach.

The global regular-embedded semi-regular approach made a real-time decompression-rendering scheme for an Auto-GCAS more viable. Two decompression approaches were developed for the semi-regular compression schemes to compute elevations corresponding to coordinate queries and for constructing local area maps around coordinate queries. The decompression process is the basis for further development in local area map construction, terrain data scanning, and terrain profile prediction processes essential to an Auto-GCAS. One method for decompressing the data using a table search algorithm was implemented in a C programming language environment; the second method, which will implement regular-to-irregular mappings, is pending development in a continuing phase of Auto-GCAS research.

**Status**

The compression and rendering methodologies and tools were implemented in a C programming language environment and delivered to the National Aeronautics and Space Administration (NASA) Dryden Flight Research Center (DFRC) (Edwards, California) customer. A study report was generated and delivered to the customer. Compressed data and decompression methods will be implemented into an aircraft simulation as a continuation of research in a new project phase.

**Contacts**
Mark Skoog, DFRC, Code RF, (661) 276-5774
Loyd Hook, DFRC, Code RF, (661) 276-5714
Shaun C. McWherter, DFRC, Code RC, (661) 276-2530
Jamie Willhite, DFRC, Code RF, (661) 276-2198

# NONLINEAR FLUTTER/LIMIT CYCLE OSCILLATIONS PREDICTION TOOL

## Summary

A toolbox has been developed to augment the current National Aeronautics and Space Administration (NASA) flutterometer $\mu$-method analysis of aeroservoelastic instability prediction with linear/nonlinear operators such that flutter and limit cycle oscillations (LCO) can be predicted. This toolbox will be useful to the flight test community by extending the current modeling capabilities to include nonlinearities identified from flight data.

## Objectives

The development of the toolbox has the following objectives:

- Develop a software package for the prediction of linear and nonlinear aeroservoelastic instability onset.
- Improve the flutterometer data-based model updating concept using a block-oriented linear/nonlinear identification setup in order to obtain a full set of advanced and computationally efficient routines for the next-generation flutterometer.
- Improve the accuracy and efficiency of flight testing by analyzing real-time flight data from test points at which the aircraft is stable, and consequently allowing a greater rate of expansion of the flight envelope process.

## Approach

This research project has proceeded using the following developments:

- General aeroelastic linear fractional transformation (LFT) modeling
- Modal extraction using a frequency-domain PolyMAX (LMS International, Leuven, Belgium) identification methodology
- Nonlinear Hammerstein model identification
- Nonlinear Wiener model identification
- Parameter-varying aeroservoelastic model estimation
- Graphical user interface (GUI) of the MATLAB® (The MathWorks, Natick, Massachusetts) toolbox
- Case application: F/A-18 (McDonnell Douglas Corporation, St. Louis, Missouri, now The Boeing Company, Chicago, Illinois) Active Aeroelastic Wing (AAW) test case.

### Aeroservoelastic Linear Fractional Transformation Modeling

The aeroelastic equation of motions can be aggregated using LFT operators to represent the structure, dynamic pressure, quasi-steady aerodynamics, unsteady aerodynamic lag terms, and inertial coupling matrices. The Simulink® (The MathWorks, Natick, Massachusetts) model of all these LFT interconnections is shown in figure 1.

6
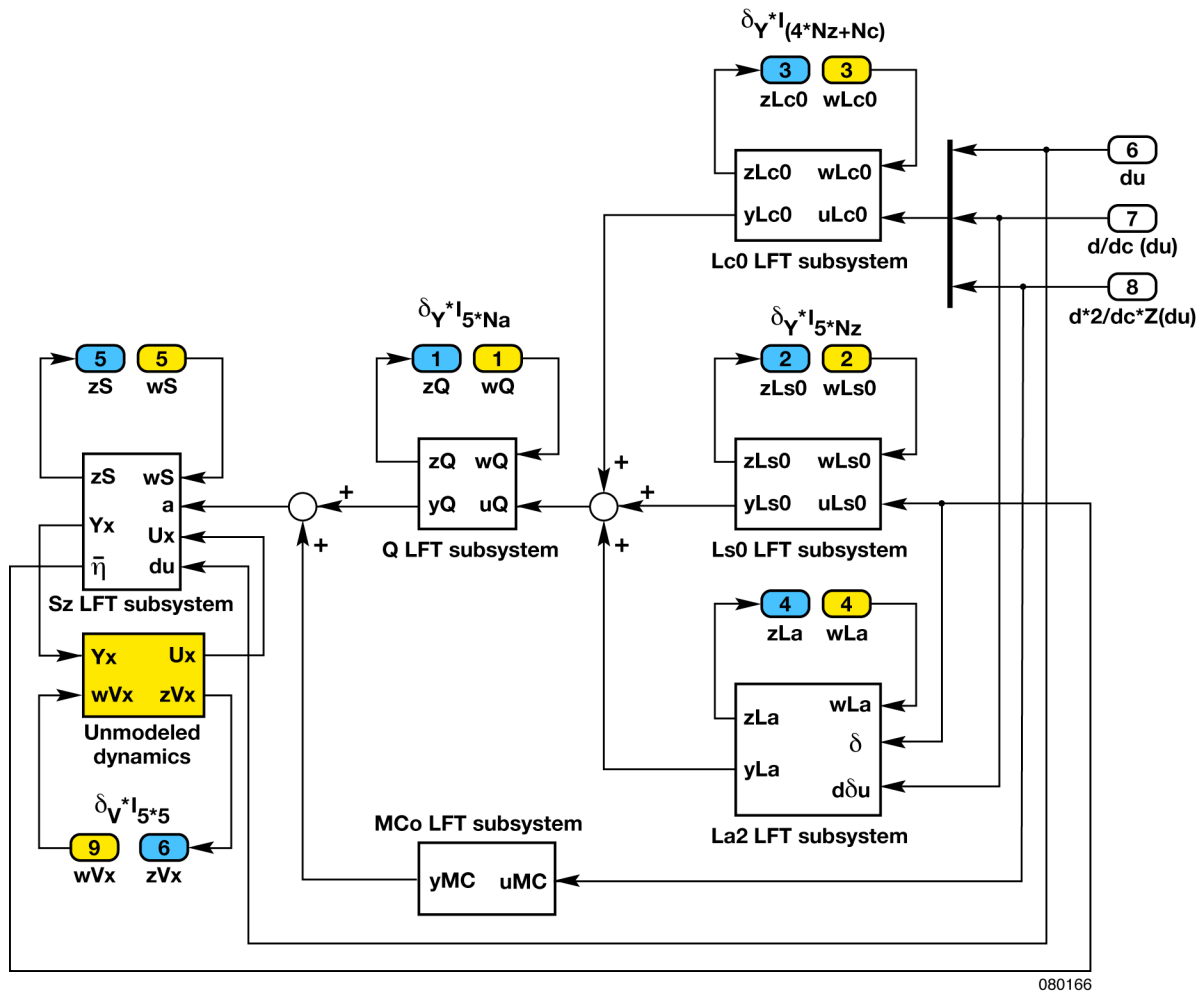
Figure 1. Aeroservoelastic LFT model.

## Mode Extraction: Frequency-Domain PolyMAX Method

The functionality of frequency-domain PolyMAX identification is to extract physical modes from experimental data by choosing the proper polynomial model parameter constraint. With the use of the correct polynomial fraction matrix to formulate the system parameter coefficients, the multiple input-output system dynamics can be approximated. This method compares favorably with the best time-domain methods in terms of accuracy, is much more efficient, and can separate stable poles and unstable poles of the system model, $H(z)$, as physical poles and mathematical (spurious) poles, respectively.

## Nonlinear Hammerstein and Wiener Model Identification

This method uses cubic spline/polynomial functions to represent the nonlinearity, orthonormal basis expansion to represent linear operator, and the separable least square (SLS) approach.

## Parameter-Varying Aeroservoelastic Model Estimation

This formulation expresses a parameter-varying model in terms of an airspeed perturbation.

7

**Status**

Figure 1 shows an aeroservoelastic LFT model including the unmodeled dynamics, and it is the basis for the data-driven, model-based, linear/nonlinear flutterometer for flight testing.

A multi-year effort has culminated in the block-oriented modeling, linear/nonlinear identification, and MATLAB$^{®}$ toolbox development with GUI. An F/A-18 AAW test case was used for analysis with flight data for flutter/LCO prediction validation. The result is a model-updating nonlinear system identification (MUNSID) toolbox.

**Contacts**

Marty Brenner, DFRC, Code RS, (661) 276-3793
Jie Zeng, ZONA Technology, Inc., Scottsdale, Arizona, (480) 945-9988

8

# NONLINEAR SYSTEM IDENTIFICATION USING ORTHONORMAL BASES: APPLICATION TO AEROELASTIC/AEROSERVOELASTIC SYSTEMS

## Summary
Iterative algorithms are developed based on identification techniques of input-nonlinearity (Hammerstein) and output-nonlinearity (Wiener) block-oriented parameter-varying aeroelastic/aeroservoelastic models.

## Objective
The objective is enhancement of the flutterometer (a model-based, data-driven aeroservoelastic instability prediction tool) with a data-based model updating concept using block-oriented linear/nonlinear identification to obtain a full set of advanced and computationally efficient routines for accurate prediction of linear and nonlinear subsonic/transonic/supersonic aeroservoelastic instabilities.

## Approach
Algorithmic development is based on separable least square (SLS) estimation using orthonormal basis functions. The linear part of the cascade system is represented by an orthonormal finite impulse response (FIR) filter, and the static nonlinear part is represented by a cubic spline/polynomial function. The advantage of using orthonormal bases in the orthonormal FIR filter lies in the possibility of incorporating prior knowledge of the system dynamics into the identification process. As a result, more accurate and simplified linear models can be obtained with a limited number of basis functions. Furthermore, using cubic spline functions instead of polynomials will greatly improve the extrapolation capability of static nonlinearities.

### Input-Nonlinear Hammerstein Model Identification
Figure 1 shows the Hammerstein model identification of the nonlinear function, $N(.)$, and linear function, $G(q)$, based on the measured data.



$$y(t) = G(N(u(t))) + v(t)$$

080167
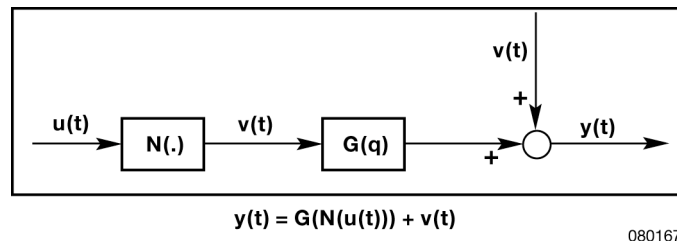
Figure 1. Hammerstein model identification.

### Output-Nonlinear Wiener Model Identification
Figure 2 shows the Wiener model identification of the linear function, $G(q)$, and nonlinear function, $N(.)$, based on the measured data.

$$z(t) = N(G(q)u(t)) + v(t)$$

080168
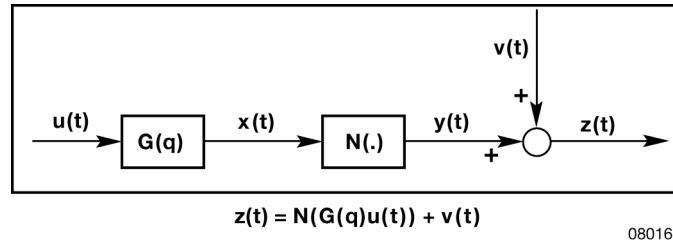
Figure 2. Wiener model identification.

**Status**

The algorithm was applied to a pitch-plunge aeroelastic system. Using the Hammerstein model setup, figure 3(a) shows the comparison of the linear system simulation output (red) and the nonlinear system output; figure 3(b) shows the comparison of the output of the estimated nonlinear error dynamics (red) and the output of the nonlinear error dynamics; figure 3(c) shows the comparison of the nonlinear simulation output (red) and the nonlinear system output; figure 3(d) shows the comparison of the true nonlinear tangent function and estimated nonlinear function (red); figure 3(e) is the plot of the unmodeled error, which is defined as the nonlinear simulated output minus nonlinear system output shown in figure 3(c); and figure 3(f) is the plot of the cost function as a function of the iteration number. From the figures, a conclusion is made that with the proper selection of the orthonormal bases to represent the linear system, and the cubic spline function to represent the static nonlinear function, the cost function converges after four iterations of the estimation process.

10
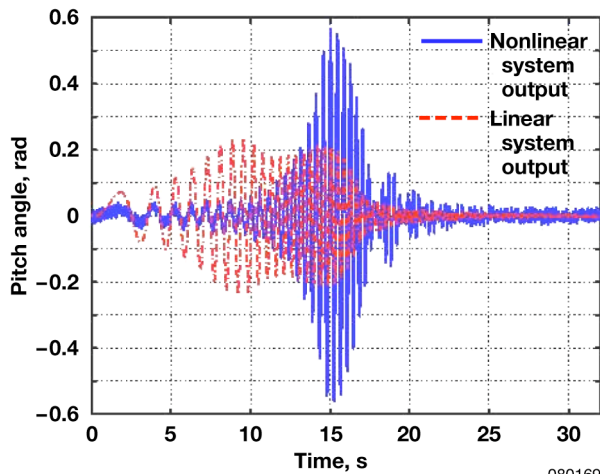
(a). Fit of response (with linear system output).
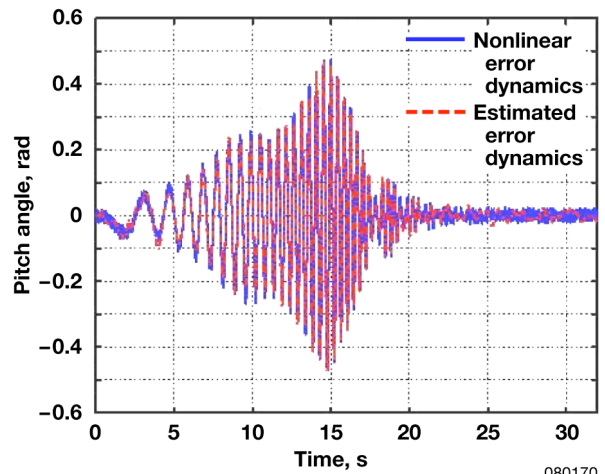
(b). Fit of unmodeled dynamics.
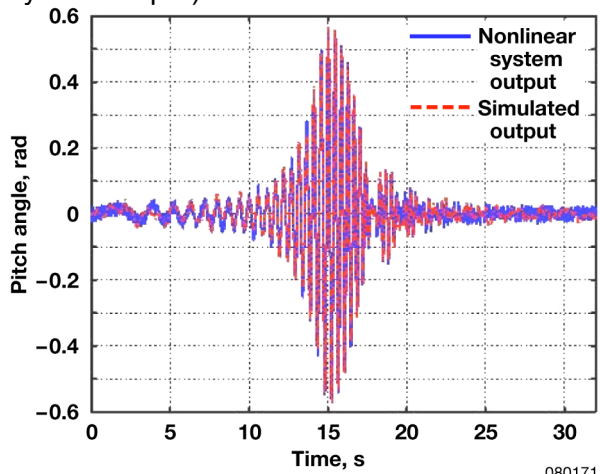
(c). Fit of response (with simulated output).
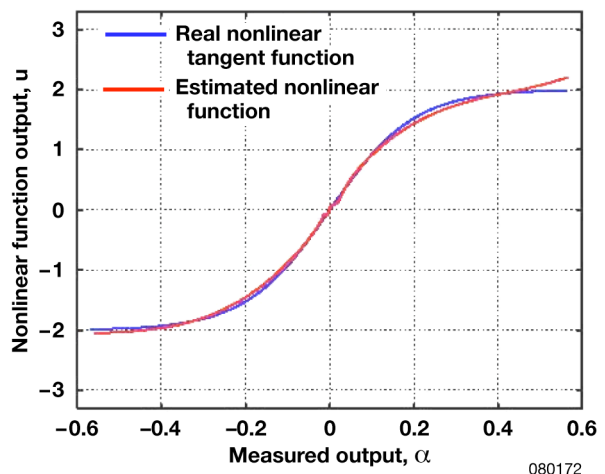
(d). Cubic nonlinear function with 13 kn.
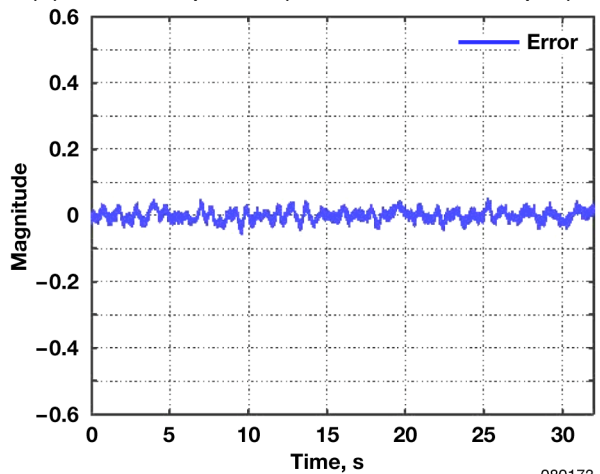
(e). Error.
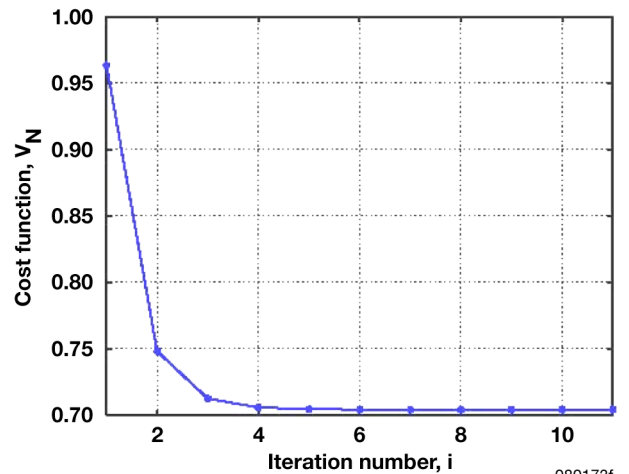
(f). Cost function.

Figure 3. Nonlinear model estimation using cubic spline represent hyperbolic tangent nonlinear representation.

11

**Contacts**
Marty Brenner, DFRC, Code RS, (661) 276-3793
Jie Zeng, ZONA Technology, Inc., Scottsdale, Arizona, (480) 945-9988

# CRITICAL AERODYNAMIC FLOW FEATURE INDICATORS:
# TOWARDS APPLICATION WITH THE AEROSTRUCTURES TEST WING

## Summary

Recent studies demonstrate the existence of a direct correlation between the unsteady aerodynamic forces and the instantaneous spatial locations of a few critical aerodynamic flow feature indicators (CAFFI), such as the leading-edge stagnation point (LESP) and flow separation point (FSP), using flush-mounted, micron-thin hot-film sensor arrays. These experiments have demonstrated that CAFFI can be used as an unsteady aerodynamic "observable" in the same manner that strain gages and accelerometers are used to measure structural response. Furthermore, since the changes in the instantaneous spatial location of CAFFI are directly related to the changes in the aerodynamic forces and moments, these "observables" can be used to initiate control actuation to realize desired load distribution and flight mission. Wind tunnel experiments have demonstrated that:

- The LESP can be used to determine the variations in the instantaneous (unsteady) lift generated by a wing section in the presence of gusts as well as structural oscillations.
- The instantaneous lift curve slope could be obtained using the LESP even without a priori calibration of the sensors.
- Absolute values of the lift coefficient in unsteady flow are obtained as a function of the instantaneous locations of the LESP and the FSP.

## Objective

The proposed experiment will extend these advanced concepts to flight research and development (R&D) applications. This effort will be devoted to minimizing the number of sensors for accurate real-time determination of CAFFI; and optimizing hardware size, weight, and power requirements for application using the aerostructures test wing (ATW2) mounted on the F-15B (McDonnell Douglas Corporation, St. Louis, Missouri, now The Boeing Company, Chicago, Illinois) aerodynamic flight test fixture (AFTF).

This flight test will be the first of its kind to measure unsteady aerodynamic loads (forcing function) in real time and to correlate them with the structural response. The ATW2 test article will be used to characterize its structural dynamic and aerodynamic behavior across a range of flight conditions, from low angle of attack to high angle of attack, from low Mach numbers to high Mach numbers, and in steady and unsteady maneuvers. Strain gages and accelerometers will be used to measure the structural response while hot-film gages will be used to characterize the aerodynamic flow features and to determine the aerodynamic forcing function. The flight experiment is expected to facilitate the development of advanced computational modeling, flutter prediction techniques, and adaptive closed-loop control technology required for the design and development of flight vehicles with active aeroelastic wings.

## Approach

The plan is to design, build, and validate a distributed aerodynamic sensing and processing (DASP) toolbox using aerodynamic "observables" for flight R&D applications, and involves the following tasks:

- Design and fabricate a flight-hardened aerodynamic sensing technology with deterministic real-time capabilities.
- Quantify the unsteady aerodynamic environment using the minimum number of sensors distributed along the wing span and chord.

- Conduct design studies for power consumption, size, and weight requirements.
- Conduct flight validation tests.

This work will basically involve the design and fabrication of a prototype DASP toolbox (including sensors with signal conditioners and signal processing software/hardware), flight system integration, and flight test support with the following tasks:

- Design and fabricate the DASP toolbox measurement electronics.
- Develop and implement the digital aerodynamic signal processor.
- Develop and validate compensation techniques.
- Ensure flight ruggedization.
- Perform system integration.
- Provide flight test support.
- Perform flight-test data analysis.

## Status

Figure 1 shows a portion of the DASP sensor array at the ATW2 wing root, with two of the macro-fiber composite (MFC) actuators to be used for structural excitation, and a ground test accelerometer at the wing-tip for a simple ground vibration test (GVT). Strain gages have been installed, and a loads test and much more extensive GVT has been completed. Design optimization and integration of sensors, signal conditioners, and signal processing components for the DASP toolbox is in progress. The MFC actuator control development and aircraft integration have been initiated.
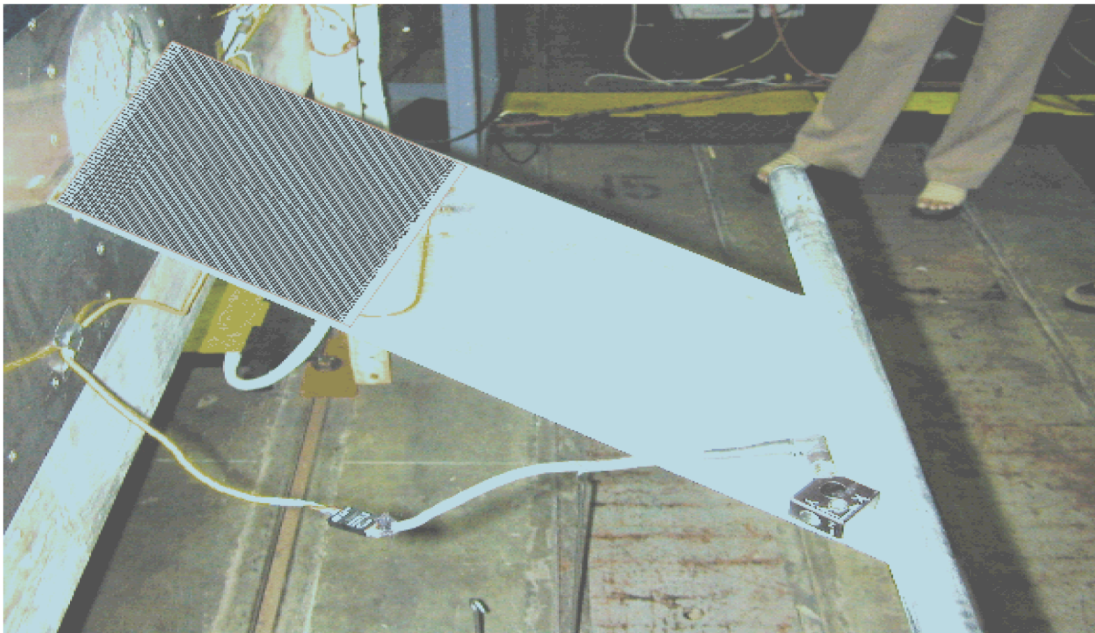


080174

Figure 1. DASP sensor array.

**Contacts**

Marty Brenner, DFRC, Code RS, (661) 276-3793
Claudia Herrera, DFRC, Code RS, (661) 276-2642
Siva Mangalam, Tao of Systems Integration, Inc., Hampton, Virginia, (757) 220-5040

# MULTIDISCIPLINARY DESIGN, ANALYSIS, AND OPTIMIZATION TOOL DEVELOPMENT USING A GENETIC ALGORITHM

## Summary

Multidisciplinary design, analysis, and optimization (MDAO) using a genetic algorithm is being developed at the National Aeronautics and Space Administration (NASA) Dryden Flight Research Center (DFRC) (Edwards, California) to automate the flutter analysis process by leveraging existing tools such as MSC Nastran™ (MSC.Software Corporation, Santa Ana, California), ZAERO™ (ZONA Technology, Inc., Scottsdale, Arizona), and the CFL3D Navier-Stokes solver to enable true multidisciplinary optimization in the preliminary design stage of subsonic, transonic, supersonic, and hypersonic aircraft. The framework has been designed to integrate analysis codes for multiple disciplines. Although a promising technology, many challenges are presented in a large-scale, real-world application. This paper describes current approaches, recent results, and challenges for MDAO as demonstrated by our experience with the Ikhana (General Atomics Aeronautical Systems, Inc., San Diego, California) fire pod design.

## Objective

In support of the Aeronautics Research Mission Directorate (ARMD) guidelines, NASA DFRC is developing an MDAO tool. This tool will leverage existing tools and practices, and allow the easy integration and adoption of new state-of-the-art software, such as the ZAERO™ aeroelastic panel code and the CFL3D Navier-Stokes solver. The primary and long-term objective of the current study is to generate the basic object-oriented framework for an MDAO tool to be used in the preliminary design stage of subsonic, transonic, supersonic, and hypersonic aircraft.

## Approach

The main goal of the development of the MDAO tool is to generate a "central executive" capable of using disparate software packages in a cross-platform network environment so as to quickly perform optimization and design tasks in a cohesive streamlined manner. Optimization can then take place within each individual tool, or in a loop between the executive and the tool, or both. Figure 1 shows a typical set of tools and their relation to the central executive.
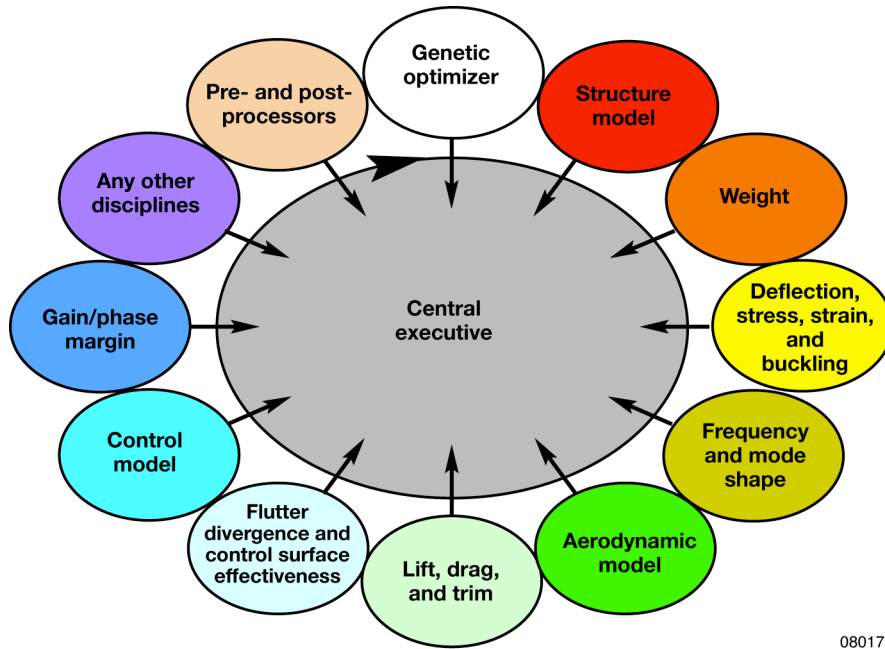
Figure 1. Central executive overview.

Currently, the central executive MDAO framework can handle structural optimization problems by using structural analysis discipline in addition to handling model update. The current MDAO framework contains five modules. The MDAO framework process is presented as a flowchart in figure 2.
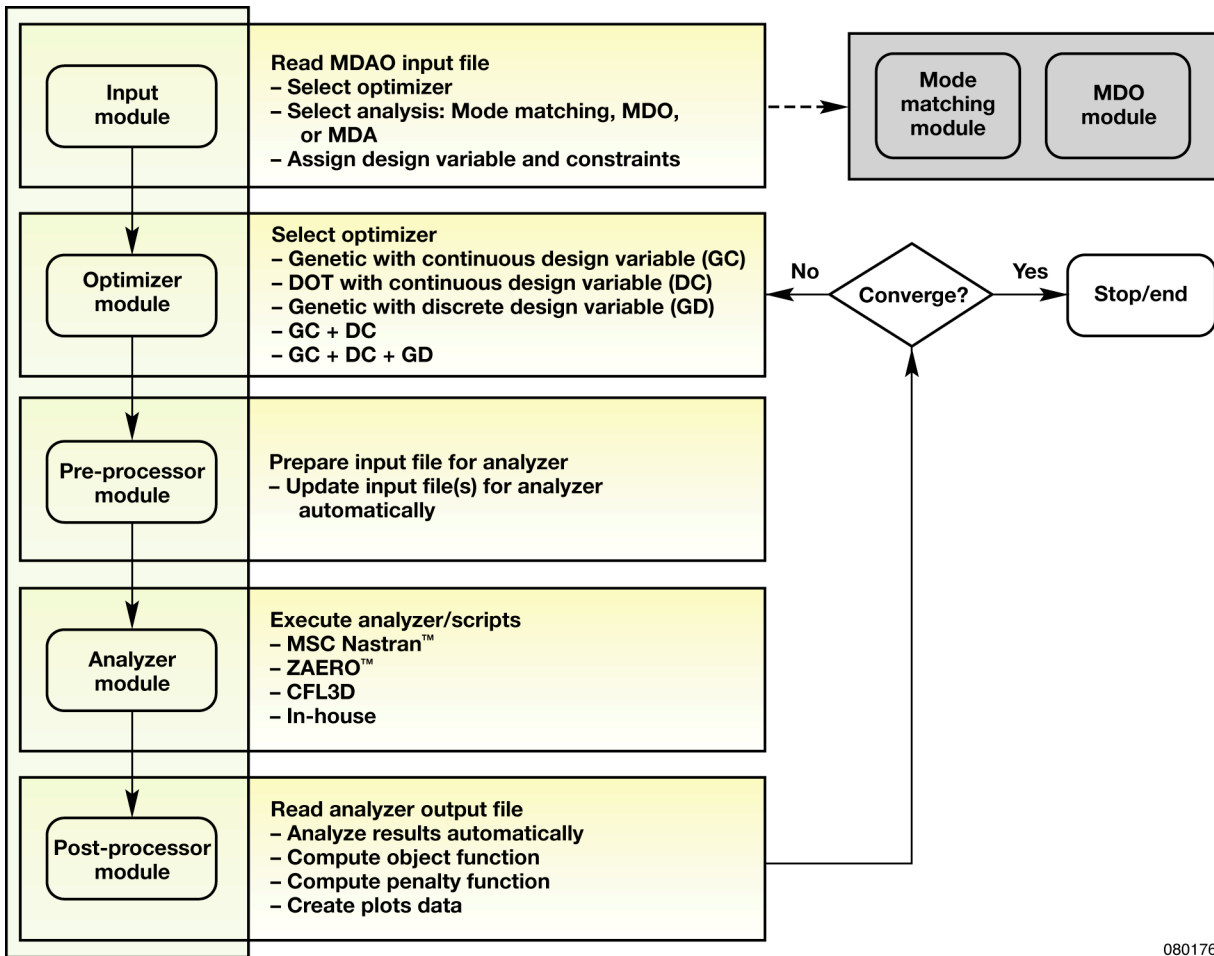
Figure 2. The basic framework of the MDAO tool central executive.

The structural analysis discipline involves loads analysis, structural dynamics, aeroelasticity, and structural optimization. The main outputs from the structural analysis discipline are structural weight, mass properties, safety factors, divergence speeds, flutter speeds, flutter frequencies, natural frequencies, and mode shapes.

**Three-Bar Truss**

The preliminary application of the MDAO tool was the optimal design of a three-bar truss subjected to an external load, as shown in figure 3. In this problem, the objective is to minimize the weight of the structure. The constraints are tensile and compressive stress constraints in member 1 and member 2 under loading $P_1$ and $P_2$. The loading $P_1$ and $P_2$ are applied separately and the material specific weight is 0.1 lb/in$^3$. The allowable stress of the tension and compression in the member is 20,000 psi and −15,000 psi, respectively. Table 1 shows the comparison of results between the MSC Nastran™ internal optimizer, MSC Nastran™ using an external optimizer (design optimization tool, DOT), and MSC Nastran™ using an external genetic optimization.
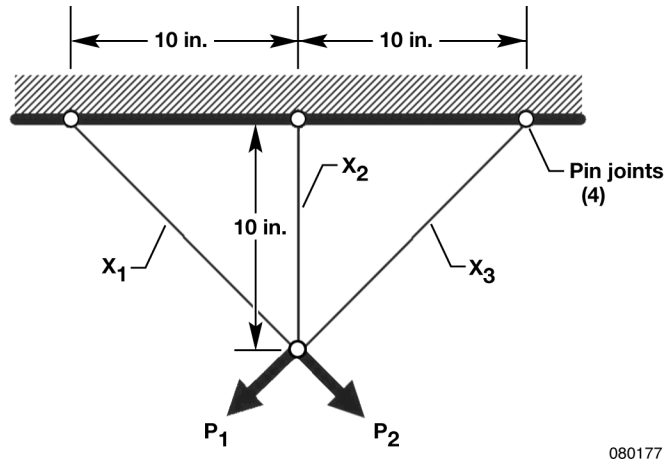
Figure 3. Three-bar truss loads conditions.

Table 1. Results of optimization on a three-bar truss.

|  | MSC Nastran™ | DOT external | Genetic external |
|---|---|---|---|
| Bar 1 | 0.77142 | 0.78798 | 0.72093 |
| Bar 2 | 0.45185 | 0.40999 | 0.66093 |
| Bar 3 | 0.77142 | 0.78798 | 0.72093 |
| Total weight | 2.6338 | 2.6388 | 2.7003 |
| Number of iterations | 5 | 7 | 50 generation and 50 propulsion |

## Ikhana with Fire Pod

A more interesting application and one of interest to NASA DFRC is the analysis and optimization of aeroelastic surfaces. The Ikhana aircraft, as shown in figure 4, will carry a fire pod that will transmit images of remote areas of the western United States down from the aircraft to a ground station. The fire pod is located under the wing near the left wing root and can alter the flutter characteristics of the baseline aircraft. The flutter flight envelope prediction of the Ikhana using the current MDAO design process is the second optimization problem in this study. The objective is to maximize the flutter and divergence speeds of the structure by varying the chordwise location and center of gravity (CG) of the fire pod from the baseline mode. The chordwise location and CG of the fire pod will be the design variables for this application.

ED07-0186-01

Figure 4. The Ikhana aircraft carrying the fire pod.

### Status

A flutter analysis determines the dynamic stability of an aeroelastic system. As with static aeroelastic analysis, flutter analysis presupposes a structural model, an aerodynamic model, and their interconnection by splines. Aircraft flutter results from coupling between the bending and torsional motions of wing and tail. Therefore, modification of the fire pod location affects both the structural finite element model and the unsteady aerodynamic model in this design optimization process. To achieve the true optimum result, new MSC Nastran™ and ZAERO™ analyses must be executed for each optimization iteration with any design variable update. The challenge of the Ikhana example is in the size of the aerodynamic influence coefficient (AIC) matrices and the complexity of the problem. With current computing resources at NASA DFRC, and using the ZAERO™ code to generate the AIC matrix, computation for a single case, one Mach number with 16 reduced frequencies, takes an average of 20 hours. Using the GA optimizer requires at least hundreds and perhaps thousands of MSC Nastran™ and ZAERO™ executions. This approach is not at all practical as a timely process. Considering the computing resource limitations and the excessive real time required for this large optimization problem, several approaches have been investigated to expedite flutter and calculations and to avoid computing a new AIC matrix for each design variable update.

### Contacts

Dr. Chan-gi Pak, DFRC, Code RS, (661) 276-5698
Wesley W. Li, DFRC, Code RS, (661) 276-3138

# STRUCTURAL MODEL TUNING CAPABILITY IN AN OBJECT-ORIENTED MULTIDISCIPLINARY DESIGN, ANALYSIS, AND OPTIMIZATION TOOL

## Summary

Updating the finite element model using measured data is a challenging problem in the area of structural dynamics. The model updating process requires not only satisfactory correlations between analytical and experimental results, but also the retention of dynamic properties of structures. Accurate rigid body dynamics are important for flight control system design and aeroelastic trim analysis. Minimizing the difference between analytical and experimental results is a type of optimization problem.

## Objective

The objective of this research is to introduce a multidisciplinary design, analysis, and optimization (MDAO) tool to optimize the objective function and constraints such that the mass properties, the natural frequencies, and the mode shapes are matched to the target data as well as the mass matrix being orthogonalized.

## Approach

Discrepancies between ground vibration test (GVT) data and numerical results are common. Discrepancies in frequencies and mode shapes are minimized using a series of optimization procedures. Recently, the National Aeronautics and Space Administration (NASA) Dryden Flight Research Center (DFRC) (Edwards, California) began developing an MDAO tool. This MDAO tool is object-oriented: users can either use the built-in pre- and post-processor to convert design variables to structural parameters and generate objective functions, or easily plug in their own analyzer for the optimization analysis. The heart of this tool is the central executive module. Users will utilize this module to select input files, solution modules, and output files; and monitor the status of current jobs. Two optimization algorithms are adopted in this MDAO tool: the traditional gradient-based algorithm and the genetic algorithm. Gradient-based algorithms work well for continuous design variable problems, whereas genetic algorithms can handle continuous as well as discrete design variable problems easily. When there are multiple local minima, genetic algorithms are able to find the global optimum results, whereas gradient-based methods may converge to a locally minimum value. In this research work, the genetic algorithm is used for the solution of the optimization problem.

## Status

A computer program for this model updating technique has been coded. An experiment known as the aerostructures test wing (ATW), as shown in figure 1, was designed by NASA DFRC to research aeroelastic instabilities and used to evaluate this process. The GVT for the first wing, ATW 1, was completed in 2002. Frequency errors of 2.97, 9.9, and 1.21 percent for the first three modes, respectively, and a total mass error of 4.13 percent were observed (table 1). After optimization, the frequency errors reduce to 0.01, 0.02, and 0.07 percent for the first three modes, respectively, and the total mass error reduces to 0.37 percent (table 2). Excellent correlations between analytical and experimental results were achieved. The GVT test for the second wing, ATW 2, is now ongoing. This model updating technique can be used again if discrepancies between measured data and analytical results are found.
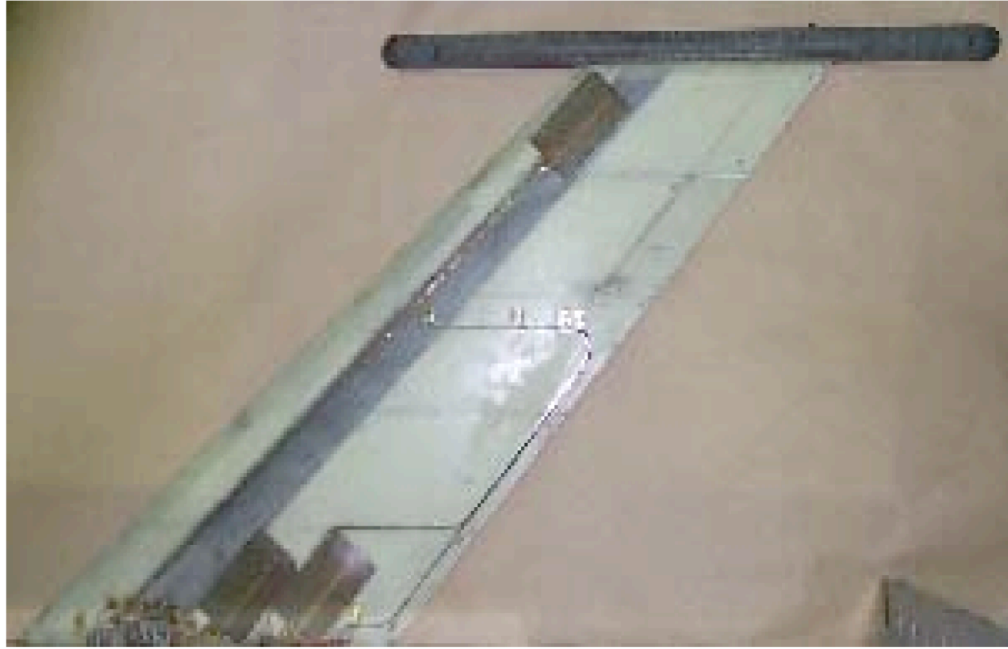
080178

Figure 1. Aerostructures test wing.

Table 1. Frequencies and total weight of the ATW 1 before optimization.

|  | GVT, Hz | MSC Nastran™, Hz | Error, % |
|---|---|---|---|
| Mode 1 | 13.763 | 13.354 | −2.97 |
| Mode 2 | 20.763 | 22.819 | 9.90 |
| Mode 3 | 77.833 | 78.771 | 1.21 |
| Total weight, lb | 2.66 | 2.77 | 4.13 |

Table 2. Frequencies and total weight of the ATW 1 after optimization.

|  | GVT, Hz | MSC Nastran™, Hz | Error, % |
|---|---|---|---|
| Mode 1 | 13.763 | 13.761 | −0.01 |
| Mode 2 | 20.763 | 20.768 | 0.02 |
| Mode 3 | 77.833 | 77.777 | −0.07 |
| Total weight, lb | 2.66 | 2.67 | 0.37 |

**Contacts**
Shun-fat Lung, DFRC, TYBRIN Corporation, Code RS, (661) 276-2969
Chan-gi Pak, DFRC, Code RS, (661) 276-5698

# EXTENSION OF KO STRAIGHT-BEAM DISPLACEMENT THEORY TO THE DEFORMED SHAPE PREDICTIONS OF CURVED STRUCTURES

## Summary

The Ko displacement theory originally developed for straight beams was applied to the deformed shape predictions of curved beams with different curvatures. The bending strains to be measured at equally spaced strain-sensing stations along the fiber-optic strain sensor lines were generated from the finite element analysis. The strains data were then input to the Ko straight-beam deflection equations for the calculations of deflections for the curved beams. The curved-beam deflections calculated from the Ko displacement theory were found to be slightly larger than the deflections calculated from the finite element computer program. The deflection prediction error was found to increase progressively with the increasing beam curvature. Mathematical functions for curvature-effect corrections were established empirically, and were incorporated into the existing Ko straight-beam deflection equation. The resulting modified Ko displacement equation was found to be able to fairly well predict the deformed shape of the curved beams up to 90° arc. For the two-point supported curved beam of 22° arc (cutout along the diameter of a generic crew exploration vehicle (CEV) spherical shell), the Ko straight-beam theory was found to provide sufficiently accurate shape predictions without using the curvature-effect corrections.

## Objective

The objective is to examine the accuracy of the Ko straight-beam displacement equations as applied to the shape predictions of curved beams, and to explore the mathematical functions for curvature-effect corrections.

## Approach

Curved beams with azimuth angles {0, 22.5, 45, 67.5, 90} deg were analyzed. Surface strains of the curved beams were generated from the finite element analysis. The strain data were then input to the Ko straight-beam displacement theory for the shape predictions of curved beams. Based on the prediction differences between the finite element analysis and the Ko displacement theory, mathematical correction functions were established to modify the Ko straight-beam displacement theory for the curved-beam shape predictions. Figure 1 shows the CEV curved beam under clamped support condition, and figure 2 provides deflection comparisons for two-end clamped CEV curved beam and equivalent straight beam.
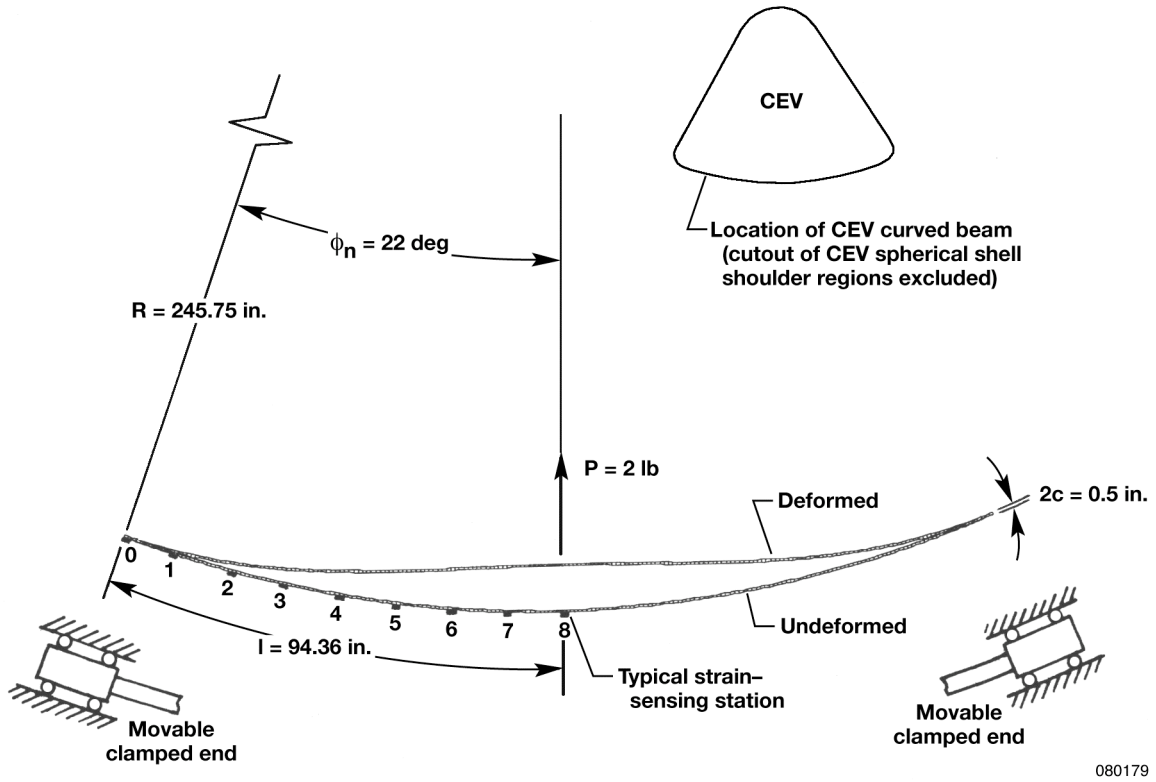
Figure 1. Two-point supported CEV curved beam under clamped support condition.
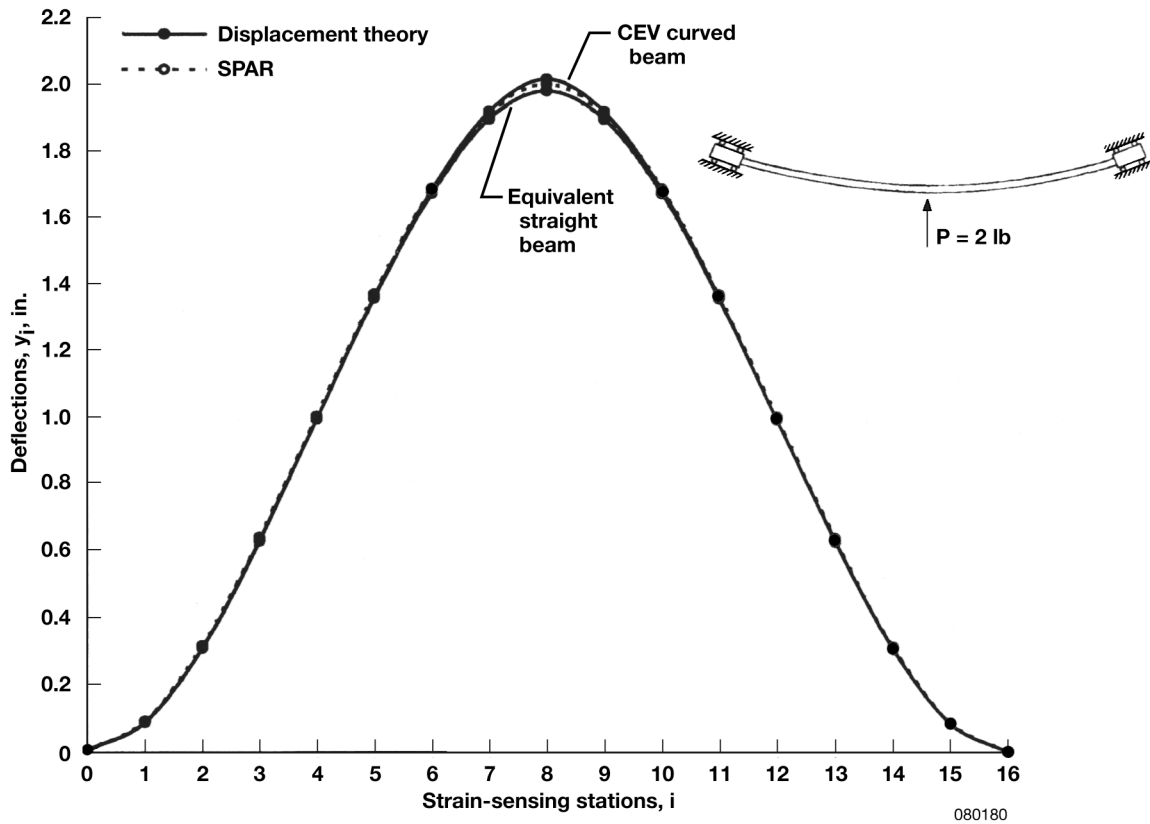
Figure 2. Comparisons of deflections calculated from SPAR program and Ko displacement theory for two-end clamped CEV curved beam and equivalent straight beam.

## Status

The modified Ko deflection equations with curvature effect introduced were found to provide reasonably accurate shape predictions for any curved beam up to 90° arc. More refined curvature-effect correction functions are being explored, however, for improving the prediction accuracy.

## Contacts

Dr. William L. Ko, DFRC, Code RS, (661) 276-3581
Dr. W. Lance Richards, DFRC, Code RS, (661) 276-3562

# F-15B WITH PHOENIX MISSILE AND PYLON ASSEMBLY–
# DRAG FORCE ESTIMATION

## Summary

The Phoenix project was a hypersonic testbed that utilized a U.S. Navy AIM-54 Phoenix (Raytheon Company, Waltham, Massachusetts) missile containing an experimental research payload that would be launched from a National Aeronautics and Space Administration (NASA) F-15B (McDonnell Douglas Corporation, St. Louis, Missouri, now The Boeing Company, Chicago, Illinois) flight research aircraft. A drag force estimation was performed using semi-empirical information from references to determine the drag of the individual components of the Phoenix Missile Hypersonic Testbed (PMHT) and of the combined F-15B and PMHT system for anticipated flight conditions. The PMHT system consisted of the AIM-54 Phoenix missile and a pylon assembly, which included the F-15 SUU-60 B/A centerline fuel tank pylon, the pylon assembly interface plate (PIP), and the F-14 (Northrop Grumman Corporation, Los Angeles, California) LAU-93 wing pylon. Flight conditions of constant airspeed, straight and level flights, and standard atmospheric conditions were assumed. The highest drag forces were found to occur at a flight condition of Mach 2 at an altitude of 34,000 ft and amounted to a 10-percent increase in overall drag of the F-15B aircraft with the PMHT system.

## Objective

A conservative drag force estimation of the individual components of the pylon assembly would aid in determining the maximum forces that would be experienced on the structural components during research flights. This estimation would help ensure adequate and safe structural design of the PMHT system. In addition, estimating the combined drag force of the F-15B and PMHT system could be used to update the NASA Dryden Flight Research Center (DFRC) (Edwards, California) F-15B flight simulator, which would aid in predicting PMHT mission performance of the F-15B aircraft.

## Approach

The pylon shapes were simplified and treated as having wedge-shaped forebodies, with straight sections following, and then ending with a sharp or blunt trailing edge. This simplification was conservative as the actual pylons have streamlined transitions and boattail trailing edges with a rounded or moderately blunt base. A review of the proposed flight envelope of the F-15B aircraft with PMHT system determined that the highest drag forces would likely occur at aircraft flight conditions of either Mach 2 at an altitude of 34,000 ft or Mach 1 at an altitude of 28,000 ft. Therefore, drag force estimations were performed at these two conditions. Significant differences exist between the local flow conditions and the ambient free-stream conditions at the PMHT system installation location on the F-15B aircraft. Local Mach numbers were determined to be Mach 1.09 and Mach 1.6 for the Mach 1 and Mach 2 flight conditions, respectively. By using air properties at the local flow conditions, the aerodynamic drag components of skin friction, pressure, and wave drag for the three components of the pylon assembly were determined.

The turbulent skin-friction drag coefficients were calculated for the components of the pylon assembly for subsonic smooth-plane wall flow using standard equations based on Blasius experimental data. These calculated values were then corrected for supersonic skin friction.

Pylon forebody pressure/wave drag coefficients were calculated using equations based on experimental data on wedge shapes. No base drag coefficients were calculated for the SUU-60 B/A pylon or the PIP as they were treated as having sharp trailing edges. A base drag coefficient was omitted for the LAU-93 pylon, although it has a moderately blunt base. This

omission was conservative as it was assumed that at supersonic speeds the drag contribution of the LAU-93 pylon base would be equal to or less than that of a double wedge-shaped pylon.

Drag information on the AIM-54 missile at the two flight conditions was obtained from a Hughes Aircraft Company stability and control design report, which provided AIM-54 trim drag coefficients as a function of angle of attack for a range of Mach numbers. Finally, the NASA DFRC F-15B flight simulator was used to determine drag coefficients and forces for the F-15B aircraft at the two flight conditions.

Initial estimations of the pressure/wave drag contributions of the pylons at the Mach 1.6 flight condition appeared to be too high. A consideration was made that the drag forces should not be more than approximately 2 times greater than those at the Mach 1.09 condition. This consideration was based on the AIM-54 and F-15B drag forces at the Mach 1.6 flight condition being approximately 2 times greater than those at the Mach 1.09 condition. Therefore, a decision was made to replace the estimations for the pylons with values that were 3 times the drag values at Mach 1.09 for conservatism. As the overall drag force predictions for the three components of the pylon assembly were considered very conservative, a 25-percent reduction of the calculated drag forces for these components was performed. In addition, no interference drag penalty was added to the total drag force predictions of the combined F-15B and PMHT system. The resulting estimated combined drag force of the F-15B aircraft with the PMHT system was 44,051 lbf at the Mach 2 flight condition.

The 25-percent reduction of the estimated drag force of the pylon assembly reduced the overall drag increase of the F-15B aircraft with the PMHT system by only a small percentage for both flight conditions. Therefore, the estimation of the drag forces was considered to be adequate. For comparison, the operation of the DFRC F-15B simulator with the centerline fuel tank installed caused an increase in drag force of 14 percent at the Mach 2 flight condition. This comparison suggested that the estimated drag contribution of the PMHT system is close to that of the simulated centerline fuel tank, which appears to be reasonable.

### Status

This drag force estimation supported the Phoenix project. No further work related to this analysis is expected for this project.

### Contact

David T. Booth, DFRC, Code RA, (661) 276-3734

# MASS PROPERTY TESTING OF PHOENIX MISSILE HYPERSONIC TESTBED HARDWARE

## Summary

The National Aeronautics and Space Administration (NASA) Dryden Flight Research Center (DFRC) (Edwards, California), in a joint effort with the Naval Air Warfare Center Weapons Division (NAWC-WD) at China Lake, California, has obtained several U.S. Navy AIM-54C Phoenix (Raytheon Company, Waltham, Massachusetts) missiles for use as hypersonic test platforms. The goal of the Phoenix Missile Hypersonic Testbed (PMHT) project is to develop a low-cost hypersonic research flight test capability that will increase the amount of hypersonic flight data to help bridge the large developmental gap between ground testing/analysis and major flight demonstrator X-planes. The missile (also known as boost vehicle) will be carried under the centerline belly of the NASA F-15B (McDonnell Douglas Corporation, St. Louis, Missouri, now The Boeing Company, Chicago, Illinois) aircraft, tail number 836, and launched from an altitude of approximately 48,000 ft at a speed of Mach 2. In order for the missile to be carried aboard the F-15B aircraft, it must be suspended from a custom-designed pylon assembly consisting of the following hardware: an F-15 centerline pylon, a custom-built interface plate, and an F-14 (Northrop Grumman Corporation, Los Angeles, California) pylon (also known as Phoenix adapter pylon). A flutter analysis of the PMHT must be performed prior to flight to help ensure the safety of the aircraft. In order to conduct the flutter analysis, finite element (FE) models of the PMHT were required to be developed with accurate mass properties of each pylon component and the boost vehicle. Due to lack of traceability and discrepancies with the original AIM-54 mass property documentation, the PMHT project elected to conduct several mass property tests on the PMHT hardware.

## Objective

The goal of the testing was to obtain mass property information of the boost vehicle (CATM-54C) and components of the pylon assembly to more accurately create FE models than could be obtained through estimation methods. The mass properties of the components involved in the stack assembly were later used to update the FE models. These FE models are critically important for the flutter analysis, which will be performed to help clear the aircraft for captive-carry envelope clearance flights. The objectives of these tests are to accurately measure the weight, center of gravity (CG), and mass moment of inertia of each test component in the stack so a more accurate flutter analysis can be completed.

## Approach

By utilizing proven methods that have been used in the aerospace industry for many years, six different tests were performed to obtain all of the desired stack mass properties. The CGs for each component were measured using various methods, which included setting pylons on knife edges or load cells (fig. 1) and then measuring reactions, or suspending the test articles from two cables and then measuring the tension in each cable. These methods allowed the CGs to be accurately marked on the pylons and the boost vehicle. After the CG was marked, measurements could then be made to place the CG in the proper aircraft coordinates used in the FE models. The mass moments of inertia of each component were measured using the bifilar pendulum method as described in NASA Technical Note No. 351. This method has been proven accurate and used in the aircraft industry for decades. For the bifilar pendulum test, two cables suspend an object such that the CG of the test article is directly between the cables (fig. 2). A custom-designed test rig allowed the MAU-12 ejector rack assembly to slide along a steel bar. This design facilitated the attachment of the interface plate, the Phoenix adapter pylon, and the boost vehicle and provided the ability to evenly locate the CGs of test articles between the cables, which is a requirement for the bifilar pendulum method. A torque in yaw

was then applied to the test article and the period of oscillation measured. From the measurements of period, cable length, distance between cables, and test article weight, the inertia of the test article was determined mathematically.



080181

Figure 1. Weight and CG test setup.



ED07-0130-20

Figure 2. Bifilar pendulum test setup.

**Status**

The PMHT mass property testing was successful, the FE models were updated, and the captive-carry flutter analysis was completed. In December 2007, however, the NASA Aeronautics Research Mission Directorate (ARMD) Hypersonics Project funding for the PMHT project was discontinued, and the project came to a work stoppage.

**Contacts**

Natalie Spivey, DFRC, Code RS, (661) 276-2790, natalie.d.spivey@nasa.gov
Thomas Williams, DFRC, Code RS Co-op, thomas.c.williams@nasa.gov

# ARMD HYPERSONICS PROJECT MATERIALS & STRUCTURES: TESTING OF SCRAMJET THERMAL PROTECTION SYSTEM CONCEPTS

## Summary

Work is being conducted under the National Aeronautics and Space Administration (NASA) Aeronautics Research Mission Directorate (ARMD) Fundamental Aeronautics Program to test and validate thermal protection system (TPS) concepts for use on scramjet-powered vehicles. The NASA Dryden Flight Research Center (DFRC) (Edwards, California) Flight Loads Laboratory (FLL) was asked to test two TPS coupons. The first coupon (fig. 1), developed by Ultramet of Pacoima, California, is a sandwich TPS concept and is to be used as a liner in a scramjet exhaust duct. The second coupon (fig. 2), developed by Materials Research & Design, Inc. (MR&D) of Wayne, Pennsylvania, is to be used as a nonparasitic integrated acreage TPS/airframe structure.

080182
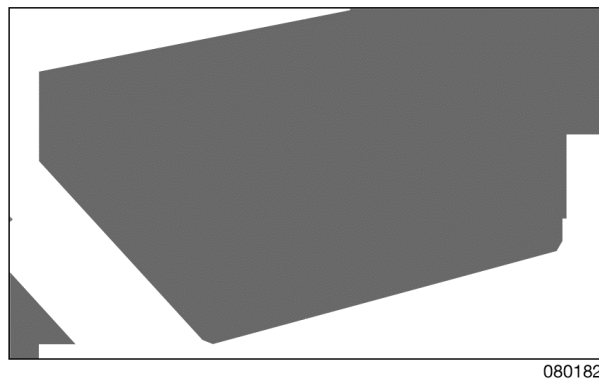
Figure 1. Ultramet TPS coupon.



080183
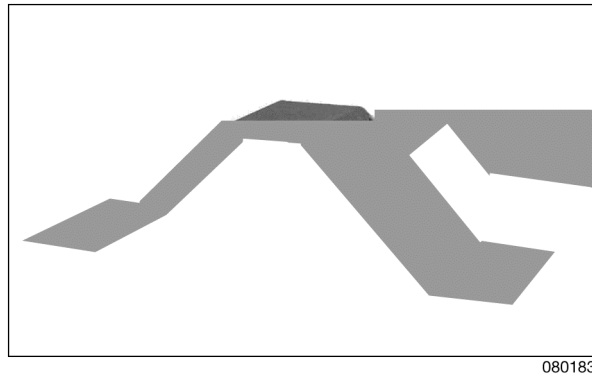
Figure 2. Materials Research & Design TPS coupon.

## Objective

The testing objective for both coupons is to validate each concept as a viable TPS option for a hypersonic vehicle. The data acquired from both tests will be used to validate pretest predictions of thermal performance. The following results and measurements acquired from testing will be used for a full analysis:

- Top side temperature distribution
- Bottom surface temperature distribution

30

- Plot of $\Delta T$ versus Time of test sample to determine $\Delta T_{max}$ and time of occurrence
- Temperature difference between bottom surface and backing plate.

**Approach**

Figure 3 shows the test setup, which utilized graphite heaters to heat one side of the coupons to the required temperature. The test articles were instrumented using high-temperature sensor techniques developed in the FLL. The heating profile was defined to match the thermal loading that the TPS panels would experience during flight. The entire test setup was enclosed within a small chamber that was purged with nitrogen. Ceramic blocks were used to create the desired adiabatic boundary conditions.



080184

Figure 3. TPS coupon test setup.

**Status**

Initial tests of the Ultramet coupon have been completed and the thermal data have been provided to Ultramet personnel. Figure 4 shows a plot of the temperature variation between the top and bottom surfaces of the Ultramet TPS coupon. (Note that the plateau seen on the top side curve is a result of temperature of the test article exceeding that of the measurement device.)

As of April 2008, the MR&D sample and the second Ultramet sample are being instrumented. After the completion of testing, each concept may be developed further.
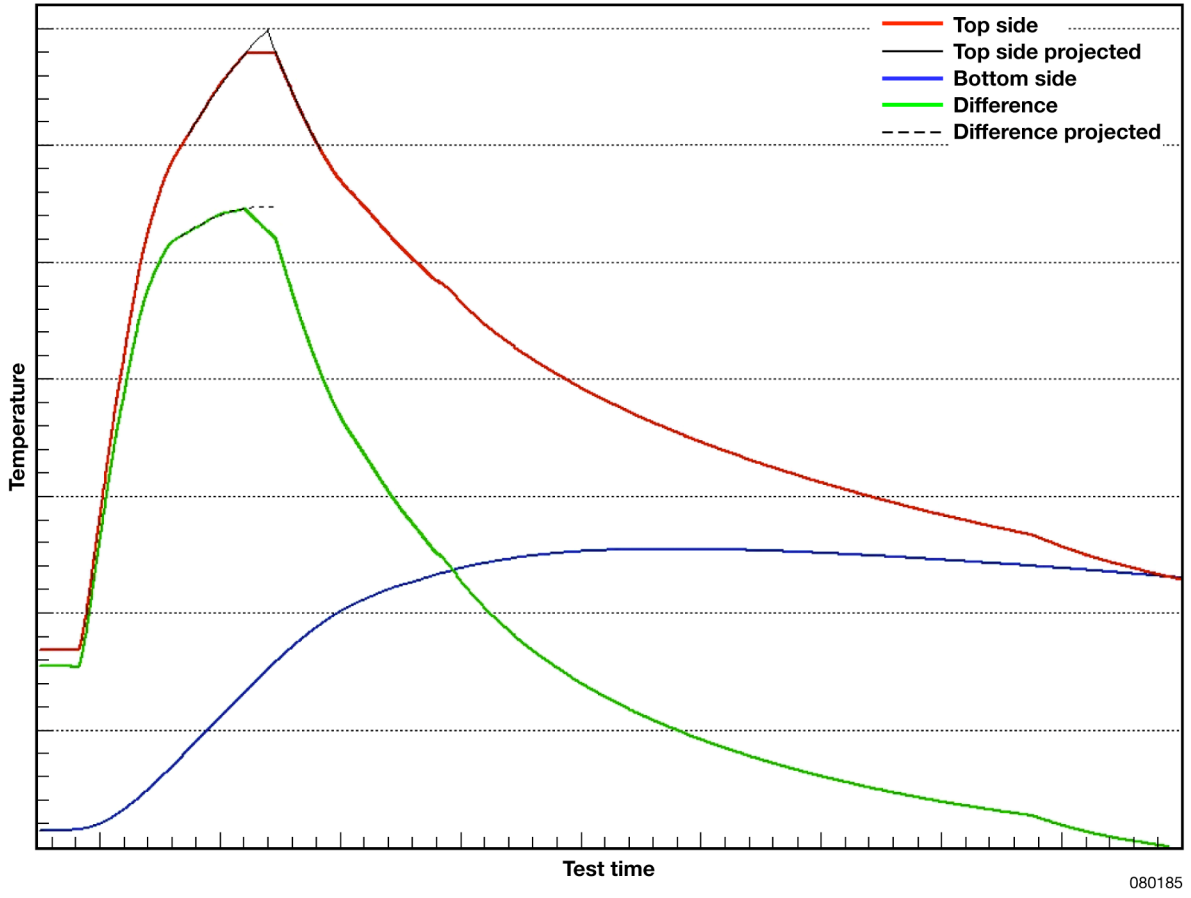
Figure 4. Temperature variation between top and bottom surfaces of the Ultramet TPS coupon.

**Contact**
Matthew Moholt, DFRC, Code RS, (661) 276-3259

# HIGH-TEMPERATURE MODAL SURVEY OF THE RUDDERVATOR SUBCOMPONENT TEST ARTICLE

## Summary

To support the National Aeronautics and Space Administration (NASA) Hypersonics Project research objectives under the Aeronautics Research Mission Directorate (ARMD) Fundamental Aeronautics Program, Dryden Flight Research Center (DFRC) (Edwards, California) has developed a program to test a carbon/silicon carbide (C/SiC) ruddervator subcomponent test article (RSTA). The C/SiC RSTA is a truncated version of the full-scale X-37 (Boeing Phantom Works, Huntington Beach, California) hot-structure control surface that was designed and fabricated under the X-37 program but was never tested. Even though it is a truncated test article, the RSTA incorporates all of the major full-scale features, including the metallic spindle and five major C/SiC quasi-isotropic lay-up components secured together with mostly C/SiC fasteners. The RSTA will undergo numerous thermal, thermal/mechanical, and thermal/vibration tests as part of the NASA ARMD Hypersonics Project research program.

Ground vibration tests (GVT) are routinely conducted for supporting flutter analysis for subsonic and supersonic vehicles; for hypersonic vehicle applications, however, GVT techniques are not well established. New high-temperature materials systems, fabrication technologies, and high-temperature sensors offer new opportunities to develop new techniques for performing GVT at elevated temperatures. These high-temperature materials have a unique property of increasing in stiffness when heated. When the materials are incorporated into a hot-structure that includes metallic components that decrease in stiffness with increasing temperature, the interaction between the two material systems needs to be understood, as it ultimately affects the hypersonic flutter analysis. Performing a high-temperature GVT that captures this material interaction will collect new data and generate this understanding. To fully understand the modal characteristics of the C/SiC RSTA at elevated temperatures, a couple of room-temperature GVT were completed; one with the RSTA suspended from a bungee cord and another mounted on the strongback in the NASA DFRC nitrogen chamber.

## Objective

The objectives of the first GVT, conducted with the RSTA in the room-temperature free-free configuration, were to measure the global frequencies to validate and correlate the RSTA analytical model, and also to verify that the new high-temperature accelerometers (maximum 900°F) output data similar to the room-temperature accelerometers. The goal of the second GVT performed was to obtain the global frequencies and mode shapes of the RSTA in the DFRC nitrogen chamber with the strongback boundary conditions at room temperature. This modal data will provide a baseline for the elevated-temperature modal tests planned during phase 2 of the RSTA project.

## Approach

For the first GVT, the RSTA was suspended from a bungee cord (fig. 1) to provide a "soft" boundary condition to compare with the finite element model free-free boundary condition results. The RSTA was instrumented with 84 external accelerometers for the test. A majority of the accelerometers were on the windward side to capture the predominant structural response. On the leeward side, the high-temperature accelerometers were placed in existing RSTA screw holes on the spar box structure with collocated room-temperature accelerometers for frequency comparison. The RSTA was excited with an impact hammer and an electromagnetic shaker; however, the shaker excitation provided better data.
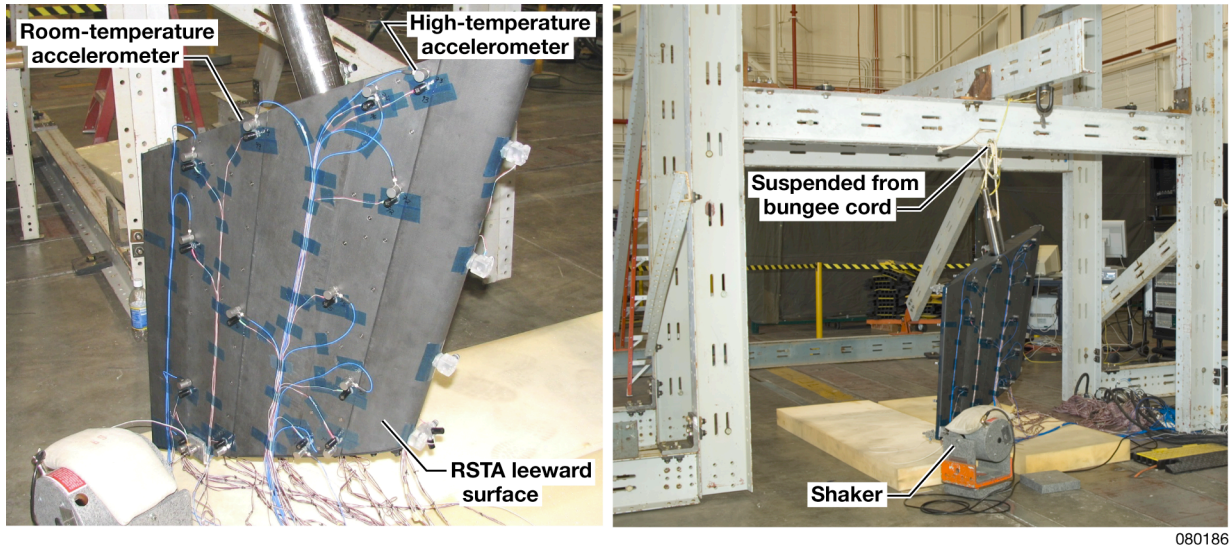
Figure 1. RSTA room-temperature free-free GVT setup.

For the second GVT, the RSTA was mounted on a strongback in the high-temperature test nitrogen chamber at the NASA DFRC Flight Loads Laboratory. A total of 14 high-temperature and 103 room-temperature accelerometers were used. The accelerometers were mounted on both the leeward and windward surfaces of the RSTA, along with numerous accelerometers mounted to the strongback and supporting structure, to capture the response of the connection stiffness and to assist in decoupling the RSTA and strongback modes. To excite the RSTA for the elevated-thermal modal testing, a modified excitation setup was designed. Numerous factors had to be considered during the design of the excitation setup for the thermal environment. The setup (fig. 2) includes an electromagnetic shaker that provides a burst random excitation in the vertical direction on the outboard aft spar box near the trailing edge of the leeward side of the RSTA.
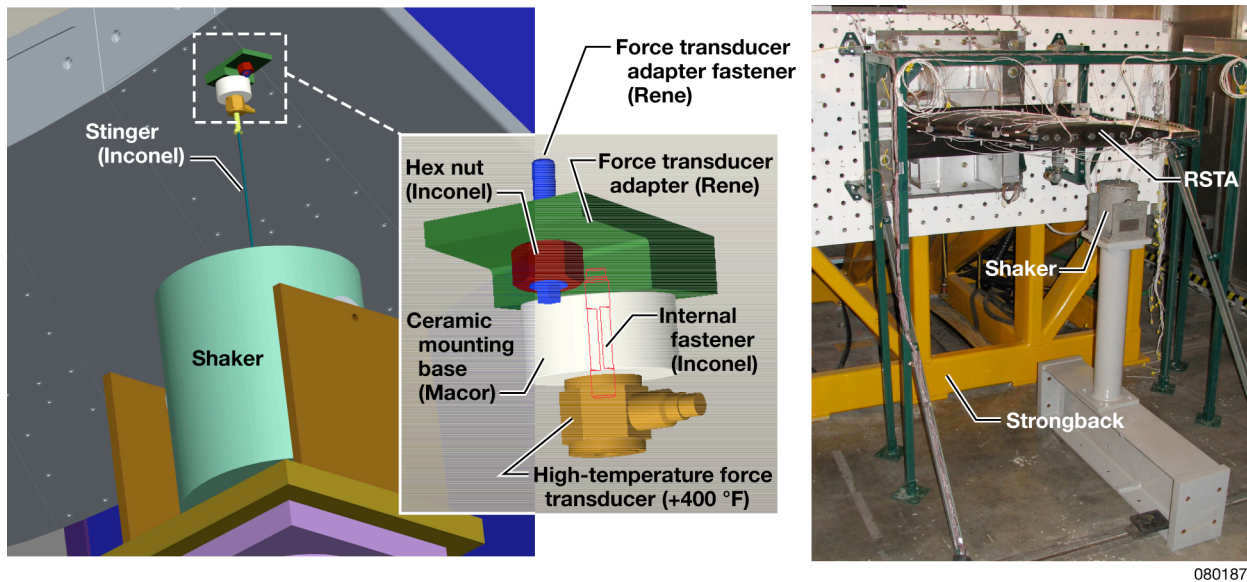


Figure 2. RSTA room-temperature strongback GVT setup.

**Status**

The RSTA phase 2 testing, which includes the thermal, thermal/mechanical, and thermal/vibration tests, is expected to begin in June 2008 and continue through October 2008.

**Contact**

Natalie Spivey, DFRC, Code RS, (661) 276-2790, natalie.d.spivey@nasa.gov

# ARMD HYPERSONICS PROJECT MATERIALS & STRUCTURES: C/SiC RUDDERVATOR SUBCOMPONENT TEST AND ANALYSIS TASK

## Summary

A multiyear effort was initiated in fiscal year 2006 (FY06) to test and analyze a carbon-silicon carbide (C/SiC) ruddervator subcomponent test article (RSTA) in cooperation with the Hypersonics Project Materials & Structures (M&S) discipline area within the National Aeronautics and Space Administration (NASA) Aeronautics Research Mission Directorate (ARMD) Fundamental Aeronautics Program. Planning, test setup design, and test hardware fabrication and partial assembly was completed in FY06–07 with final test setup assembly and testing to occur in FY08.

## Objective

The C/SiC RSTA (fig. 1) is a hot-structure control surface that was designed, fabricated, but never tested under the X-37 (Boeing Phantom Works, Huntington Beach, California) long-duration orbital vehicle technology development program. The RSTA was designed by Materials Research & Design, Inc. (Wayne, Pennsylvania) and manufactured by Power System Composites LLC ( a subsidiary of General Electric Company, Fairfield, Connecticut) of Newark, Delaware. The RSTA is a truncated version of the full-scale X-37 control surface, but it incorporates all of the major full-scale features including the metallic spindle, five major C/SiC quasi-isotropic lay-up components fastened together with mostly C/SiC fasteners, and face-sheets that serve as access panels for assembly of the RSTA.
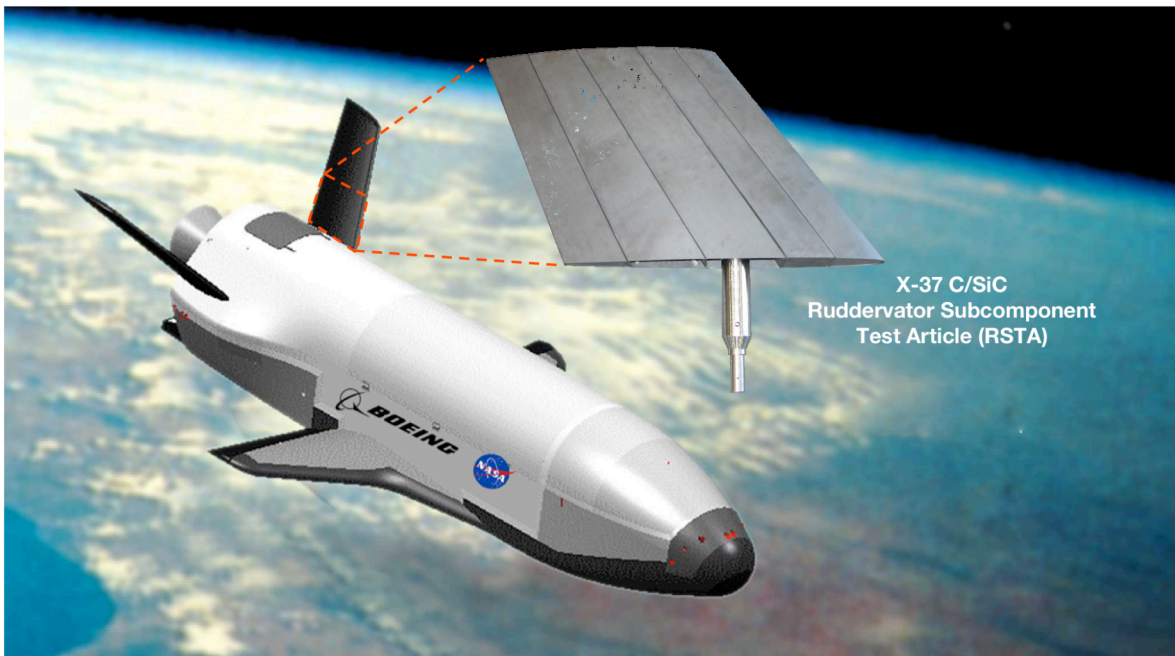


080188

Figure 1. Location of the RSTA on the X-37 vehicle.

The research objectives that were proposed to the Hypersonics Project M&S program were as follows:

- Test and evaluate the thermal, structural, and dynamic performance of the C/SiC RSTA through the application of relevant hypersonic thermal, structural, acoustic, and vibration loads.
- Establish an extensive database for current and future structural analysis developments and evaluation.
- Perform pretest and posttest thermal-structural analysis to support test operations and evaluation of NASA subsequent advanced analysis methods.

## Approach

A four-phase, multiyear test program has been developed to subject the C/SiC RSTA to relevant thermal, structural, acoustic, and vibration loads expected for hypersonic reentry and transatmospheric flight trajectories. Phase 1, acoustic and vibration testing at X-37 ascent conditions, was completed at NASA Langley Research Center (LaRC) (Hampton, Virginia). Phases 2 and 3, thermal and mechanical testing at X-37 reentry and hypersonic cruise conditions, are currently active at NASA Dryden Flight Research Center (DFRC) (Edwards, California). Phase 4, vibration and thermal-acoustic testing at hypersonic cruise conditions, will be conducted at NASA LaRC.

## Status

After the completion of phase 1 acoustic and vibration testing at NASA LaRC, the RSTA underwent a series of activities in preparation for phase 2 testing, which include thermography and modal survey testing, instrumentation installation, and test setup development. Baseline thermography testing has identified material defects in the structure that will be tracked throughout the tests to study the impact of testing on defect propagation. The baseline thermography results will also help to identify and track any damage initiated by testing. Modal survey testing provided a baseline understanding of the natural frequencies and mode shapes for the RSTA. These data, along with data collected from a posttest modal survey, will provide an understanding of the impact of testing on changes to the natural frequencies and mode shapes. In addition, modal survey testing will be performed at high temperatures to attempt to assess the impact of temperature on natural frequencies and mode shapes on a hot-structure control surface. The RSTA was fully instrumented with thermocouples, high-temperature fiber-optic strain sensors, and high-temperature accelerometers (fig. 2). The test setup design and most of the component fabrication has been completed. A significant portion of the test setup has also been assembled, including the assembly of the quartz lamp heating system (fig. 3).
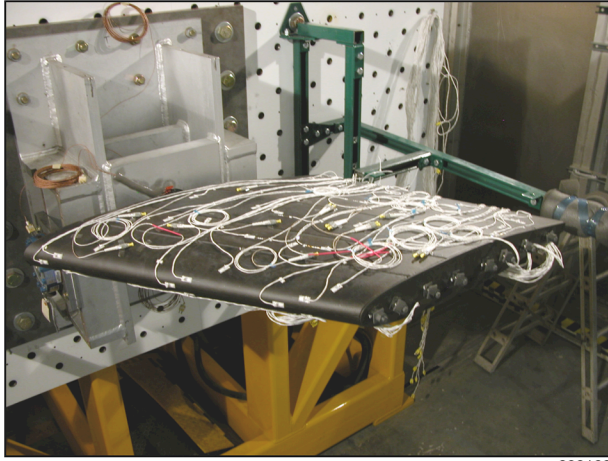
080189



080190

Figure 2. Instrumented RSTA installed in the test setup.
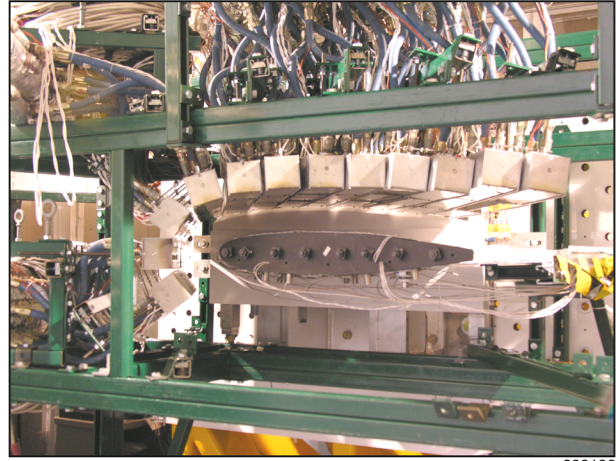
Figure 3. Fit check of RSTA quartz lamp heating system.

**Contacts**

Larry Hudson, DFRC, Code RS, (661) 276-3925
Craig Stephens, DFRC, Code RS, (661) 276-2028

# GROUND VIBRATION TESTING AND MODEL CORRELATION OF THE PHOENIX MISSILE HYPERSONIC TESTBED

## Summary

The National Aeronautics and Space Administration (NASA) Dryden Flight Research Center (DFRC) (Edwards, California) and the Naval Air Warfare Center Weapons Division (NAWC-WD) (China Lake, California) have been working together on the Phoenix Missile Hypersonic Testbed (PMHT) project to develop a low-cost hypersonic research flight test capability. The missile (boost vehicle) will be carried on the NASA F-15B (McDonnell Douglas Corporation, St. Louis, Missouri, now The Boeing Company, Chicago, Illinois) aircraft, tail number 836, on the centerline with a series of pylons and launched from an altitude of approximately 48,000 ft at a speed of Mach 2. To ensure flight safety of the F-15B aircraft, ground vibration testing (GVT), finite element (FE) models, and a flutter analysis are required to quantify the boost vehicle and pylon assembly structural modes, frequencies, and aeroelastic stability before the PMHT captive-carry flights.

## Objective

The goal of the GVT was to measure the frequency, modal damping, and mode shape of the primary structural modes of the boost vehicle and pylon assembly mated to the F-15B aircraft in the configuration for the captive-carry flights. The objective of the model correlation was to update the boost vehicle and pylon assembly analytical FE models with the measured GVT data, such that the models matched the "as-assembled configuration" of the mode shapes and frequencies of the test article. These FE models will be used for the flutter analysis, which is used as a guide for flight clearance.

## Approach

The GVT was conducted with the boost vehicle in the captive-carry configuration, as shown in figure 1. The aircraft was on soft tires to simulate a free-free boundary condition, and 107 accelerometers were placed in all three translational directions on the boost vehicle, pylon assembly, and aircraft to capture the required structural response. The GVT data was analyzed and used for the correlation of the FE models during the mode-matching technique.

ED07-0073-40

Figure 1. GVT test setup.

The mode-matching technique utilized was a series of optimizations used to match the mass and stiffness properties of the beam FE models to the GVT data. Three optimization steps were used: the mass properties were modified to match measured mass properties; the mass matrix was orthogonalized; and then the natural frequencies and mode shapes were matched. The optimization took into account hundreds of mass and stiffness design variables such as mass properties information (mass, center of gravity location, and mass moments of inertia), structural sizing information (thickness, cross-sectional area, area moment of inertia, torsional constant), material properties (Young's modulus), and spring constants. Figure 2 shows the three mode shapes that were used during the mode matching process and how successful the FE model eventually correlated to the GVT data by comparing frequency results.

**GVT data**

**FE model**

| **Mode 1 – Lateral bending Frequency error, –0.102 percent** | **Mode 2 – Yaw frequency error, –0.027 percent** | **Mode 3 – Pitch frequency error, –0.013 percent** |

080191
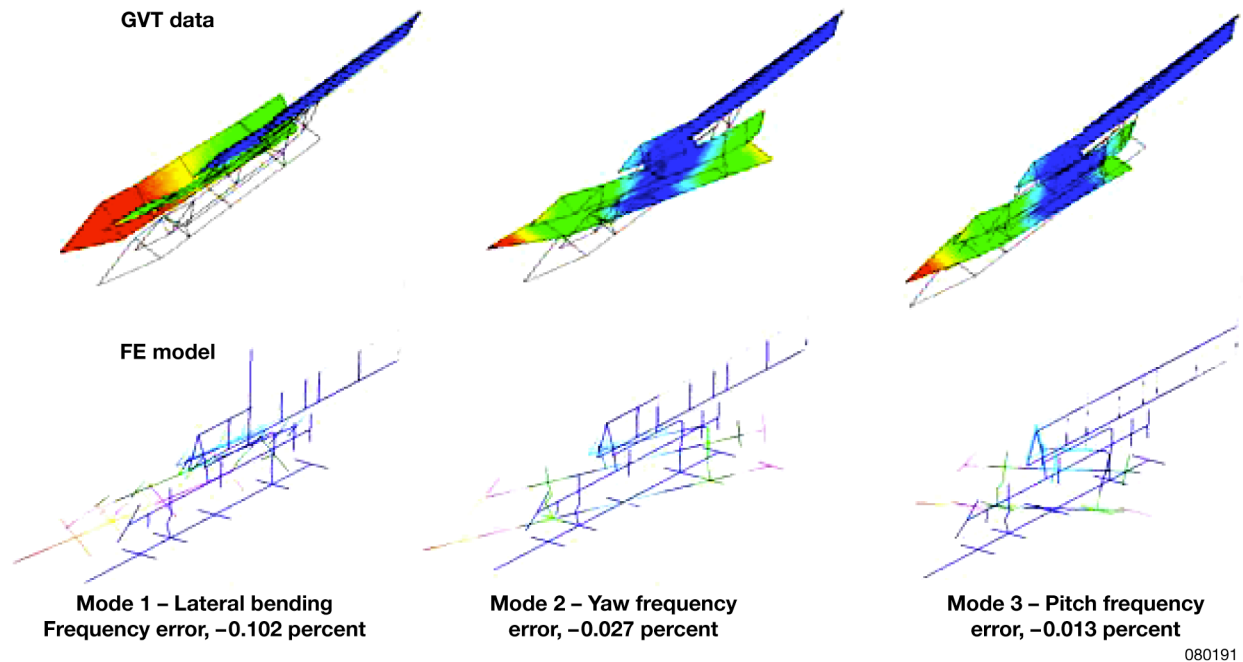
Figure 2. Mode shapes and matching results of the Phoenix stack.

## Status

The PMHT GVT was completed, the FE models were correlated, and the captive-carry flutter analysis was completed. In December 2007, however, the NASA ARMD Hypersonic Project funding for the PMHT project was discontinued, and the project came to a work stoppage.

## Contacts

Natalie Spivey, DFRC, Code RS, (661) 276-2790, natalie.d.spivey@nasa.gov
Darin Flynn, DFRC, Code RA, (661) 276-3450, darin.c.flynn@nasa.gov

# PHOENIX MISSILE HYPERSONIC TESTBED: PERFORMANCE DESIGN AND ANALYSIS

## Summary

The Phoenix Missile Hypersonic Testbed (PMHT) project goal is to convert surplus U.S. Navy AIM-54 Phoenix (Raytheon Company, Waltham, Massachusetts) missiles into research testbeds to accurately deliver research payloads through programmable guidance to hypersonic test conditions at a low cost with a high flight rate. The National Aeronautics and Space Administration (NASA) F-15B (McDonnell Douglas Corporation, St. Louis, Missouri, now The Boeing Company, Chicago, Illinois) aircraft, tail number 836, will launch the testbed missile from the centerline pylon. The PMHT performance group (including flight controls, propulsion/performance, aerodynamics, and simulation) is responsible for the primary deliverable of guidance and control flight software for the modified missile.

## Objective

The overall objective of the PMHT performance group is to enable the missile to reach mission-specific test conditions, including Mach number, dynamic pressure, angle of attack ($\pm1°$), and roll angle ($\pm5°$), for a minimum test time duration. Except for the angle requirements, mission test conditions vary according to the modified missile weight. The first testbed demonstration objective is to achieve a speed of Mach 5, a dynamic pressure of 500 psf, and test time duration of 8 s at the same launch weight as the original AIM-54 missile.

## Approach

Two simulations are used for missile performance design and analysis: Program to Optimize Simulated Trajectories II (POST II), an optimal trajectory generation simulation; and the standard National Aeronautics and Space Administration (NASA) Dryden Flight Research Center (DFRC) (Edwards, California) six-degree-of-freedom (6-DOF) nonlinear simulation for guidance and control design. Both simulations use a thrust model and an aerodynamic model that are digitized from AIM-54 documents. Tools have been developed or enhanced for digitization of the AIM-54 final wind tunnel report plots with a digitization error of less than 1 percent. The simulations are validated against each other to ensure that the dynamics compare well. The POST II simulation explores the following features:

- Optimize simulated trajectory for Mach number or downrange distance at the end of the motor burn.
- Tightly constrain the initial launch angle.
- Tightly constrain the pitch during the first few seconds after launch for a safe separation.
- Constrain flight dynamics for the vehicle limits.

Guidance and control algorithms are designed and autocoded in MATLAB® and Simulink® (both by The MathWorks, Natick, Massachusetts). For improved design iterations using the DFRC 6-DOF, the Simulink® diagrams are directly interfaced to the simulation through shared memory. This interface is referred to as "talk" and allows the guidance and control designer to analyze the design with the high-fidelity, nonlinear simulation without coding. Guidance preliminary design implements linear quadratic regulator (LQR) tracker architecture for vertical guidance. Three state feedback (altitude, climb rate, and angle of attack) are used to generate an angle-of-attack command. Controller preliminary design implements Nesline architecture inherited from the original missile design for pitch/yaw control and a simple proportional-integral for roll control. The Nesline algorithm computes gains from aerodynamic data with scheduling on Mach number, altitude, and motor on/off discrete.

To obtain the maximum Mach number test condition, the F-15B PMHT launch envelope development is conducted in the DFRC-piloted simulation. For improved modeling of high Mach number flight conditions, engine models from Pratt & Whitney (East Hartford, Connecticut) and The Boeing Company (Chicago, Illinois) are incorporated into the simulation and await flight test validation. Potential launch conditions, at an altitude under the 50,000-ft ceiling and within the fuel limit and dynamic limits, were developed by the project pilot to simulate flight to launch conditions with and without pitch maneuvers for varying the launch angle.

## Results

Validation of the missile simulations shows good dynamic comparison between POST II and the DFRC 6-DOF. Trajectories have been generated in POST II and incorporated into the guidance algorithm as the target trajectory to follow. The guidance and control algorithms have been incorporated into the DFRC 6-DOF for simulated missions. The initial stability analysis of the Nesline controller at altitudes from 40,000–100,000 ft and Mach 0.6–6.0 shows adequate stability margin. Also, guidance and control algorithms have been successfully autocoded and incorporated into the DFRC 6-DOF for batch analysis.

Two studies were conducted to plan the launch condition for the first demonstration flight by using POST II to compute optimized maximum test Mach number trajectories. First, the launch flight condition at an altitude of 40,000 ft at Mach 2 was fixed, and sensitivities to launch pitch angle (0°, 5°, and 10°), fixed pitch angle safe separation fly-out duration (0 s, 3 s, and 6 s), and launch weight (1008 lb, 908 lb, and 808 lb) were examined. Results of the first study are shown in figure 1. The bars above the Test Mach scale indicate the test Mach number achieved for various launch weights, with sensitivity to the other aforementioned factors. Second, at a launch weight of 1008 lb and fixed-pitch angle, safe separation fly-out duration of 6 s, the F-15B PMHT piloted simulation was used to simulate various launch conditions of altitude (40,000–48,000 ft), launch pitch angles (0°, 5°, 10°, and 15°), and the maximum F-15B Mach number speed (Mach 2.0–2.2). Results are shown in figure 1 below the Test Mach scale, indicating a range of Mach 4.5–4.9. From these studies and discussion of flight operation simplicity, a first demonstration launch condition was chosen at an altitude of 48,000 ft, Mach 2.0, level launch reaching test Mach 4.68. An example full trajectory from this launch condition is shown in figure 2. Maximum test Mach number achievable does not reach the previous conceptual design estimate incorporated into the requirements. The project is reevaluating the test condition requirements based on this analysis.
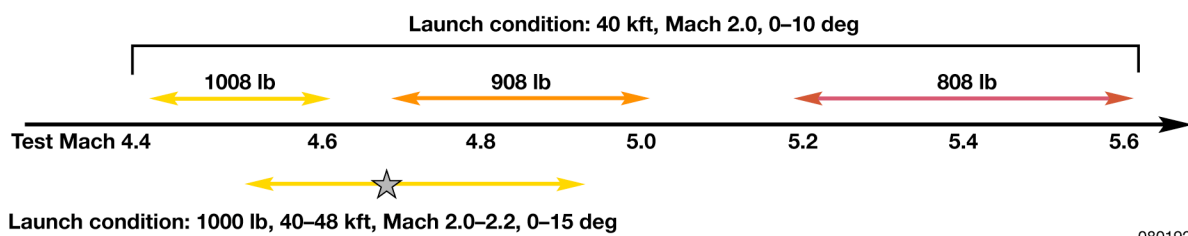


Figure 1. Ranges of optimized maximum Mach number trajectories from sensitivities to launch conditions: weight, altitude, Mach number, pitch angle, and fixed angle fly-out duration.
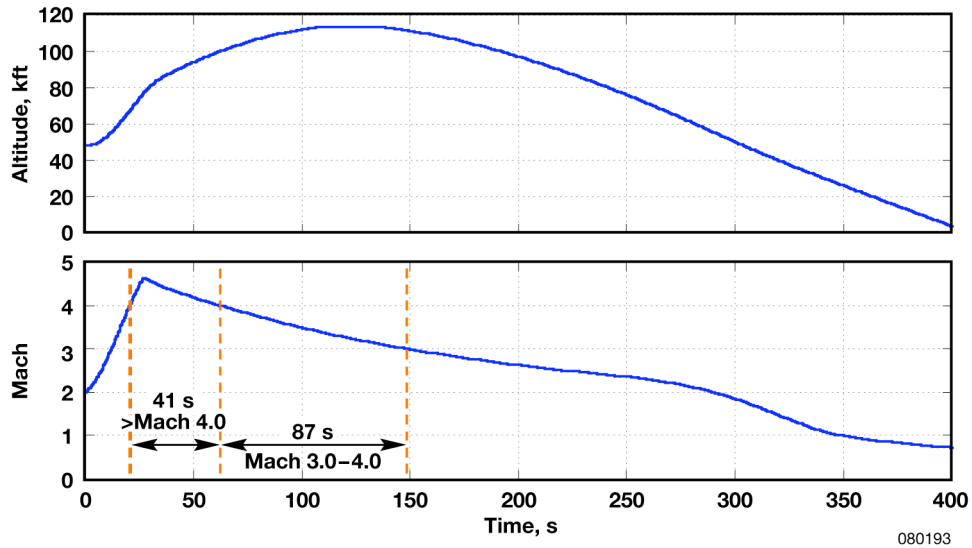
Figure 2. Example optimized maximum Mach number trajectory from demonstration flight launch condition (48,000 ft, Mach 2.0, level).

## Status

The program was near completion of a preliminary design for a Preliminary Design Review in December 2007. Performance test flights of the NASA F-15B launch aircraft to validate the engine model are scheduled in winter 2008. In December 2007, however, the funding for the PMHT project under the NASA Aeronautics Research Mission Directorate (ARMD) Hypersonics Project was discontinued, and the project came to a work stoppage. The project was looking for customers and partners to complete the testbed development.

## Contacts

Mark Buschbacher, DFRC, Code RC, (661) 276-3838
Kurt Kloesel, DFRC, Code RA, (661) 276-3121

# CREW EXPLORATION VEHICLE LAUNCH ABORT SYSTEM–PAD ABORT-1 (PA-1) FLIGHT TEST

## Summary

The Constellation program is an organization within the National Aeronautics and Space Administration (NASA) whose mission is to create the new generation of spacecraft that will replace the space shuttle after its planned retirement in 2010. In the event of a catastrophic failure on the launch pad or launch vehicle during ascent, the successful use of the launch abort system (LAS) will allow crew members to escape harm. The pad abort-1 (PA-1) flight test is the first of six planned unmanned flight tests to verify the LAS to be used in future operational missions. These flight tests will be performed at the White Sands Missile Range (WSMR) in New Mexico. The PA-1 launch is scheduled for December 2008.

## Objective

The objective of the flight tests is to examine the performance of the LAS rocket used to initiate pad, mid- and high-altitude aborts. In the event of a catastrophic failure on the launch pad or during the early ascent portion of spaceflight, the LAS will initiate an abort that will pull the crew module (CM) to a safe distance away from the launch pad or failed booster. The primary flight test objectives for PA-1 are to demonstrate a ground-initiated abort as well as to demonstrate the capability of the LAS to propel the CM to a safe distance from a launch vehicle.

## Approach

The PA-1 flight test article (FTA) is composed of a CM and LAS, and the combination is referred to as the launch abort vehicle (LAV). The CM boilerplate vehicle for PA-1 is being built by NASA Langley Research Center (Hampton, Virginia). The boilerplate vehicles are not representative in structure of the operational CMs, but have an outer mold line that is representative of the operational vehicle. The boilerplate CM is designed to match mass properties targets that are reasonable reflections of the mass properties of future operational vehicles.

The LAS is being built by Orbital Sciences Corporation (Dulles, Virginia) and consists of an abort motor, an attitude control motor (ACM), and a jettison motor. During an LAS abort, the abort motor will fire and provide the impulse necessary to pull the CM away from the launch pad or malfunctioning booster. The abort motor will deliver the majority of its thrust within the first 4 s after ignition to provide 15 g of acceleration away from the launch pad or failed launch vehicle. At the same time the abort motor fires, the ACM will fire to maintain stable flight. The ACM consists of eight equally spaced nozzles, each 45° apart around the LAS housing near the top of the casing. These eight nozzles will provide the ability to control motion in the pitch and yaw axes. The ACM will burn for approximately 20 s, providing thrust that can be diverted through the eight nozzles to produce controlling moments. After the abort motor burns out and the LAV is stabilized, the two canards on the LAS will deploy, and the combination of the canards and the ACM will reorient the CM and LAS so that the heat shield on the bottom of the CM will be forward with respect to the air stream. Once the LAV reorients with the heat shield forward, the LAS jettison motor will fire and provide the impulse necessary to separate the LAS from the CM after the LAV is stabilized.

The Flight Test Flight Dynamics group will determine and analyze the flight dynamics and trajectories of the FTA for all abort flight tests performed by the Flight Test Office, for the purpose of ensuring mission success and safety. The team's work currently addresses the software simulations and models held by the various organizations involved with Orion abort flight test. Figure 1 shows an example of recent analysis performed on the PA-1 FTA. The figure

shows the resulting trajectories for 1000 simulation runs using dispersions on mass properties, winds, and aerodynamic uncertainties.
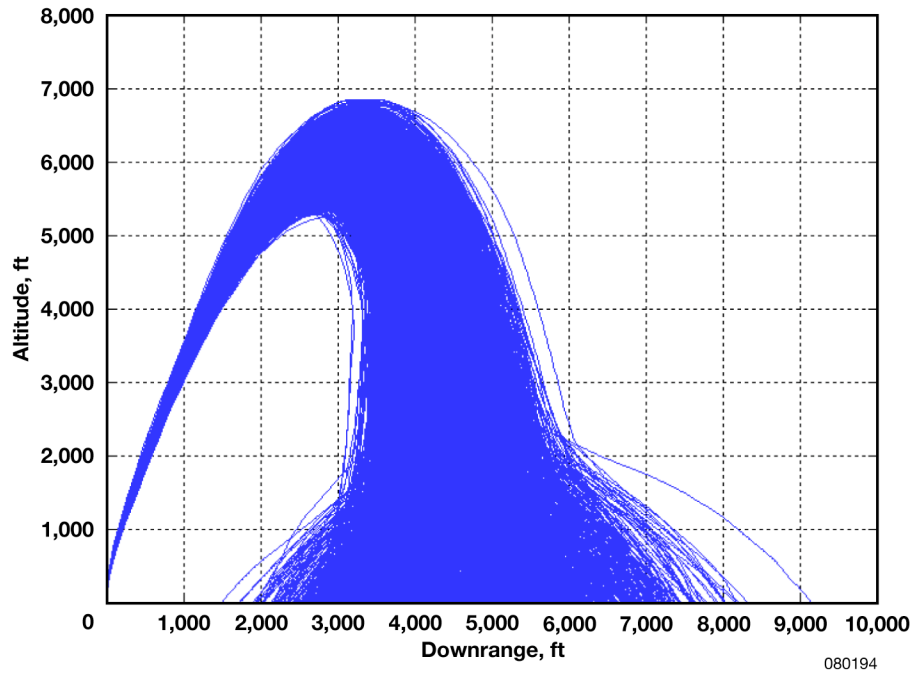


Figure 1. PA-1 FTA simulation runs trajectories.

## Status

The flight tests will occur at WSMR in New Mexico. The initial site selection for PA-1 is near launch complex 32. The PA-1 is slated to be launched in a due north direction relative to the launch pad.

## Contacts

Peggy Hayes, Flight Test Flight Dynamics lead, DFRC, Code RC, (661) 276-2508
Bob Clarke, Flight Test Office lead engineer, DFRC, Code RC, (661) 276-3799
Ryan Dibley, DFRC, Code RC, (661) 276-5324
Jinu Idicula, DFRC, Code RC, (661) 276-2892
Prasad Kutty, DFRC, Analytical Mechanics Associates, Inc., Code RC, (661) 276-6810

# TESTING THE ORION (CREW EXPLORATION VEHICLE) LAUNCH ABORT SYSTEM–ASCENT ABORT-1 (AA-1) FLIGHT TEST

## Summary

The National Aeronautics and Space Administration (NASA) has announced a plan to retire the space shuttle fleet in 2010, but for the U.S.-manned exploration of space to continue, a next generation spacecraft needs to be designed. The Constellation team was given the task to create the spacecraft that will take astronauts and materials to the International Space Station, the Moon, and beyond. In the event of a catastrophic failure during the launch, the successful use of the launch abort system (LAS) will allow crew members to escape harm. The ascent abort-1 (AA-1) flight test is the second of six planned unmanned flight tests to verify the functionality of the LAS, and the first test to occur from the abort test booster (ATB). All of the flight tests are scheduled to occur at White Sands Missile Range (WSMR) in New Mexico. The AA-1 launch is scheduled for February 2010.

## Objective

In the event of a catastrophic failure on the launch pad or during the early ascent portion of spaceflight, the LAS will initiate an abort that will pull the crew module (CM) to a safe distance away from the failed booster. The objective of the abort flight tests is to examine the performance of the LAS through a series of six unmanned flight tests. Two of the flight tests that the Flight Test Office team has proposed are launch pad abort tests that will be performed from a launch stand instead of from an external booster. The remaining four proposed flight tests are ascent abort tests that will use an ATB to take the CM and LAS to a predetermined flight condition. The primary flight test objectives for AA-1 are to demonstrate an abort at the maximum dynamic pressure (maximum load) condition of the operational launch vehicle trajectory, as well as to demonstrate the capability of the LAS to propel the CM to a safe distance from a launch vehicle.

## Approach

The AA-1 flight test article (FTA) is composed of an ATB, a CM boilerplate, and an LAS. The CM boilerplate vehicle for AA-1 is being built by NASA Langley Research Center (Hampton, Virginia). The boilerplate vehicles are not representative in structure of the operational CMs, but have an outer mold line and center of gravity that is representative of the operational vehicle. The ATB for AA-1 is being built by Orbital Sciences Corporation (Dulles, Virginia) Launch Systems Group in Chandler, Arizona, and will be a single-stage booster unlike the five-stage booster for the operational launch vehicle.

The Flight Test Flight Dynamics team determines and analyzes the flight dynamics and trajectories of the FTA for all abort flight tests performed by the Flight Test Office. The first flight test, pad abort-1 (PA-1), will not use an ATB and will be traveling a much shorter distance than the AA-1 flight test. Due to the increased altitude, downrange, and velocity of the AA-1 test flight, additional constraints have been placed on the AA-1 trajectory design. The CM, LAS, ATB, and any other objects of significant mass will be tracked as they return to Earth through six-degree-of-freedom (6-DOF) Monte Carlo simulation runs. The debris must remain clear of the White Sands National Monument on the north side and highway 70/82 that runs through the testing area. The AA-1 trajectory has been adjusted to 37° east of north to provide the farthest traveling ATBs a chance to impact to the south of the White Sands National Monument. Figure 1 shows an example of the sequence of events superimposed on the AA-1 nominal trajectory. Figure 2 shows the results from the 6-DOF Monte Carlo simulation of the AA-1 CM trajectory. The work to be performed by the NASA Dryden Flight Research Center (DFRC) (Edwards, California) team involves the generation of the 6-DOF trajectories, analysis of the

various vehicle sensitivities, and validation of simulations and models held by the various organizations involved with the Orion abort flight test.
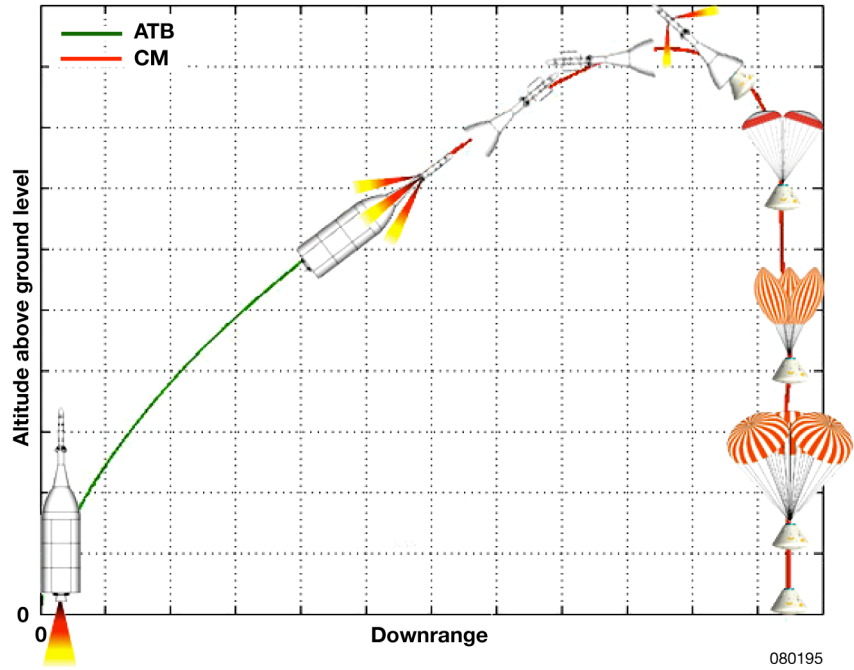


Figure 1. Sequence of events for AA-1 flight test.
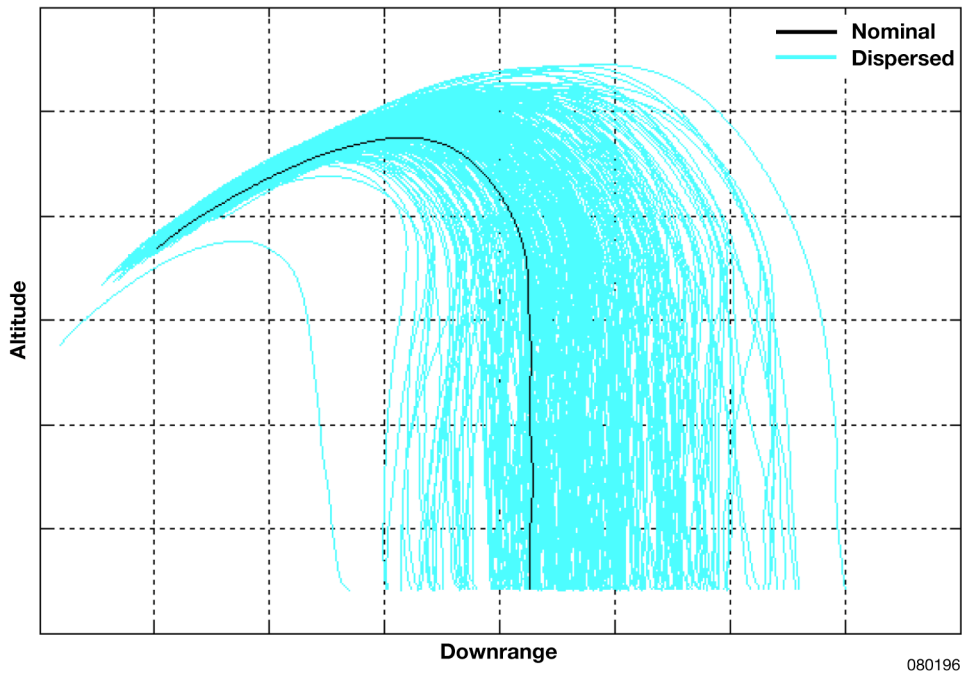


Figure 2. CM trajectories resulting from the 6-DOF Monte Carlo simulation runs of the AA-1 flight test.

**Status**

All of the flight tests are scheduled to occur at WSMR in New Mexico. The initial site selection for AA-1 is near launch complex 32 and is slated to be launched in a 37° east of north direction relative to the launch pad in February 2010. The DFRC team has released the initial 6-DOF trajectories, performed initial sensitivity analysis of the moments of inertia and aerodynamics, and analyzed the effectiveness of the p-Beta controller for roll control.

**Contacts**

Ryan Stillwater, DFRC, Code RC, (661) 276-3591
Peggy Hayes, Flight Test Flight Dynamics lead, DFRC, Code RC, (661) 276-2508
Bob Clarke, Flight Test Office lead engineer, DFRC, Code RC, (661) 276-3799

# SOFIA FLIGHT-TEST FLUTTER PREDICTION METHODOLOGY

## Summary

The Zimmerman flutter prediction method has existed for decades but has not been used at the National Aeronautics and Space Administration (NASA) Dryden Flight Research Center (DFRC) (Edwards, California) for control room envelope expansion. For the Stratospheric Observatory for Infrared Astronomy (SOFIA) flight test program, the Zimmerman method was used for preflight predictions, for postflight comparisons with flutter analysis, and during closed-door envelope expansion flights. The method requires precise modal curve fitting of frequency and damping and at least three test points to make a good prediction. With an inconsistent team of dynamists in the control room for each flight, uniform frequency and damping curve fits were difficult to provide with the constant change in fuel configurations. For this flutter prediction method to work accurately and quickly in the control room, an automated procedure for identifying frequency and damping for particular modes needs to be implemented. The Zimmerman method successfully made postflight comparisons between flight flutter data and the flutter analysis, even with shifts in frequency and damping seen during the flight test, as compared to the finite element model predictions.

## Objective

The Zimmerman flutter prediction method has been shown to work very well for flutter mechanisms consisting of two modes. For the SOFIA aircraft, a modified 747SP (The Boeing Company, Chicago, Illinois) airplane, an attempt was made to pair up modes in a multiple-mode flutter mechanism to determine whether the method was applicable with such mechanisms. For this aircraft, the theoretically predicted wing bending and torsion, nacelle lateral and aft fuselage torsion, and antisymmetric critical flutter mechanism have at least four modes participating.

## Approach

The analytical prediction from MSC Nastran™ (MSC.Software Corporation, Santa Ana, California), and ZAERO™ (ZONA Technology Inc., Scottsdale, Arizona) gave the same flutter results of conditions at sea level, Mach 0.85, and 525 *KEAS*. The SOFIA aircraft has a five-mode flutter mechanism. Mode 1 represents wing first bending antisymmetric; mode 2 represents wing first torsion antisymmetric; mode 3 represents engine nacelles in-phase; mode 4 represents engine nacelles out-of-phase; and mode 5 represents aft fuselage torsion. Ten analytical mode pairs were input into the Zimmerman method for a flutter prediction. Mode pair 1,5 started making predictions at 335 *KEAS* (36-percent flutter margin) and mode pair 2,5 at 402 *KEAS* (24-percent margin), but the majority of pairs made the first prediction at 475 *KEAS* (10-percent margin). Figure 1 shows a summary plot of the 10 mode pairs and their flutter prediction results. The mode pairs that gave conservative results were modes 1,5, modes 2,5, modes 3,5, and modes 4,5.
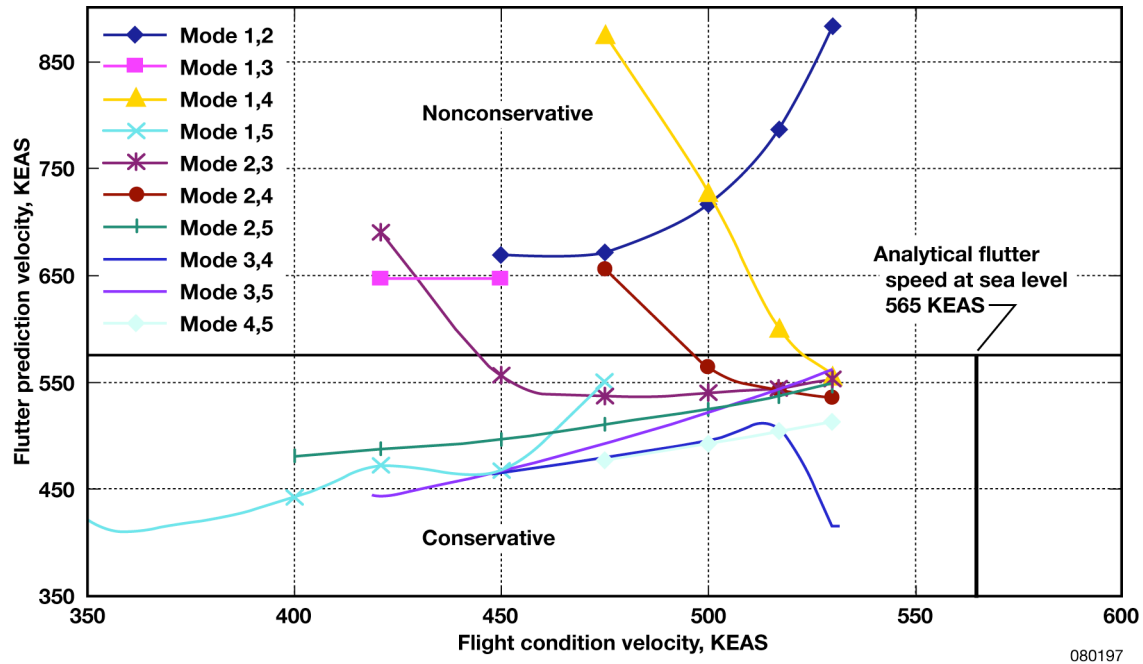
Figure 1. Flutter prediction summary of mode pairs.

The initial plan was to use these four mode pairs in the control room; unfortunately, once the data from the first flight was reviewed, engine nacelle modes 3 and 4 apparently would be impossible to track in real time. The engine nacelle modes are dense (that is, very close together in frequency), noisy, and nonlinear. Frequency and damping of modes 1, 2 and 5 were curve-fit, and modes 1,2, 1,5, and 2,5 were paired. The process took an average of 3 to 4 min to make a flutter prediction once the test point was complete. With varying personnel in the control room curve-fitting the data, the most accurate predictions in real time were unable to be made. Postflight analysis results would correct the real-time predictions. Figure 2 shows the postflight results of curve-fitting the frequency of modes 1, 2, and 5 as compared to the analytical data.
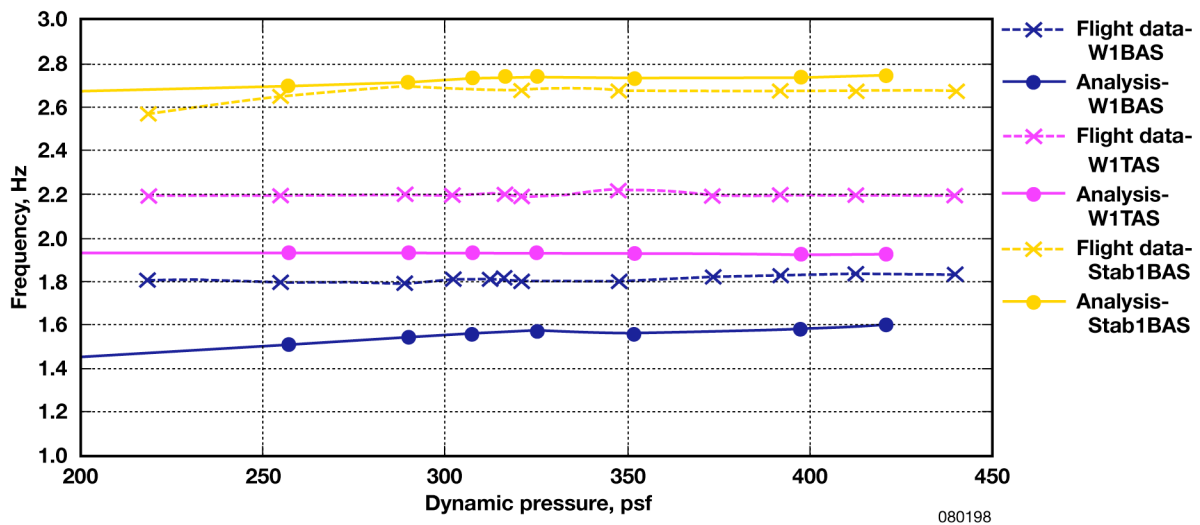


Figure 2. SOFIA Flight 007 frequency comparison with analytical data.

51

The flight conditions used in figure 1 near flutter, which the Zimmerman solution gives the most accurate prediction. The data in figure 2 has flight conditions 44-percent away from the predicted flutter point. At the 400-*KEAS* flight condition shown in figure 1, a limited amount of data points will output a conservative flutter solution. The SOFIA envelope is restricted to 330 *KEAS* at sea level, so identification of a mode pair that would make a conservative and early prediction with few data points was important. Analytically, modes 2,5 gave the best flutter predictions. Using flight test data, modes 1,2 gave the best flutter prediction because the actual airplane shows modes 1 and 2 coalescing closer together than the analytical model. When using the same flight conditions analytically and for flight test, the Zimmerman method gives a 7-percent decrease in flutter speed because the actual airplane has lower frequencies and lower damping.

## Status

No current plans exist to implement an automated curve-fitting routine for the control room. The Zimmerman method will be used during postflight analysis to compare flight test data with the analytical model and real-time predictions with more control room training.

## Contact

Starr Ginn, DFRC, Code RS, (661) 276-3434

# SOFIA CLOSED-DOOR AERODYNAMIC ANALYSES

## Summary

The Stratospheric Observatory for Infrared Astronomy (SOFIA) aircraft, a modified 747SP (The Boeing Company, Chicago, Illinois) airplane, conducted a series of flight tests in the closed-door configuration. One of the primary goals during these flights was to determine the aerodynamic characteristics of the aircraft in this configuration. Several different facets of the aerodynamic characteristics of the SOFIA aircraft were explored, including flying qualities, airflow around the modified portion, performance of the flush airdata sensing (FADS) system, and accuracy of the production pitot-static system.

## Objective

The objective of these flight tests is to determine the aerodynamic characteristics of the SOFIA aircraft in the closed-door configuration.

## Approach

Various approaches were used to accomplish the diverse aerodynamic goals for the closed-door segment of SOFIA testing. Standard parameter estimation techniques were used to evaluate the flying qualities of the aircraft. Tufting was used to characterize the airflow around the modified portion of the aircraft. A FADS system was designed and incorporated into the existing flush port system that was previously used for determination of angle of attack and angle of sideslip. This system was calibrated using standard calibration maneuvers, such as push-over/pull-ups (POPU) and rudder sweeps. Due to the age of the aircraft and the modifications made, the accuracy of the pitot-static system required verification. This verification was done using tower flyby and acceleration-deceleration maneuvers.

Parameter estimation results indicate that the flying qualities of the vehicle have not been significantly changed from a baseline 747SP airplane. Analysis of tufting video has allowed for a general characterization of the flow around the modified area of the aircraft. This data will serve as baseline data for comparison with tufting video and pressure data from open-door flights. The FADS system was used effectively throughout the flight tests. The system was calibrated to within accuracies of approximately ±0.5° for the majority of the flight envelope. The production pitot-static system in the airplane was determined to be sufficiently accurate for flight-testing purposes to within an accuracy of ±0.005 Mach.

## Status

The SOFIA segment 1 closed-door flight tests have been completed. Various aerodynamic data from these flights are currently being analyzed.

## Contacts

Stephen Cumming, DFRC, Code RA, (661) 275-3732
Mike Frederick, DFRC, Code RA, (661) 276-2274
Mark Smith, DFRC, Code RA, (661) 276-3177
David Booth, DFRC, Code RA, (661) 276-3734

# SOFIA HANDLING QUALITIES EVALUATION FOR CLOSED-DOOR OPERATIONS

## Summary

The Stratospheric Observatory for Infrared Astronomy (SOFIA) mission objective is to provide a safe and robust platform on which a wide variety of infrared science instruments can be flown in an attempt to gain a greater understanding of the Universe. The platform is a highly modified Boeing 747SP (The Boeing Company, Chicago, Illinois) airplane with a 2.5-m telescope in the aft section. The installation of this telescope required the removal of a large (approximately 90°) portion of the fuselage above the telescope, installation of a movable door over the opening, installation of a new pressure bulkhead just in front of this open port cavity, and a rerouting of the empennage control cables. The magnitude of this modification forced extensive verification of the handling qualities of the SOFIA aircraft. The nature of the input response (large amplitude control inputs required to generate measurable airplane response) of the 747SP airplane, and the desire to test as efficiently as possible, has made it impractical to analyze the traditional frequency-domain low-order equivalent systems (LOES) from frequency sweep-type pilot inputs. As a result, a novel time-domain nonlinear least-squares technique was utilized to examine the handling qualities. Additionally, the response of the vehicle to large disturbances from trim needed to be reevaluated. Despite the magnitude and complexity of the airplane modification, the SOFIA aircraft has not been shown to behave differently in any substantial ways from the unmodified airplane in either a dynamic or static sense, and is therefore considered cleared throughout the closed-door envelope.

## Objective

The primary objective of this work is to support the development of the SOFIA platform from a flight controls and handling qualities standpoint and to ensure that the laboratory is both safe and capable of fulfilling more than 20 years of science missions. An important component of the plan that will ensure the operability of this observatory throughout its operational envelope is to determine the input response and stability characteristics of the vehicle.

## Approach

The basic approach to show that the modified SOFIA airframe does not have objectionable handling qualities is to determine both the dynamic responses of the aircraft near trim and the degree of linearity of the aircraft response in regimes far from trim. The near-trim dynamic responses have been analyzed using time-domain LOES. A more qualitative approach was utilized to evaluate aircraft behavior far from trim with guidance taken from the Flight Aviation Rules (FAR) part 25 requirements. These qualitative metrics included pilot comments; evaluation of the linearity of the longitudinal stick force verses normal acceleration, and rudder pedal displacement verses sideslip angle curves; and the speed stability of the vehicle to large slow disturbances from trim.

### Qualitative Evaluation of Aircraft Behavior Far from Trim

The guidance for qualitative evaluation of the aircraft flight characteristics out of trim was taken from the FAR part 25 regulations for commercial jet airliners. These regulations basically state that the response of the airplane should be substantially linear in pitch, but that a moderate amount of stick force lightening is tolerable and expected in some portions of the flight envelope for swept-wing aircraft, as long as no control reversals are observed and sufficient deterrent buffet exists prior to substantial lightening. In the directional axis the response should be mostly linear, but stiffening is allowable and often desirable near the pedal limit. Examples of behavior in both the pitch and yaw axes is clearly shown in figure 1. The lateral response of the aircraft is substantially linear with stiffening near the ends throughout the operational envelope. The pitch

response, however, does exhibit some mild lightening (decreasing slope of the stick force versus normal acceleration trace) at low dynamic pressure after the onset of aircraft buffet.
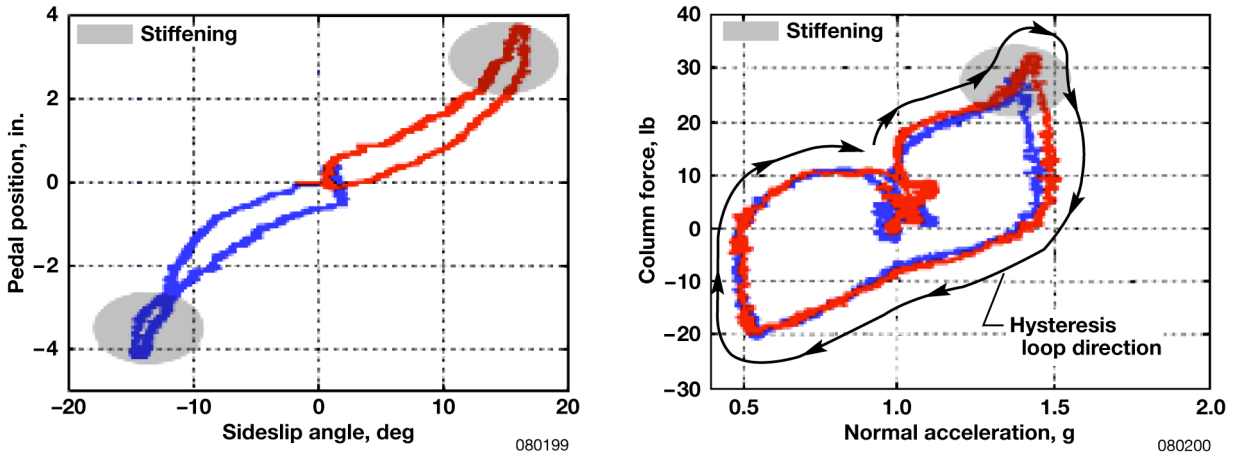


(a). Rudder pedal response.  (b). Column response.

Figure 1. Aircraft response far from trim.

## LOES Analysis for Behavior Near Trim

The time-domain LOES algorithm developed and employed for handling qualities metric evaluation uses a nonlinear least-squares technique to minimize the root mean square (RMS) error between the simulated response and the actual measured vehicle response. Figure 2 shows the fit characteristics for the time-domain method and a more traditional frequency-domain method. Figure 3 is a graphical representation of how the SOFIA handling qualities, as determined by the LOES analysis for the short period mode, align with the MIL-STD-1797B metrics. Figure 3 clearly shows that the natural frequency and control anticipation parameter are within the level 1 for the operational envelope; however, some of the time delay and n/α numbers are between the level 1 and level 2 boundaries. The short period damping values were all level 1. An important note is that almost all of the other LOES-determined parameters for all of the other modes (Dutch roll, spiral, roll, phugoid) are within the level 1 region, and none are outside of the level 2 boundary.
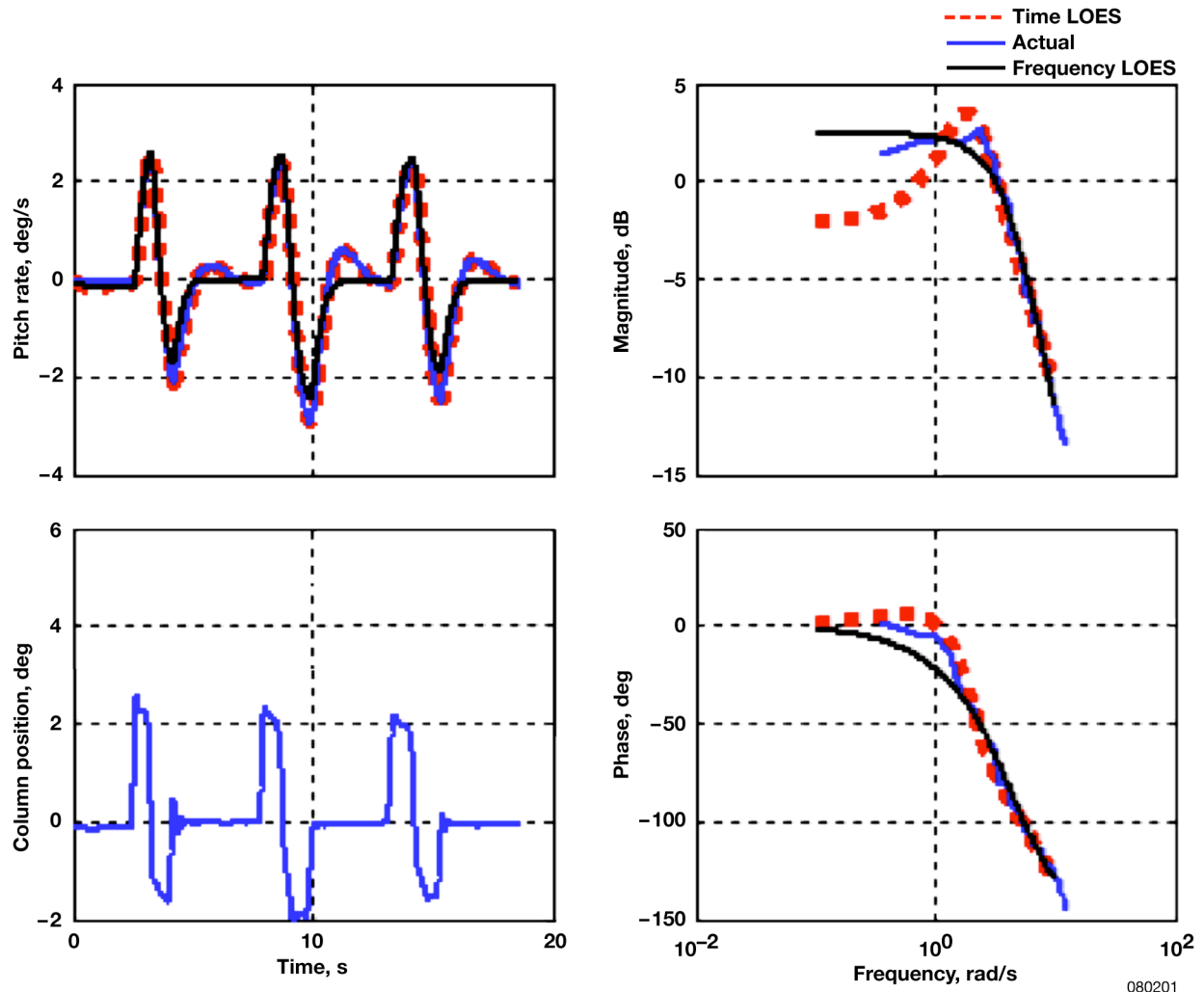
Figure 2. LOES comparison for SOFIA short-period mode.
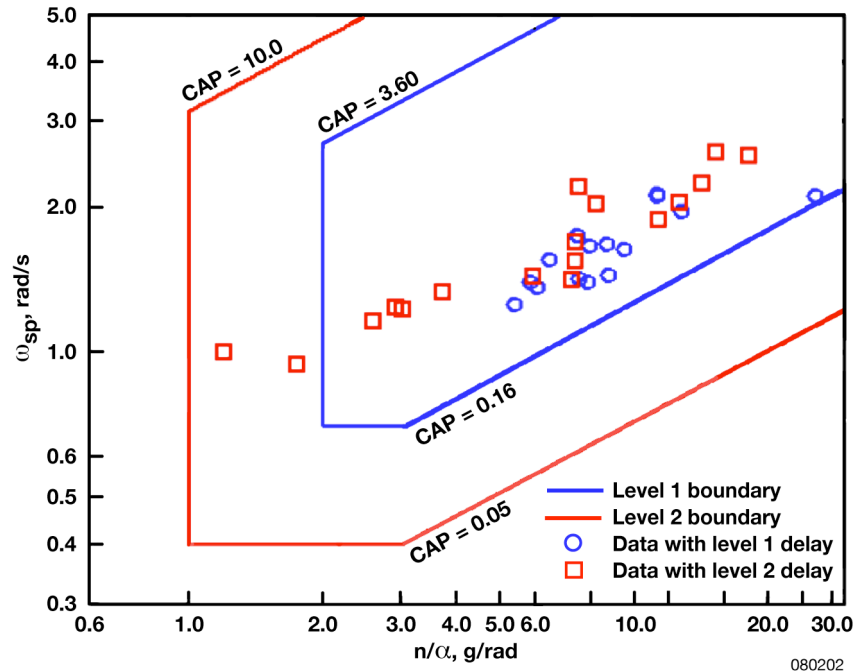
Figure 3. Short-period handling qualities.

**Status**

The envelope expansion and recertification for the closed-door envelope for the SOFIA platform is nearly complete. All that remains from a flight controls perspective is the engine-out minimum control speed testing. The aircraft has been shown to have damping and natural frequency numbers for the Dutch-roll and short-period modes in the level 1 or 2 handling qualities zones from MIL-STD-1797B, and these modes have not been shown to have been affected by the SOFIA modification. The roll mode has also not been affected by the modification. The spiral and phugoid modes both appear to be stable and have been shown to be well within acceptable tolerances. Demonstrations have shown that the aircraft substantially responds linearly to increasing column and pedal inputs, and that the aircraft does not have unacceptable pitch-up tendencies anywhere in the flight envelope. Demonstrations have also shown that the modification has not reduced the allowable crosswind landing limits of the airframe. Handling qualities evaluations for operations with the cavity door open are planned for the upcoming year and will be performed in a similar manner to those presented in this report, but with many more data points.

**Contact**

Christopher J. Miller, DFRC, Code RC, (661) 276-2902

# C-17 SUPPORT OF IRAC ENGINE MODEL DEVELOPMENT

## Summary

Pratt & Whitney (P&W) (East Hartford, Connecticut) and the National Aeronautics and Space Administration (NASA) Dryden Flight Research Center (DFRC) (Edwards, California) collaborated on a series of engine data collection flights in June and December 2007. An engine was highly instrumented, and data from both the aircraft and engine were collected using the NASA-developed onboard computer rack. Customized cockpit displays were created to facilitate the pilots and flight test engineer performing the precision test objectives. A total of three flights were flown on the Boeing C-17 Globemaster III T-1 (The Boeing Company, Chicago, Illinois) aircraft operated by the U.S. Air Force at Edwards Air Force Base, California, to successfully meet all flight milestones for this project. Ultimately, the data are used by P&W to help NASA Glenn Research Center (GRC) (Cleveland, Ohio) develop engine models.

## Objective

The objective of these flights was to collect flight test data to assist in the modeling of engine dynamics and engine calibration as part of the Damaged Aircraft Good Engine (DAGE) project of the Integrated Resilient Aircraft Control (IRAC) program.

## Approach

The data to be collected was primarily the compressor flow, temperatures, and pressures at the inlet and exhaust of the high-pressure compressor (HPC) section of the engine. Data collection was accomplished by the use of existing and new engine sensors including flow meters, pressure probes, and temperature probes (fig. 1). The design and installation of the sensors were accomplished through collaboration between P&W and DFRC. Engine and aircraft data were recorded and displayed in real time using the DFRC-developed data rack, which served as a flying control room. The DFRC and P&W flight test engineers observed the data integrity and quality to ensure all test points were met.
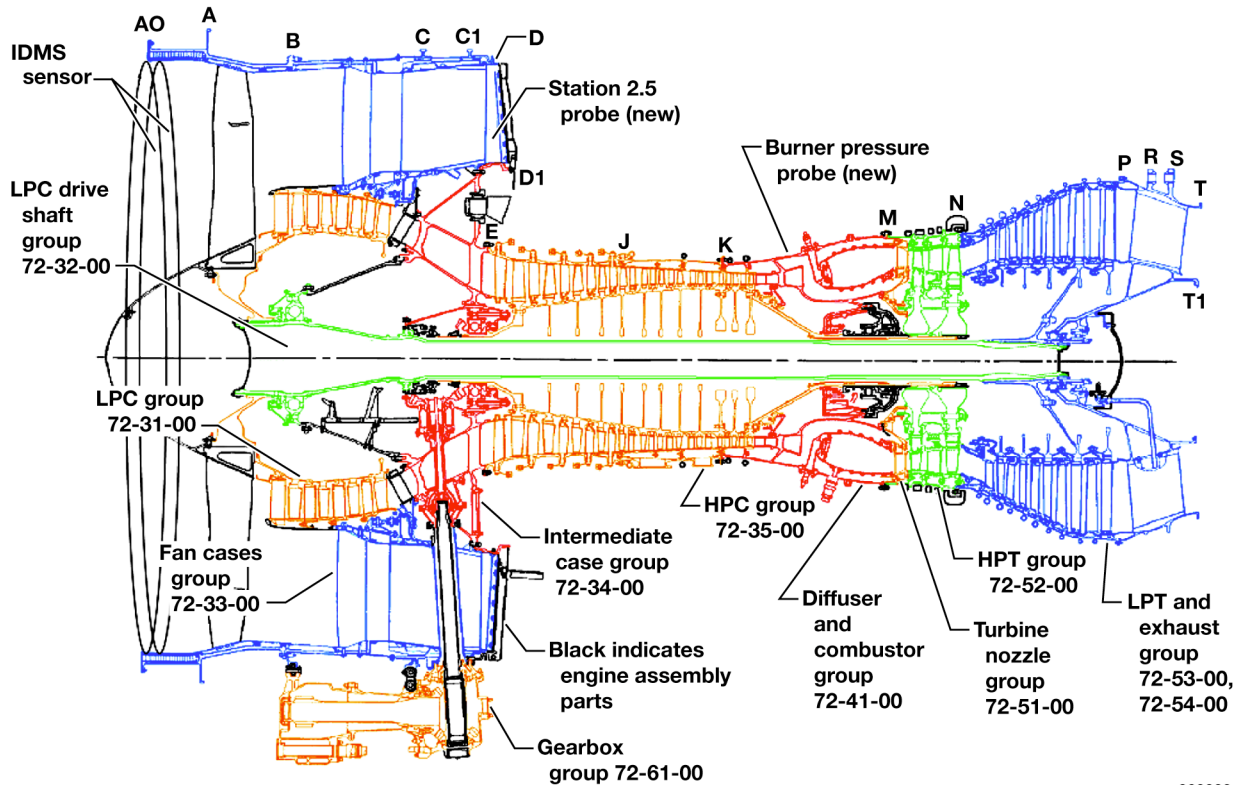
Figure 1. Gas path sensors.

Because of the precise nature of the engine throttle transients required for this program, special cockpit display screens were created to assist pilots. These transients include both snap throttle movements and steady ramps, as shown in figure 2. To maintain airspeed and altitude, a highly coordinated balancing of all engine throttles was required. The pilot displays were a tremendous asset both in training at the DFRC C-17 simulator and in flight. An example pilot display is shown in figure 3. The coordination of the flight test engineers using similar rack displays and the pilot displays enabled a rapid completion of flight test points. It also served as the first line to catch sensor failures. Two such failures occurred in flight and were first recognized on the rack.
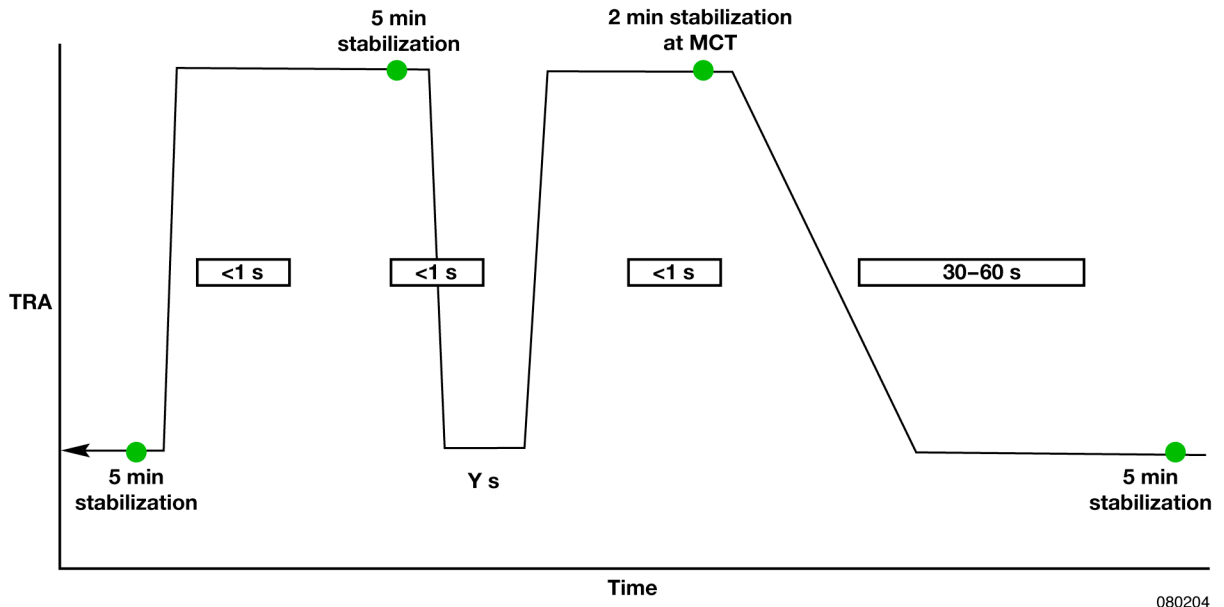
Figure 2. Transient maneuvers profile with engine 3.



Figure 3. Pilot display for calibration and thrust transient maneuvers.

## Status

The summation of all three flights resulted in capturing the required test points, as shown in table 1. Ongoing DFRC support with data reduction is being provided to P&W, and DFRC is collaborating with GRC on future engine models.

Table 1. Altitude test matrix.

| Flight condition (altitude/speed) | Test point description |
|---|---|
| 15,000 ft/Mach 0.45 | Performance calibration |
| 15,000 ft/Mach 0.45 | Transient engine bodies |
| 15,000 ft/< Mach 0.36 | Transient engine bodies |
| 10,000 ft/Mach 0.45 | Transient engine bodies |
| 10,000 ft/< Mach 0.36 | Transient engine bodies |
| 20,000 ft/Mach 0.50 | Transient engine bodies |
| 20,000 ft/< Mach 0.41 | Transient engine bodies |
| 25,000 ft/Mach 0.45 | Transient engine bodies |
| 30,000 ft/Mach 0.65 | Transient engine bodies |
| 35,000 ft/< Mach 0.70 | Performance calibration |
| 35,000 ft/< Mach 0.70 | Transient engine bodies |

**Contacts**

Ross Hathaway, DFRC, Code RA, (661) 276-3618
Mike Venti, DFRC, TYBRIN Corporation, Code RA, (661) 276-2513
Dave Berger, DFRC, Code RA, (661) 276-5712

# CURRENT CAPABILITIES AND FUTURE UPGRADE PLANS OF THE C-17 DATA RACK

## Summary

The data rack was developed for data collection and as an airborne control room for the Boeing C-17 Globemaster III T-1 (The Boeing Company, Chicago, Illinois) aircraft. The rack was recently used to support propulsion research in both Integrated Vehicle Health Management (IVHM) and Integrated Resilient Aircraft Control (IRAC).

## Objectives

The data rack provides an onboard data recording and display capability and is used as a mission control center for the National Aeronautics and Space Administration (NASA) flights onboard the C-17 T-1 aircraft.

## Approach

The major components of the data rack are a Systel, Inc. (Atlanta, Georgia) rack-mounted PC, a Wyle Electronics (Irvine, California) Series-3000/OMEGA™ rack-mounted PC/Decommuter, and a Metrum Technologies, LLC (Waco, Texas) tape recorder. Figure 1 shows the rack, and figure 2 shows the rack as installed in the C-17 T-1 aircraft during the 2007 IRAC flights.
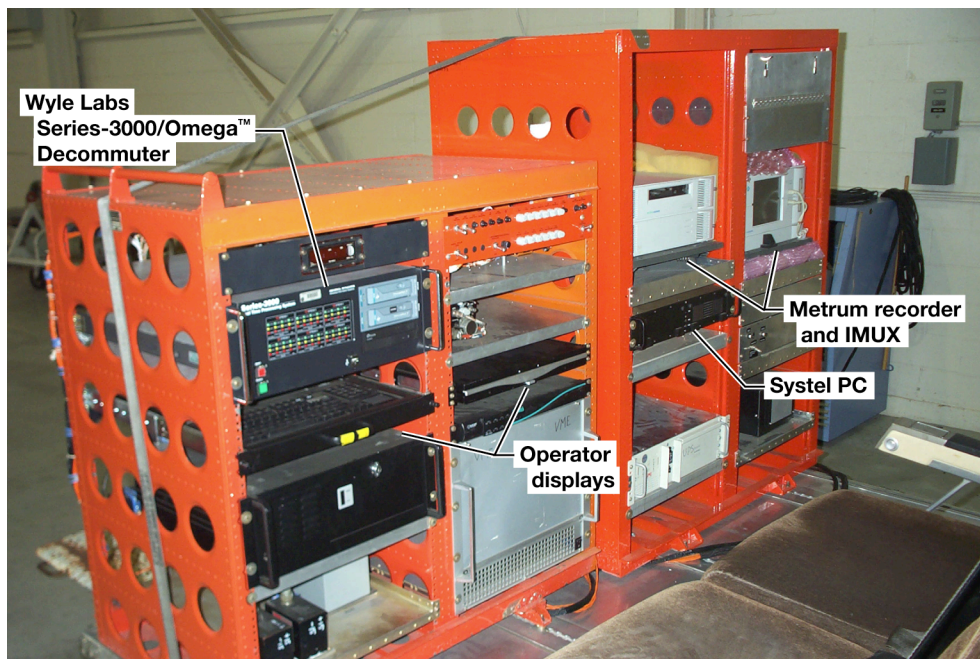


Figure 1. C-17 data rack.

080207

Figure 2. Data rack installed in the C-17 T-1 aircraft.

Data from NASA-installed sensors are sent to the rack as pulse code modulation (PCM), and aircraft bus data are available in the rack. Both data streams can be recorded on the PC systems; additionally, PCM is recorded on the Metrum recorder, and bus data is recorded on a U.S. Air Force intelligent multiplexer (IMUX) system from Wyle Electronics. A block diagram of the instrumentation is shown in figure 3. Displays can be created in the OMEGA™ environment and used similar to the interactive display system and project data system displays used in the Dryden Flight Research Center (DFRC) (Edwards, California) control room.

The rack provides two workstations, and additional flight test engineers can be accommodated with laptops in the side jump seats. A laptop can also be placed in the cockpit as a pilot display, as was used in the 2007 IRAC flights.
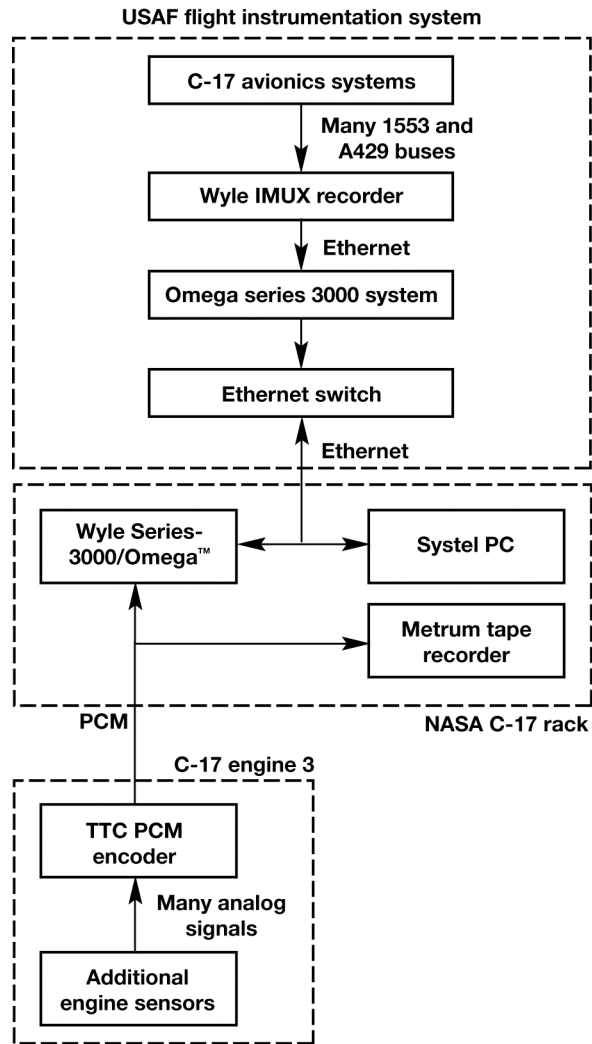
Figure 3. Data system block diagram.

## Status

The IRAC flights were completed, and the data were sent to Pratt & Whitney (East Hartford, Connecticut). Current rack work includes software development to allow advanced models and prognostic algorithms to be ran in real time onboard the C-17 aircraft. The DFRC IVHM team considers this upgrade to be an enabling technology to assist in advancing prognostics development.

## Contributors

Tony Branco, DFRC, RI, (661) 276-3195, Antonio.E.Branco@nasa.gov
Mike Delaney, DFRC, RI, (661) 276-6059, Michael.M.Delaney@nasa.gov
Mike Venti, DFRC, TYBRIN Corporation, RA, (661) 276-2513, Mike.W.Venti@nasa.gov
Glenn Sakamoto, DFRC, RI, (661) 276-3679, Glenn.M.Sakamoto@nasa.gov

## Contact

Mike Delaney, DFRC, RI, (661) 276-6059, Michael.M.Delaney@nasa.gov

# INTELLIGENT DATA MINING CAPABILITIES AS APPLIED TO INTEGRATED VEHICLE HEALTH MANAGEMENT

## Summary

Intelligent data mining is one of the grand challenges as outlined by the National Aeronautics and Space Administration (NASA) Aeronautics Research Mission Directorate (ARMD) Aviation Safety Program and represents an enabling technology for Integrated Vehicle Health Management (IVHM). Recently, in support of NASA C-17 (The Boeing Company, Chicago, Illinois) IVHM, the ARMD funded a commercial-off-the-shelf (COTS)-developed intelligent data mining toolset called OMEGA™ Data Environment (ODE) (Wyle Electronics, Irvine, California) for the NASA Dryden Flight Research Center (DFRC) (Edwards, California) C-17 IVHM project. During the recent NASA C-17 Integrated Resilient Aircraft Control (IRAC) Damaged Aircraft Good Engine (DAGE) engine performance test, this COTS toolset, through its publishing and mining capability, was successfully deployed to support the postflight analysis as a prognostic and diagnostic tool for an engine sensor discrepancy evidence during the flight mission. The toolset afforded a quick-look root cause analysis for this sensor discrepancy and mitigated the long lead times associated with heritage postflight data processing and analysis techniques.

## Objective

The objective of this flight research effort in support of C-17 IVHM is to demonstrate the applicability of this COTS intelligent data mining toolset as follows:

- To provide secure mining and exploitation of large datasets derived from flight data
- To demonstrate real-time publishing capability towards verification and validation of experimental data with embedded systems modeling
- To demonstrate both the prognostic and diagnostic evidence gathering capability with the "stat-pack" technology of the toolset
- To support the development of the IVHM Intelligent Data Mining Laboratory by providing flight-derived research-quality data.

## Approach

For this initial research phase, the approach was to apply the publishing tool to the datasets as a postflight data processing task. The datasets, one set consisting of aircraft avionic bus and states, and the other engine-mounted sensor data, were acquired with the NASA C-17 instrumentation data system rack, herein called the rack. Both datasets, which were recorded on the storage equipment of the rack, were offloaded onto portable storage media that was easily connected to an equivalent ground-based system for postprocessing, data warehousing, and distribution. The postprocessing equipment, a standard ground station running the identical airborne processing software and project setup, was enhanced with the ODE intelligent data mining toolset.

## Results

The ODE toolset became the prime diagnostic tool to perform the root cause analysis for the sensor discrepancy observed during the flight monitoring on the rack. Once the publishing tool was applied to the dataset (that is, creating XML metadata for the dataset), the desktop visualization viewer provided the rendering of the metadata. From the rendered metadata on a time basis, the viewer provided easy selection of time segments for view in real time, for correlation, and for data product creation for follow-on analysis. Figure 1 shows approximately 1 hour of published and visually rendered metadata for which each bar represents 1 percent of the total rendered time, in this case approximately 0.6 min. Figure 2 shows a time history of

sample data for a selected time segment identified as an event. Created data products as comma separated values (CSV) and MATLAB® (The MathWorks, Natick, Massachusetts) can be extracted from data products utility.
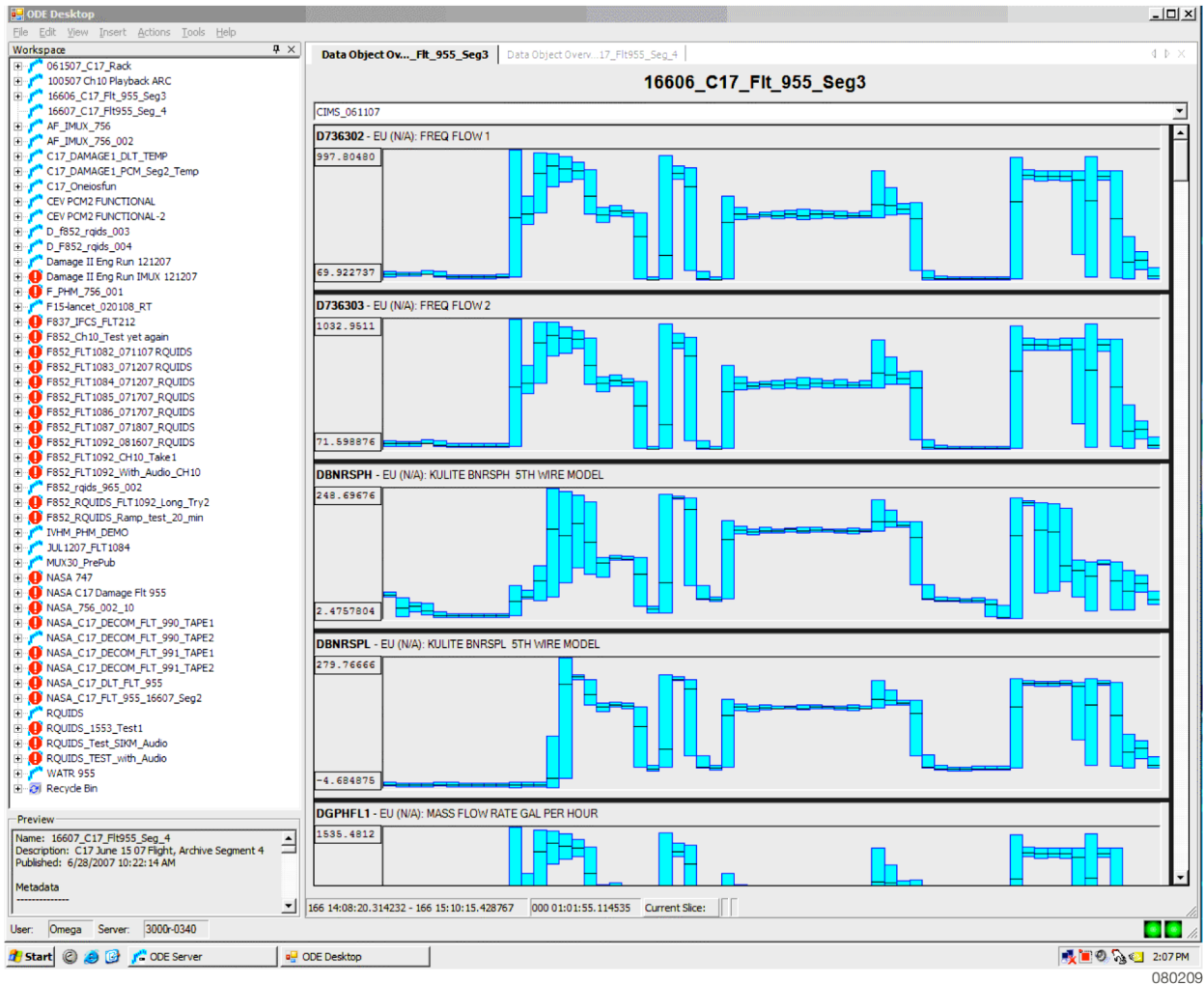


Figure 1. ODE desktop visualization metadata of flight 995 for burner probe root cause analysis.
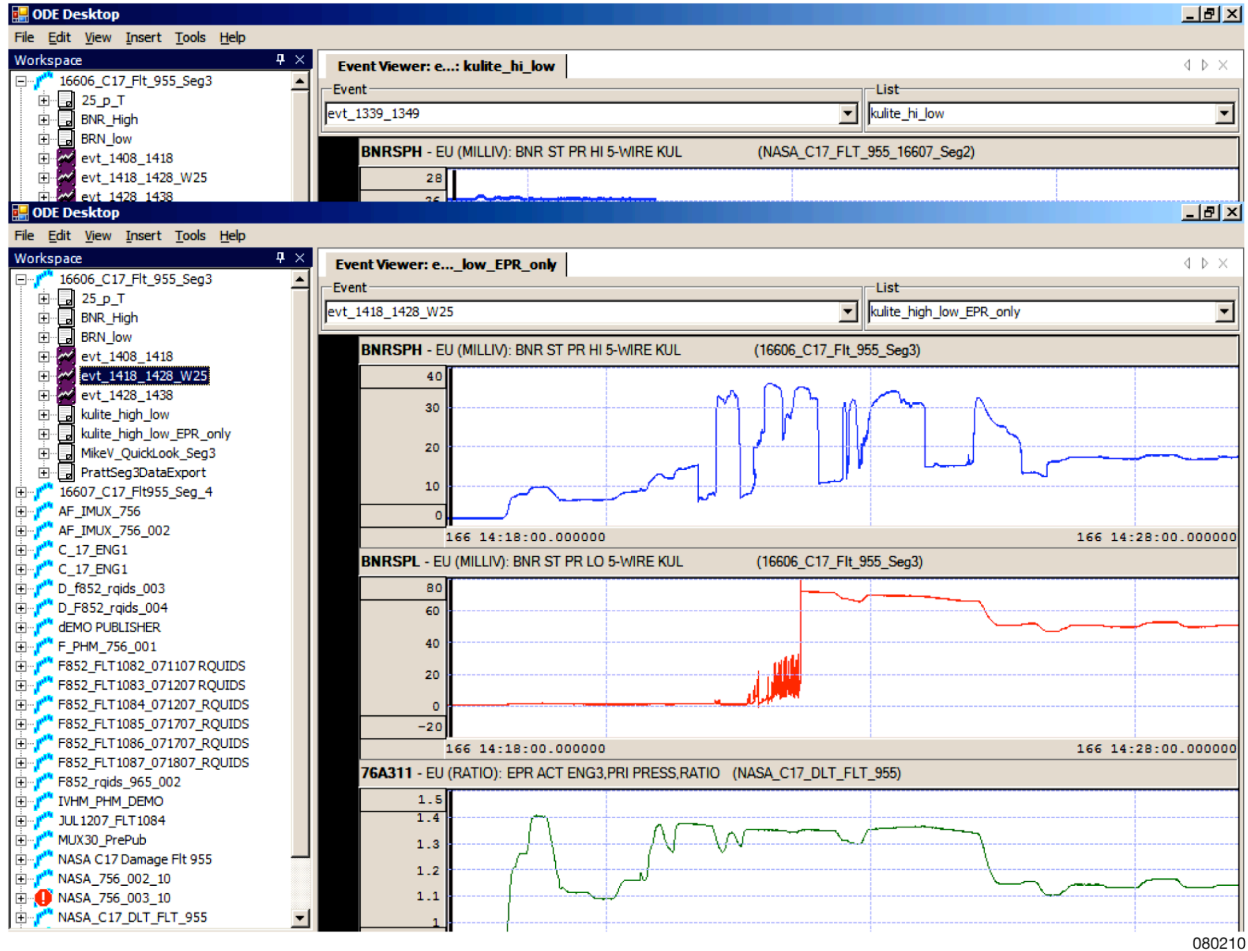
Figure 2. Selected metadata time segment and sensor data in real time.

## Status

The ODE publishing and visual mining capability was successfully demonstrated on the C-17 IRAC DAGE dataset during the initial postflight data processing by performing a diagnostic and root cause analysis of the sensor discrepancy. The ODE, as applied to other DFRC research testbeds, showed that the tools promise as a mining and analysis tool. The query capability of the ODE is still being investigated. Additionally, ODE has been shown to work with a newly emerging, self-describing recording format called Chapter 10.

Work is in progress to support the NASA Ames Research Center (Moffett Field, California) IVHM Intelligent Data Mining Laboratory with the flight-derived dataset from this IVHM testbed.

## Contributors

Mike Delaney, DFRC, RI, (661) 276-6059, Michael.M.Delaney@nasa.gov
Mike Venti, DFRC, TYBRIN Corporation, RA, (661) 276-2513, Mike.W.Venti@nasa.gov
Dave Berger, DFRC, RA, (661) 276-5712, Dave.A.Berger@nasa.gov
Ross Hathaway, DFRC, RA, (661) 276-3618, Ross.W.Hathaway@nasa.gov
Chris R. Miller, DFRC, PA, (661) 276-2482, Chris.R.Miller@nasa.gov

## Contact

Glenn Sakamoto, DFRC, RI, (661) 276-3679, Glenn.M.Sakamoto@nasa.gov

# STARS FLIGHT DEMONSTRATION #2 IP DATA FORMATTER

## Summary

An airborne system was developed for the Space-Based Telemetry and Range Safety (STARS) flight demonstration #2 flights that could provide a network data path to the control room for both network-ready and legacy instrumentation subsystems. The Internet protocol (IP) data formatter was successfully used to transfer onboard data through the Range User phased-array antenna satellite downlink during each flight.

## Objectives

The four main objectives for the IP data formatter are as follows:

1. Format pulse code modulation (PCM) data from legacy equipment into user datagram protocol (UDP) packets for telemetry.
2. Forward UDP packets from network-ready systems for telemetry.
3. Time-stamp each PCM minor frame and UDP packet with inter-range instrumentation group B (IRIG-B).
4. Record the time-stamped PCM and UDP data.

## Approach

The NetAcquire® Corporation (Kirkland, Washington) was chosen to develop a ruggedized PC/104-based system as the IP data formatter (fig. 1). The system contained four high-speed synchronous/asynchronous RS-422 ports, four 10/100-Mbps Ethernet ports, an IRIG-B input, and a 4-GB solid-state hard drive. The system was capable of being programmed to input data from any source, decommutate, perform calculations, time-stamp, reformat, record, and output the data. For development and preflight operation, a web server on the IP data formatter allowed a user with a laptop and a web browser to monitor status, reconfigure, reprogram, and manage data recordings via an Ethernet connection. Figure 2 shows the web browser interface for programming the system by allowing a user to simply choose from predefined blocks with customizable parameters.



Figure 1. IP formatter.
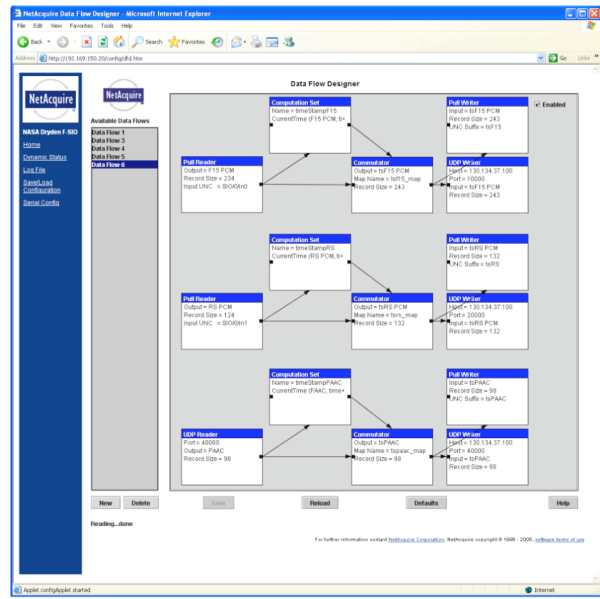
080212

Figure 2. IP formatter web interface.

For the STARS application, the system was programmed to receive a 1-Mbps PCM stream, a 10-Kbps PCM stream, and a 100-Kbps UDP stream. Each stream was time-stamped before being recorded and output as UDP packets with unique destination port numbers. Prior to being telemetered, the network data was formatted according to the high-level data link control (HDLC) standard using equipment developed and flight tested by the High-Rate Wireless Airborne Network Demonstration (HiWAND) project. A lab version of the IP data formatter was used in the Telemetry and Radar Acquisition Processing System (TRAPS) to time-stamp each packet and forward them to multiple destinations. The time stamps allow for measuring latency on a packet-by-packet basis in real time. One destination of the UDP data was the Flexible Acquisition Processing System (FLAPS) in TRAPS. The FLAPS was modified to accept, decommutate, and distribute UDP data to project application graphics executable (PAGE) displays in the control room. Another destination of the UDP data was a laptop. The laptop was programmed using Microsoft® (Microsoft Corporation, Redmond, Washington) Visual Basic® 2005 to accept the UDP data, decommutate and display parameters, perform calculations, determine packet latency and loss, and record and play back the raw data. One additional feature programmed for the laptop was a Google Earth™ (Google, Inc., Mountain View, California) interface. This interface provided a real-time update of the position and attitude of a three-dimensional model of the NASA NF-15B (McDonnell Douglas Corporation, St. Louis, Missouri, now The Boeing Company, Chicago, Illinois) research aircraft, tail number 837, over terrain. A screenshot of this display is shown in figure 3. The interface also allowed the user to control the heading, tilt, and range of the camera view to get a perspective from a chase plane.
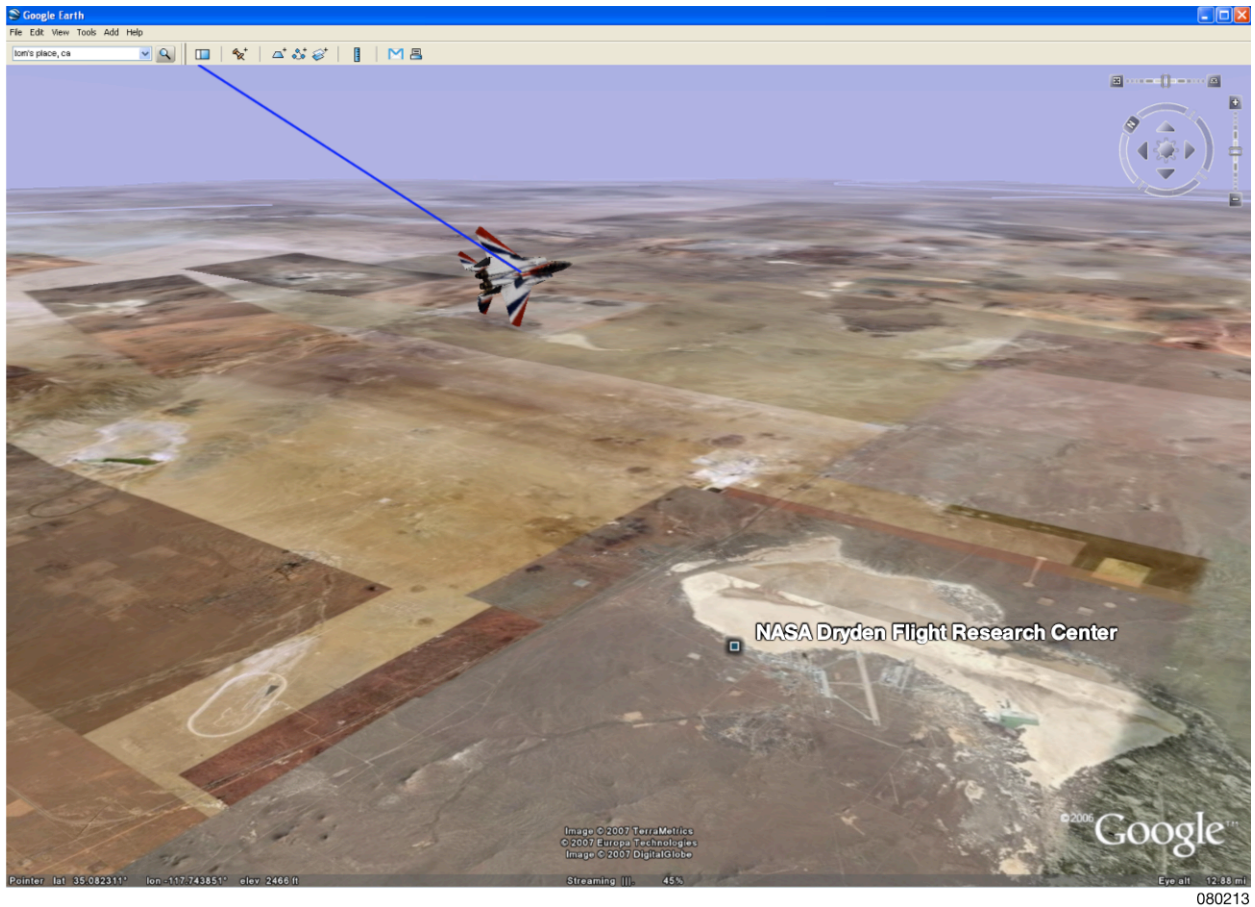
69

Figure 3. Network data-driven three-dimensional display.

**Status**

The STARS flight demonstration #2 has been successfully completed, and a second system with more features was purchased by the Ikhana (General Atomics Aeronautical Systems, Inc., San Diego, California) project.

**Contact**

Russ Franz, DFRC, Code RI, (661) 276-2022

# SPACE-BASED TELEMETRY AND RANGE SAFETY (STARS) FLIGHT DEMONSTRATION #2 RANGE USER FLIGHT TEST RESULTS

## Summary

A Ku-band phased-array antenna system was installed and flight tested on the National Aeronautics and Space Administration (NASA) NF-15B (McDonnell Douglas Corporation, St. Louis, Missouri, now The Boeing Company, Chicago, Illinois) research aircraft, tail number 837, to provide a high bit-rate video and data downlink through the Tracking and Data Relay Satellite System (TDRSS). Flight test results for this system are presented.

## Objectives

There were two main objectives for the Range User antenna system:

1. Increase the maximum downlink bit-rate from 500 Kbps during flight demonstration #1 to at least 5 Mbps.
2. Maintain a minimum link margin of 3 dB for antenna pointing elevations greater than 30°.

## Approach

The phased-array antenna was hybrid, such that the azimuth control was mechanical and the elevation control was electronic. The azimuth steering was therefore limited in angular velocity and acceleration, whereas the elevation steering was only limited by the maximum command rate of 100 Hz. Because the elevation was controlled electronically through phase shifters, the radiated beam became distorted and the peak gain dropped off steeply below elevations of 30°. Flight test maneuvers included both low- and high-dynamic periods intended to test the antenna within and beyond the designed performance.

## Results

Figure 1 shows the results of four flights conducted that were configured for a bit-rate of 5 Mbps. Although dedicated maneuvers were performed throughout the flights, link margin is plotted versus the commanded elevation over the entire time from prior to takeoff until after landing. Link margin was calculated from measured bit errors, and zero bit errors corresponded to a link margin of 9.3 dB. One horizontal line (at a value of 3 dB link margin) and one vertical line (at a value of 30° commanded elevation) separate the plot into four distinct quadrants. The upper-left and upper-right quadrants correspond to points meeting and exceeding the second stated objective. The lower-right quadrant defines points when the commanded elevation was greater than 30° but the link margin was below 3 dB. With the exception of four points, possibly due to blockage by the vertical tail or chase aircraft, all points within the lower-right quadrant were caused by either the TDRSS satellite passing through the antenna zenith or the aircraft intentionally performing dynamic maneuvers.
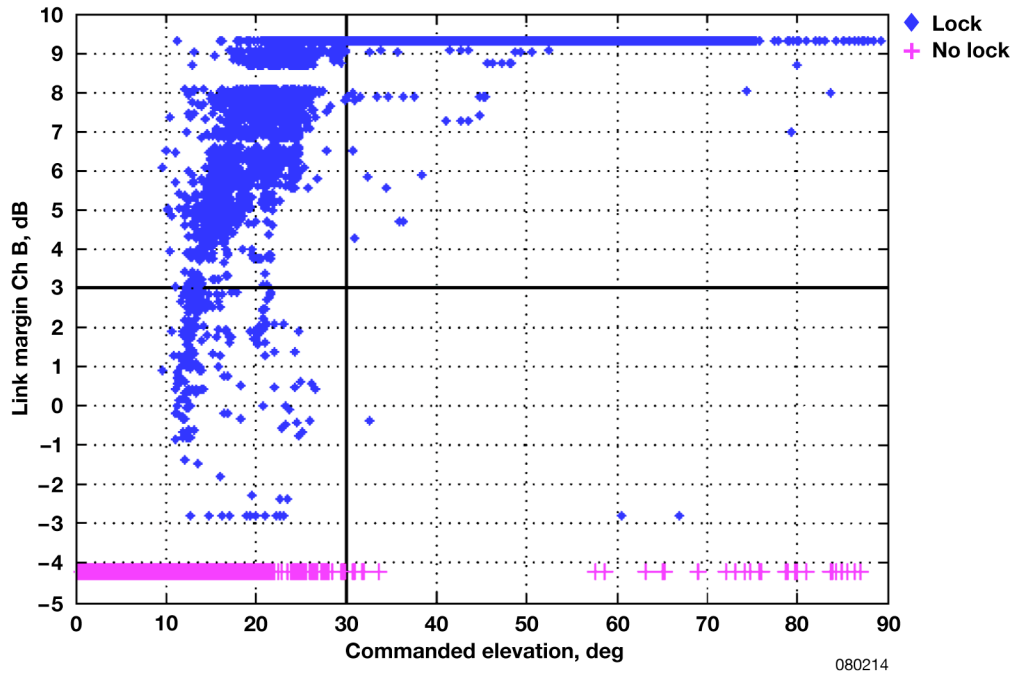
Figure 1. Link margin for 5-Mbps Range User flights.

A similar plot was generated for two 10-Mbps bit-rate flights and is shown in figure 2.
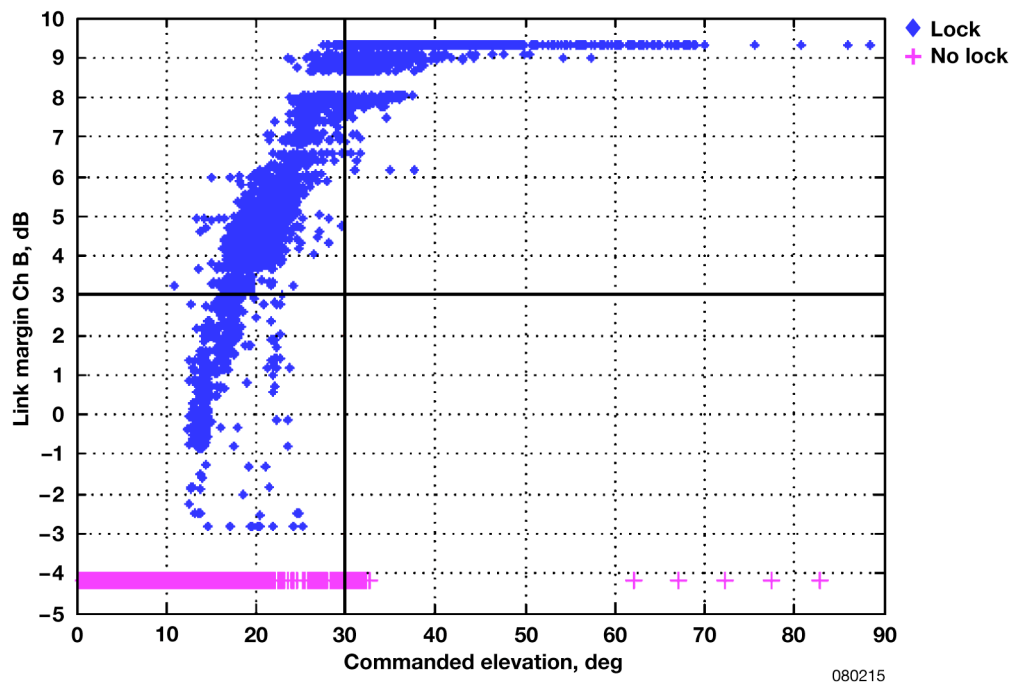


Figure 2. Link margin for 10-Mbps Range User flights.

Figure 3 is a three-dimensional representation of the antenna pointing vectors projected to the surface of a unit sphere. Each pointing vector was color-coded according to the associated link margin. Because of the mechanical control of the antenna azimuth, whenever the TDRSS

satellite passed through the antenna zenith, a momentary loss of signal occurred as the antenna slewed at maximum performance. Figure 4 shows a frame of the video that was digitized, compressed, and transmitted through the phased-array antenna. This particular video frame was taken during a 70°-bank maneuver. The video was time-stamped both on the aircraft and in the Telemetry and Radar Acquisition Processing System (TRAPS). Comparison of these time stamps agrees well with time stamps in the data and results in an overall latency of 300 msec.



080216
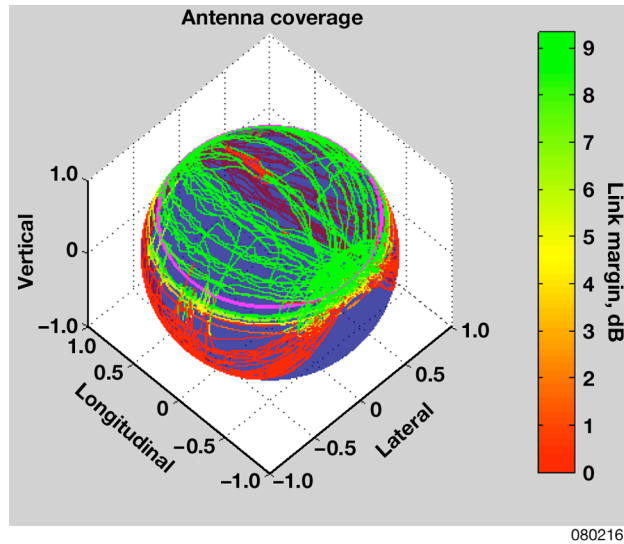
Figure 3. Antenna coverage.



080217
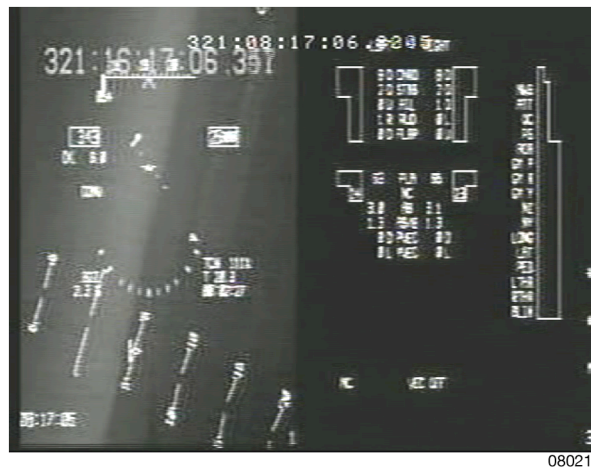
Figure 4. Cockpit video frame during 70° bank.

## Status

A NASA Technical Memorandum is currently being generated to document the flight test results in more detail.

## Contact

Russ Franz, DFRC, Code RI, (661) 276-2022

# AERODYNAMIC EFFECTS OF THE QUIET SPIKE™ ON AN F-15B AIRCRAFT

## Summary

The Quiet Spike™ (Gulfstream Aerospace Corporation, Savannah, Georgia) nose boom was flown on a National Aeronautics and Space Administration (NASA) F-15B (McDonnell Douglas Corporation, St. Louis, Missouri, now The Boeing Company, Chicago, Illinois) aircraft for structural integrity testing and computational fluid dynamics (CFD) validation. The Quiet Spike™ consisted of multiple sections and could be extended during flight to a length of 24 ft. Preliminary analyses indicated that the addition of the experimental nose boom could adversely affect vehicle flight characteristics and airdata systems. Flight data indicated that the presence of the experimental boom reduced the static pitch and yaw stability of the aircraft. The boom also adversely affected the static-position error of the aircraft, but did not significantly affect angle-of-attack or angle-of-sideslip measurements.

## Objective

The objective is to characterize the aerodynamic effects of the Quiet Spike™ on the F-15B aircraft.

## Approach

Preliminary analyses indicated the Quiet Spike™ test article could adversely affect both the flight characteristics and the airdata systems of the F-15B aircraft. Pitch and yaw stability derivatives were both predicted to be less stable with the addition of the Quiet Spike™. Prior to flights with the Quiet Spike™ installed, baseline flights of the F-15B aircraft were flown to characterize the flying qualities and airdata systems of the vehicle. Doublet maneuvers and standard parameter estimation techniques were utilized to estimate flying qualities. Airdata system characterization was achieved through standard calibration techniques using push-over/pull-up (POPU) maneuvers, rudder sweeps, and level accelerations.

A total of 30 research flights were flown with the Quiet Spike™ test article installed on the F-15B aircraft. Analysis of these flights indicates that the experimental boom did affect the aircraft. As predicted, static pitch and yaw stability were reduced. Figures 1 and 2 show the parameter estimation results for pitching moment coefficient due to angle of attack, $C_{m_\alpha}$, and yawing moment coefficient due to angle of sideslip, $C_{n_\beta}$, respectively, from the baseline and research flights. Figure 1 shows that static pitch stability was reduced from the baseline configuration, noticeably more than had been predicted in the subsonic region. Figure 2 shows that weathercock stability was also reduced by the presence of the experimental nose boom. While stability was reduced more significantly than expected for much of the subsonic regime, it was not reduced by as much as predicted at high supersonic flight conditions.

74
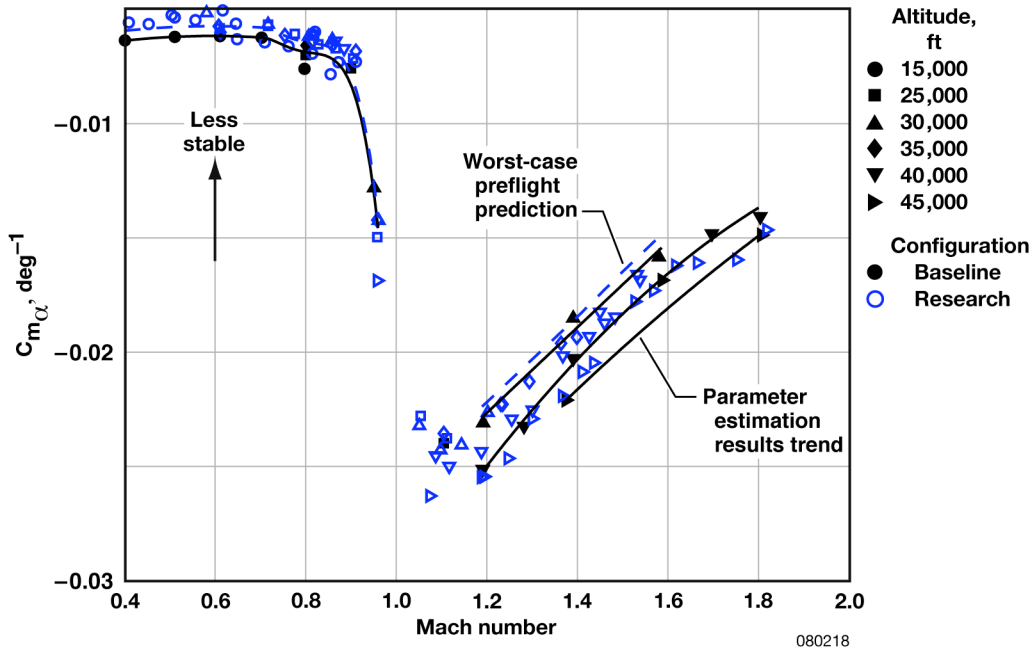
Figure 1. Estimated pitching moment due to angle of attack for baseline and research configurations.
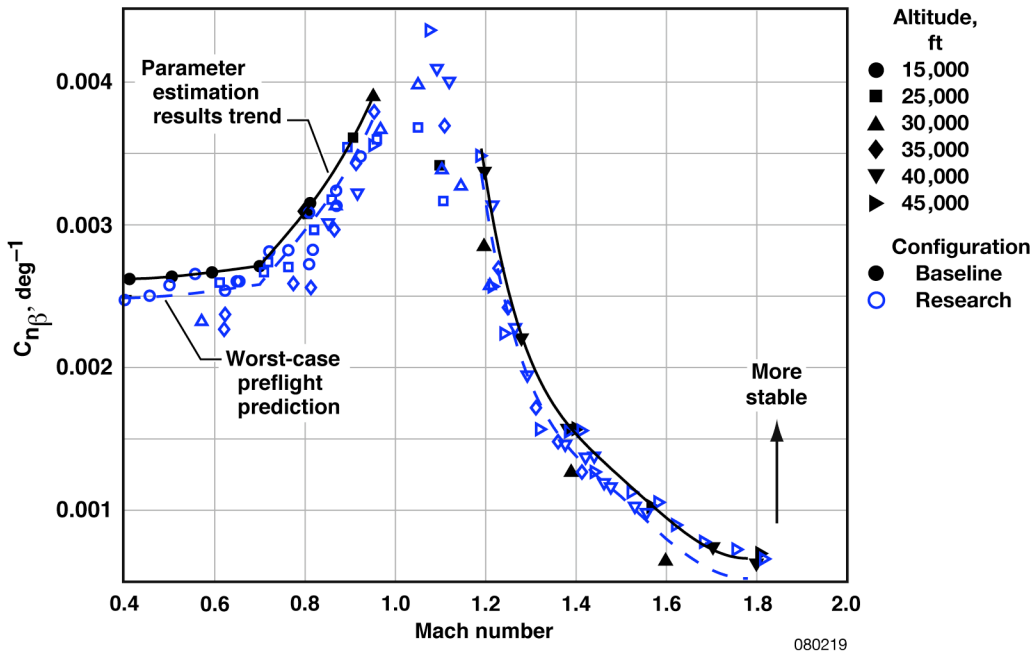


Figure 2. Estimated yawing moment due to sideslip angle for baseline and research configurations.

75

The experimental nose boom also affected the pitot-static system of the aircraft. Discernable changes to the Mach number correction curves were noted in the subsonic flight region, as well as in the supersonic region above Mach 1.4. The general trend for both subsonic and supersonic flight regimes was that the error induced by the presence of the experimental nose boom increased as Mach number increased. In the subsonic flight regime, the Mach number correction was changed by as much as 0.005 Mach, and in the supersonic flight regime, the change in correction was as high as 0.007 Mach.

While there were definite effects of the Quiet Spike™ on the F-15B aircraft, none prevented safe operation of the aircraft through a large portion of its flight envelope.

### Status

The research flights have been successfully completed, and flight test results have been published as NASA/TM-2008-214634.

### Contacts

Stephen Cumming, DFRC, Code RA, (661) 276-3732
Mark Smith, DFRC, Code RA, (661) 276-3177
Mike Frederick, DFRC, Code RA, (661) 276-2274

# F-15 INTELLIGENT FLIGHT CONTROLS–INCREASED DESTABILIZATION FAILURE

## Summary

Seven flights were flown in 2007 providing evaluation of a direct adaptive, neural-network-based flight control concept. A highly modified NF-15B (McDonnell Douglas Corporation, St. Louis, Missouri, now The Boeing Company, Chicago, Illinois) aircraft, tail number 837, was used as the demonstration vehicle. These flights increased the severity of a simulated destabilization failure. The adaptation provided increased stability margins in the presence of the simulated failure as compared to the nonadaptive system.

## Objective

The use of neural network and similar adaptive technologies in the design of highly fault and damage tolerant flight control systems shows promise in making future aircraft system failures far more survivable than current technology allows. During the flight evaluations performed in 2007, the neural network was engaged and allowed to learn in real time to dynamically alter the aircraft handling qualities characteristics in the presence of simulated failure conditions. The objective was to demonstrate that the adaptive system provides for a better-controlled system compared to the nonadaptive system when subjected to a simulated failure.

## Approach

A simplified sigma-pi neural network was implemented in a direct adaptive control architecture. When significant feedback errors are encountered, the neural network adjusts to counteract them. A destabilizing failure was simulated by changing an angle-of-attack feedback to the canard command to artificially destabilize the vehicle. Previous flight results showed modest improvement with the adaptive system engaged; however, the failure was much more benign than predicted by simulation. As a result, a new series of flight tests were conducted with the destabilizing feedback gain increased from a range of 1.0 to –0.5 dB to a new range from 0.0 to –1.75 dB.

## Results

The larger destabilizing feedback gains reduced the vehicle stability down very close to the neutral stability point (fig. 1). Stability margins without adaptation were reduced from –9.1 dB for a canard multiplier (CM) of 0.0 to –0.6 dB for a CM of –1.75.
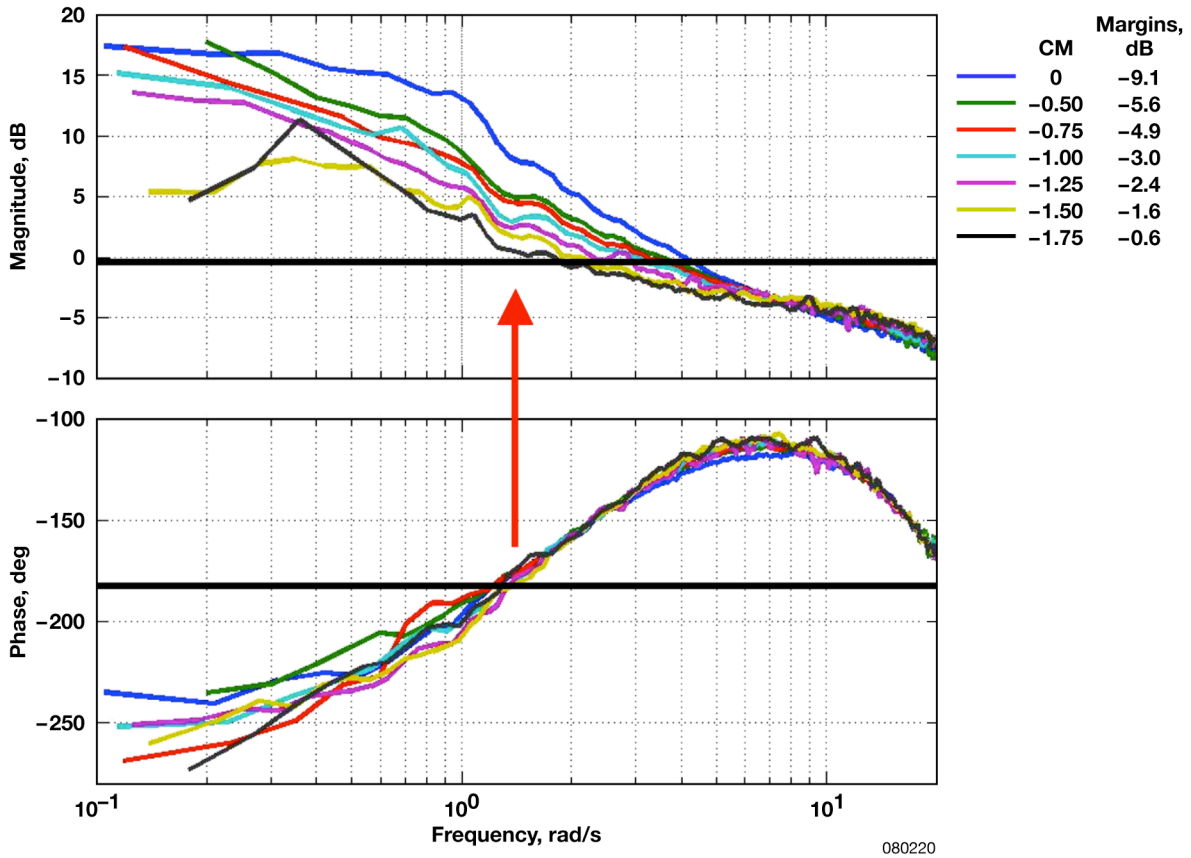
Figure 1. Flight-measured symmetric stabilator open-loop frequency response with a destabilizing feedback gain and no adaptation.

When adaptation was engaged, the system adjusted to gain back stability margin. Even with a destabilizing gain of –1.75, with adaptation, the stability margin was measured to be about –5.0 dB (fig. 2).
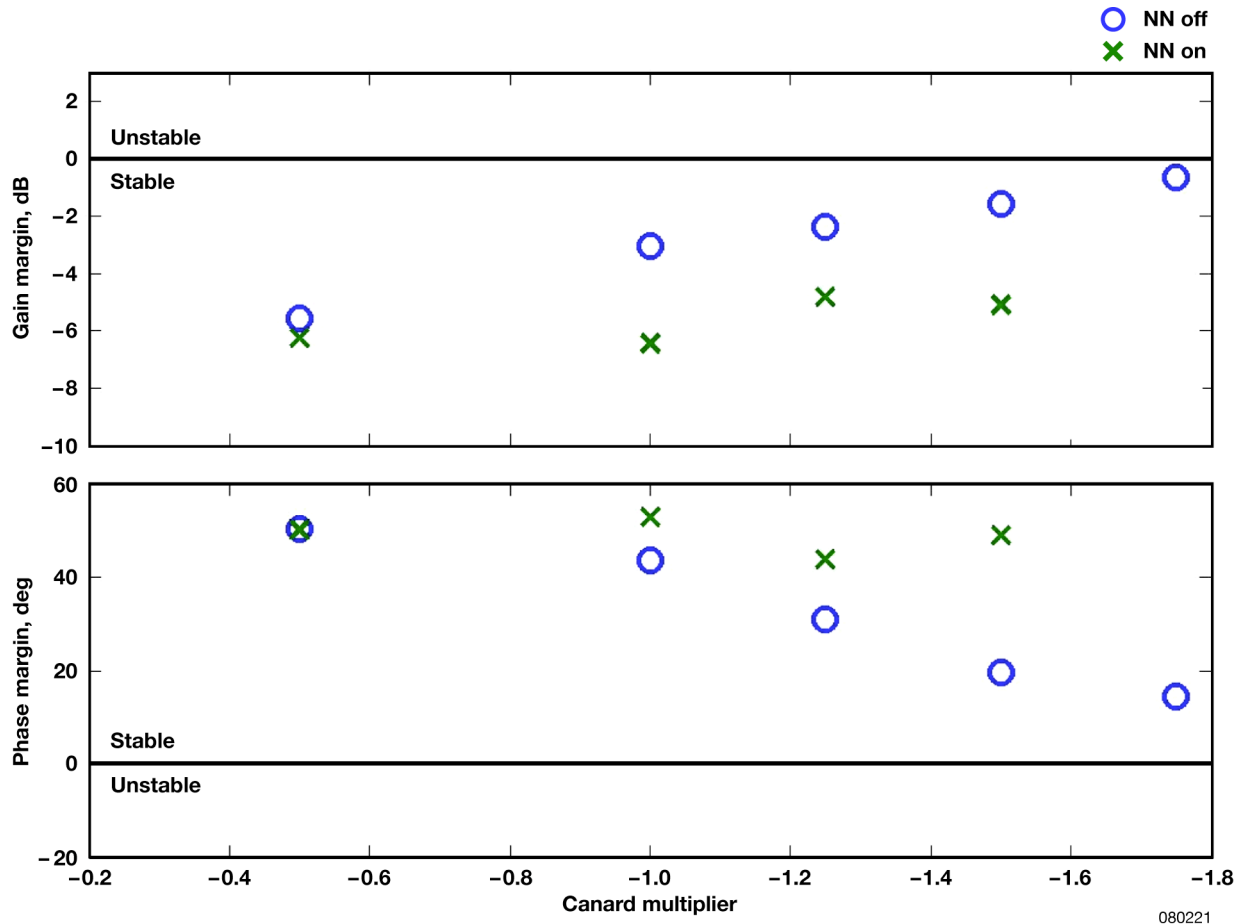
Figure 2. Symmetric stabilator loop stability margins with and without adaptation.

## Status

The F-15 Intelligent Flight Control System (IFCS) project will continue to support research in adaptive controls under the Integrated Resilient Aircraft Controls (IRAC) project under the Aeronautics Research Mission Directorate (ARMD). The work will include further refinement to the existing adaptive controller algorithm.

## Contacts

John T. Bosworth, DFRC, Code RC, (661) 276-3792
James A. Lee, DFRC, Code RC, (661) 276-3385
John J. Burken, DFRC, Code RC, (661) 276-3726
Curtis E. Hanson, DFRC, Code RC, (661) 276-3966

# F-15 INTEGRATED RESILIENT AIRCRAFT CONTROL (IRAC) IMPROVED ADAPTIVE CONTROLLER

## Summary

Past flight tests have shown that adaptation is helpful in the majority of in-flight failure situations but can become problematic with certain control surface failures. Flight tests of the Intelligent Flight Control System (IFCS) Generation 2 (Gen-2) direct adaptive model following controller began in early 2006 on the National Aeronautics and Space Administration (NASA) F-15B (McDonnell Douglas Corporation, St. Louis, Missouri, now The Boeing Company, Chicago, Illinois) aircraft, tail number 837. Overall, the neural adaptive flight controller provided improvement in performance. Control surface failures produced mixed results, which showed that for some failure cases the performance with the neural networks was worse than the nonadaptive controller. The goal of the project, however, is to develop an adaptive system that improves performance over the entire range of in-flight failure scenarios. Two improved adaptive controllers, Gen-2a and Gen-2b, have been designed and evaluated in simulation. Formal verification and validation testing of these controllers started in February 2008. The next flight phase of the NASA F-15B aircraft will evaluate the performance of the improved adaptive controllers.

## Objective

The global objective of this project is to determine whether future adaptive controllers, as compared to the current technology, will improve the survivability of damaged aircraft. The objective of this study is to develop and flight-test improved adaptive algorithms (Gen-2a and Gen-2b) over the previously flight-tested version (Gen-2). This study will help improve the flying qualities of the failed or damaged aircraft. During flight test evaluations of Gen-2, the aircraft handling qualities with emulated surface jams did not improve with adaptation and in some cases were worse than the nonadaptive controller. The poor handling qualities of the Gen-2 system are primarily due to cross-coupling between the pitch and roll axes. The main emphasis of the design of the improved adaptive algorithms was to reduce the cross-coupling induced by a simulated jammed stabilator.

## Approach

Under normal operations conditions (without failures), a roll input produces little or no longitudinal response such as Nz (normal acceleration). During a failure such as a single jammed stabilator, however, roll command inputs by the pilot will produce a pitch response. The improved adaptive controllers were designed with an emphasis on reduced cross-axis coupling. The neural networks are engaged and allowed to learn in real time to dynamically alter the aircraft response characteristics in the presence of simulated failure conditions. Air-to-air tracking and formation flight-handling qualities tasks will be flown for a back-to-back comparison of the improved adaptive controllers, as compared to the original Gen-2 controller and the controller without adaptation.

## Results

Figure 1 shows a time history of the improvement with the new adaptive systems (Gen-2a and Gen-2b) over Gen-2. The failure was a right stabilator jam at 10 s. The pilot inputs are simple roll doublets. For a healthy aircraft, very little normal acceleration exists with a roll input, as shown by the response of all three controllers before the failure occurs. Following the stabilator failure, however, all three adaptive systems exhibit some degree of coupling in the pitch axis. The two improved adaptive systems are shown to significantly reduce the amount of undesired pitch response, and they should produce better handling quality ratings than the Gen-2 system. The project intends to demonstrate these improved ratings through flight test.
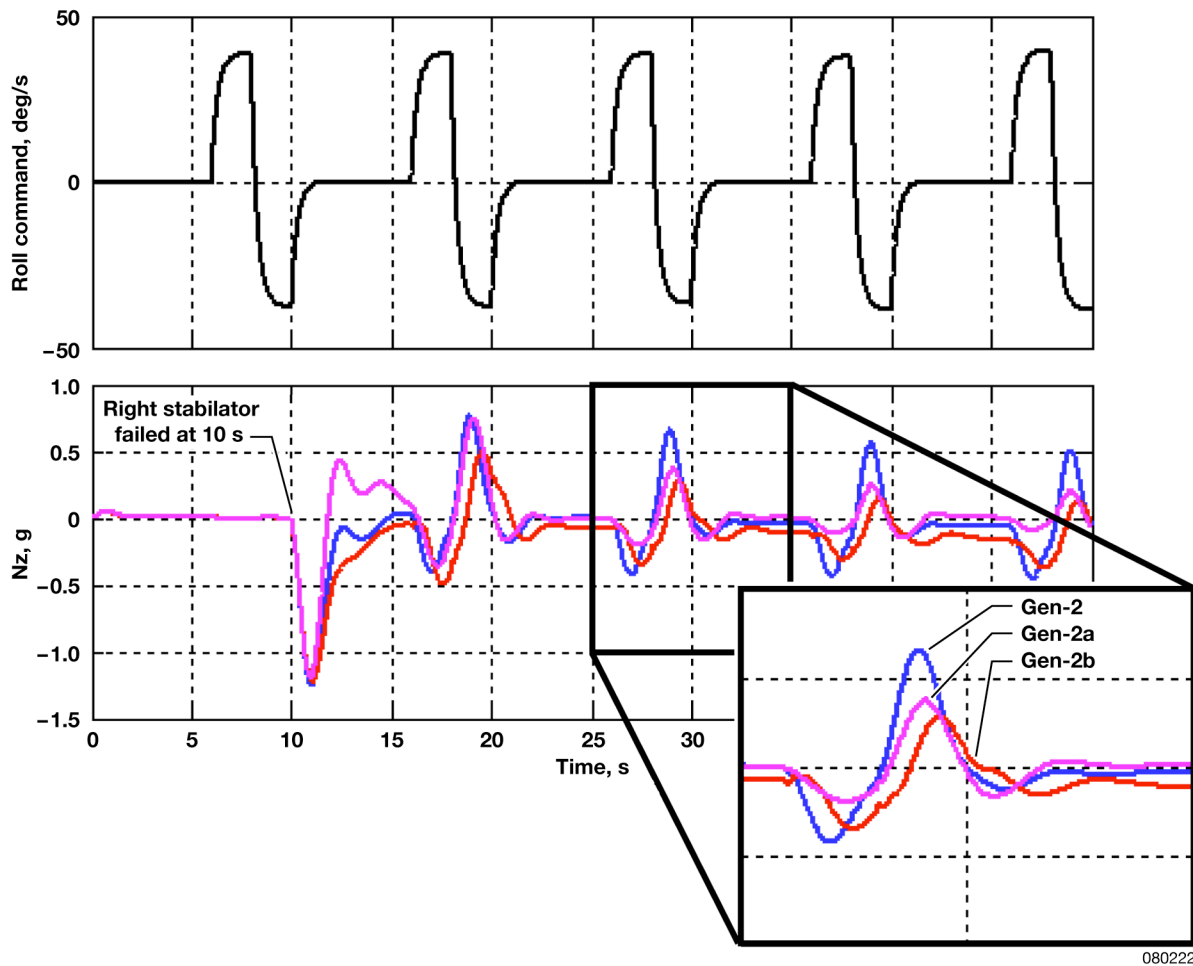
Figure 1. Pitch-axis coupling due to roll-axis commands.

**Status**

The F-15B IFCS project will continue to support research in adaptive controls under the Integrated Resilient Aircraft Controls (IRAC) project under the Aeronautics Research Mission Directorate (ARMD). Formal verification and validation of the improved adaptive algorithms is underway and flight evaluation will follow.

**Contacts**

John J. Burken, DFRC, Code RC, (661) 276-3726
Curtis E. Hanson, DFRC, Code RC, (661) 276-3966
John T. Kaneshige, Ames Research Center (ARC), Code T, (650) 604-1710
John T. Bosworth, DFRC, Code RC, (661) 276-3792
Nilesh Kulkarni, ARC, Perot Systems Corporation, Code T, (650) 604-0453

# AEROELASTIC ANALYSIS OF THE IKHANA/FIRE POD SYSTEM

## Summary

The Western States Fire Mission (WSFM) of 2007 is a partnership between the National Aeronautics and Space Administration (NASA) Dryden Flight Research Center (DFRC) (Edwards, California), NASA Ames Research Center (ARC) (Moffett Field, California), and the U.S. Forest Service (USFS) established to demonstrate high-altitude data collection by an unmanned aerial vehicle (UAV) over a wildfire. To support this effort, the WSFM fire pod was mated to a NASA DFRC UAV, the Ikhana aircraft built by General Atomics Aeronautical Systems, Inc. (GA-ASI) of San Diego, California. The Ikhana aircraft is a civilian version of a Predator® B (GA-ASI) aircraft and was already cleared for flight. The fire pod was cleared for the WSFM 2006 flights while attached to the GA-ASI Altair aircraft (fig. 1).

ED06-0208-1

Figure 1. The WSFM Altair/Fire Pod system configuration.

Because the Altair and Ikhana aircraft are not the same and the interfacing hardware was new, it was necessary to evaluate the airworthiness of this configuration. A ground vibration test (GVT) was conducted to update the WSFM 2007 structural dynamics finite element (FE) models. The FE models obtained from this update were used in the flutter analyses, which supported clearing this configuration for flight.

## Objective

The objective of this work was to determine the aeroelastic stability of the fire pod installed on the Ikhana aircraft using a custom-designed and manufactured pylon. In particular, this configuration was assessed for the mission flight envelope for the WSFM 2007 as required for mission objectives.

## Approach

As with any flutter analysis, a model validation was needed. A GVT was conducted to validate and/or update the Ikhana and fire pod structural dynamics FE models. Various configurations were tested, which included the aircraft baseline configuration for empty and full fuel, and a mated Ikhana/fire pod configuration with empty fuel (fig. 2).

Figure 2. GVT configurations.

During this test, a determination was made that installing the fire pod at the inboard station would not provide the necessary landing gear clearance, and a decision was made to relocate the pod to the mid-board station. Because the interfacing hardware would remain the same, a second GVT was unnecessary, but extra analysis was required. A model update with the fire pod at the inboard station was done using the results from this test. The fire pod and interfacing hardware were analytically translated to the mid-board station, maintaining the same stiffness to represent the physical change of location. The frequencies and mode shapes from the modal analysis of this FE model were used in the Ikhana/Fire Pod system flutter analysis.

The model update performed rendered less than adequate results, which guided the methodology for the flutter analyses. Three possible sources for aeroelastic instability were analyzed at Mach 0.42: aircraft flutter, aircraft/pod flutter, and pod flutter. Two sets of flutter analyses were performed. The first analysis used the component FE model of the fire pod updated to match the pod frequencies and mode shapes. This analysis would provide the pod flutter speed. The second analysis used the mated Ikhana/fire pod FE model updated to primarily match the coupled aircraft/pod modes. This analysis would quantify the effect of the fire pod on the aeroelastic stability of the aircraft, as well as provide flutter speeds and flutter mechanisms for the mated configuration.

Preliminary flutter analyses included all local modes present in the FE model, and this later proved to be of great significance, which was unexpected. The inclusion of these local modes affected the results of the flutter analysis–both speeds and mechanisms. Because these local modes (fig. 3) do not interact with the free stream, their effect on the flutter speed was deemed a numerical artifact, and they were omitted from the flutter analysis.
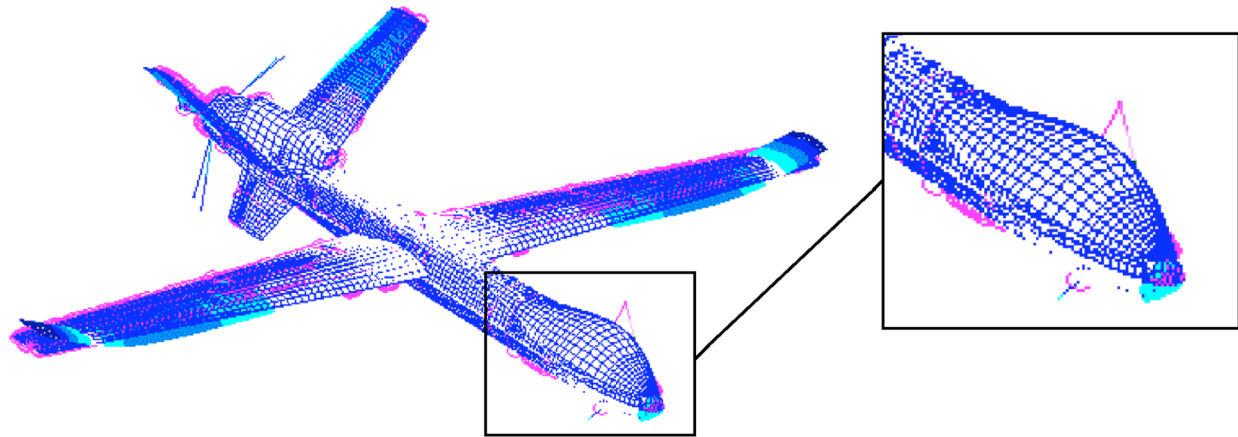
Figure 3. Nose internal local mode.

In addition, no flutter crossings were existent with the integration of the local modes; therefore, omitting these modes resulted in a conservative analysis. Any purely local modes were omitted, and any local modes with global motion reaching 25 percent or less of the maximum normalized deflection were also omitted.

The addition of the fire pod had no major effect on most of the primary modes, with only two modes having a frequency shift greater than 5 percent; therefore, the addition did not change the flutter mechanism. The aeroelastic stability margin increased with the addition of the fire pod by 28 *KEAS*, which was a change in a favorable direction.

## Status

Based on the test and analytical work done for the Ikhana/Fire Pod system, it was cleared for flight in August 2007. The Ikhana/Fire Pod aerial system provided successful support for the WSFM of 2007.

## Contact

Claudia Herrera, DFRC, Code RS, (661) 276-2642

# IKHANA: WESTERN STATES FIRE MISSIONS UTILIZING THE AMES RESEARCH CENTER FIRE SENSOR

## Summary

The National Aeronautics and Space Administration (NASA) has acquired an MQ-9 Predator® B unmanned aircraft system (UAS) built by General Atomics Aeronautical Systems, Inc. (GA-ASI) of San Diego, California, to be used as a research testbed. One of the first science payloads to be carried onboard the aircraft, named Ikhana, was the NASA Ames Research Center (ARC) (Moffett Field, California) Western States Fire Missions (WSFM) Fire Sensor and Pod system. This payload has high-resolution multispectral imaging capabilities with real-time image downloads that enabled the fire crew on the ground to see the hot spots and temperature gradients in a live fire. Several technologies were incorporated to improve the usefulness of the data, including overlaying the global positioning system (GPS) coordinates of the images onto a three-dimensional ground map generated by Google Earth™ (Google Inc., Mountain View, California). The results were so successful that the State of California asked NASA headquarters for emergency Ikhana support to assist with the San Diego fires after its missions had officially ended.

## Objective

The objective of the WSFM was to test the many enhancements made to the original fire sensor pod produced by NASA ARC researchers through flight tests and real-time use in the actual environment. The test objectives were to test the accuracy of the visual and infrared light sensor suite, the accuracy of the GPS coordinates associated with the images, the ability to overlay the real-time images onto Google Earth™ terrain maps, and the methodology of producing geo-rectified maps for flight planning. The last objective was to push the current data to an ARC server, which could then be provided simultaneously to fire teams, crews, and coordinators.

## Approach

The existing payload pod from a previous Altair (GA-ASI)/Fire Pod project was examined and determined to be reusable. A contractor performed the design and stress analysis on a newly designed pylon and the existing pod. The analysis determined that improvements were required to the pylon-to-wing attachment to achieve an adequate factor of safety for stress on the bolts. A ground vibration test and weight and balance tests were performed. A power budget was calculated by performing generator power analysis at different altitudes. Additional batteries were added to account for a generator-out hazard scenario when far from a landing site. The project designed all the wiring for the fire sensor experiment, as it required control, data, and power from the aircraft. The ARC researchers designed the telemetry solution and data server, and coordinated with the fire teams.

## Status

In this first science mission using the Ikhana as a platform, the aircraft was used extensively for surveying forest fires in the Western States from southern California to Montana. At least one researcher was on the ground providing data received at the Ikhana ground control station to the ARC server via a data link. This researcher provided the U.S. Forest Service fire crew with an interpretation of the real-time infrared images and data on the severity, location, and activity of the fires and hot spots that remained after fires had swept through an area. The real-time availability of data has saved lives in the opinion of the fire teams. The fire pod will be refitted and flown this fire season. The collaborative effort between NASA ARC researchers and NASA Dryden Flight Research Center (DFRC) (Edwards, California) engineers and flight crew made the mission effort simple and responsive, and has provided a framework for continuing collaboration on future projects.

**Contacts**
Kurt Sanner, DFRC, Code RF, (661) 276-2535
Tom Rigney, DFRC, Code PA, (661) 276-2452
Yohan Lin, DFRC, Code RF, (661) 276-3155

# IKHANA: FIBER-OPTIC WING SHAPE SENSORS

## Summary

The National Aeronautics and Space Administration (NASA) has acquired an MQ-9 Predator® B (General Atomics Aeronautical Systems, Inc., San Diego, California) unmanned aircraft system (UAS) to be used as a research testbed. This aircraft has been equipped with fiber-optic sensors that will measure the shape of the wing in flight, real time, with a rate high enough to be used for flight control. The technology can be used to prevent dangerous fluttering encountered with highly flexible wings, to enable true active aeroelastic control by changing the shape of the entire wing surface for better performance, and to make lighter, higher flying aircraft safer and more maneuverable.

## Objective

The primary objective of the fiber-optic wing shape sensor (FOWSS) system is to obtain the shape of the wing in real time with an accuracy that will enable realistic modeling of the aerodynamic forces involved with the airframe. The second objective is to obtain the wing shape data fast enough, and with a frame rate that is high enough, to be an input to a feedback control loop for an advanced flight control algorithm.

## Approach

Because the fiber-optic sensors require a control to verify their accuracy against, standard strain gages were embedded into the top of the wing alongside the fiber-optic lines. The first test of the approach occurred when an analysis was required to verify that the fiber-optic lines and sensors would not disrupt the airflow over the wing to the point that it would delaminate and cause a loss of lift. Then, a payload tray was designed for the existing pod to hold a pallet that contains the FOWSS system test equipment. The Fourier transforms on the acquired signals are performed onboard in real time. All of the equipment underwent thorough environmental testing, which showed a weakness with the design of the hard drive. A replacement was made using a solid-state hard drive that has no moving parts or stored air. The plans for the layout of the fibers were made; the wings were carefully sanded by hand; the fibers and sensors were attached; and the wings were repainted. A power budget was made and found to be adequate to support the FOWSS system. Control, data, and power cables were made and routed to the pod. Finally, the weight and balance tests were performed with the payload pod with the FOWSS system tray. For telemetry, an independent S-band antenna, transmitter, and receiver were used.

## Status

The FOWSS system has been fully installed and ground tested. During the combined systems test, the aircraft was taxied up and down the runway with the FOWSS system active. During this test, the vibration of the wings provided real-time data from the fiber-optic sensors and from the strain gages that verified proper system operation. Now, after preliminary test flights, the FOWSS system flights will begin. When the research flight control computer, the Airborne Research Test System III (ARTS III) (West Virginia High Tech Consortium Foundation, Fairmont, West Virginia), is ready, the FOWSS system will have a flight control computer to provide input for the next generation of flight control algorithms.

**Contacts**
Kurt Sanner, DFRC, Code RF, (661) 276-2535
Tom Rigney, DFRC, Code PA, (661) 276-2452
Lance Richards, DFRC, Code RS, (661) 276-3562
Allen Parker, DFRC, Code RS, (661) 276-2407
Yohan Lin, DFRC, Code RF, (661) 276-3155

# IKHANA: ARTS III

## Summary

The National Aeronautics and Space Administration (NASA) Dryden Flight Research Center (DFRC) (Edwards, California) is using the Ikhana, a modified Predator[®] B built by General Atomics Aeronautical Systems, Inc. (GA-ASI) of San Diego, California, for high altitude (above 42,000 ft), long endurance (over 28 mission hours) flights while being remotely piloted from a ground control station. An airborne research test system, ARTS III (West Virginia High Tech Consortium Foundation, Fairmont, West Virginia), has been developed for the Ikhana to test advanced flight control algorithms and integrated experiments in an aircraft capable of autonomous operation without risking the safety of pilots or crew. The ARTS III not only supports flight control algorithms, but also supports advanced sensor integration, health monitoring, intelligent mission planning, and other experiments that enhance the capabilities of command, control, or situational awareness.

## Objective

The objective of the ARTS III is to allow different autonomous flight control methods that will enable the Ikhana to be used to test flight control algorithms, including the use of active wing shape sensing for aircraft control. The flight control methods include waypoint control via automatically generated mission plans, heading and altitude control, and stick, rudder, and throttle control. To obtain an authoritative research experiment, one objective is to prove that the primary flight control computer will maintain authority and rescind control from the ARTS III in case of an anomalous event, or in case a control outside of the predefined allowed envelope is prescribed.

## Approach

The ARTS III was built and functionally qualified through ground testing by the ISR. Extensive software modifications were made to the flight control system of the Ikhana for integration of the ARTS III with the aircraft. A pilot interface was designed to provide the pilot with supervisory control over the ARTS III. The ground station was modified to have a crew member operate the ARTS III engineering work station for health and status monitoring. A software functional quality test for the ARTS III with an Ikhana flight control computer was performed by the ARTS III engineers. Next, the ARTS III will be integrated with the lab station at GA-ASI for full integration testing with the ground station, telemetry system, and aircraft system components. After corrections to any problems discovered in integration testing have been made, the ARTS III will be installed in the Ikhana to undergo thorough ground testing again in a ground combined systems test. After all ground tests have been passed, the aircraft will be flown to ensure proper behavior while pushing all limits to verify that the flight control computer of the Ikhana will disengage the ARTS III as required.

## Status

The ARTS III has been built and successfully tested with the pilot interface and the engineering work station. All software has been completed and delivered with all documents by ISR. All of the ARTS III equipment is currently at GA-ASI undergoing extensive integration testing to test all design requirements. The software modifications to the Ikhana ground station and flight control computer have been made and are being tested in the current integration tests.

## Contacts
Kurt Sanner, DFRC, Code RF, (661) 276-2535
Tom Rigney, DFRC, Code PA, (661) 276-2452
Yohan Lin, DFRC, Code RF, (661) 276-3155

# SOFIA CLOSED-DOOR FLUTTER ENVELOPE FLIGHT TESTING

## Summary

A 747SP (The Boeing Company, Chicago, Illinois) airplane that has been modified to carry a relatively large infrared telescope has completed closed telescope door, flight flutter envelope clearance without incident. A typical buildup approach of risk was used for configuration and dynamic pressure. Preflight, real-time, and postflight predictions of aeroelastic stability, using computer models and flight data, were employed to assist flight test safety.

## Objective

The primary objective of this effort was to safely clear the Stratospheric Observatory for Infrared Astronomy (SOFIA) closed-door, telescope assembly (TA) flight envelope to be free of flutter instability. A secondary objective was to identify other less critical events, such as limit cycle oscillation or buffet. The linear flutter analysis predictions, using a ground vibration test (GVT)-correlated finite element (FE) model, were to be confirmed as well as the possibility of nonlinear events not considered in the analysis. The effects of fuel loading and TA to aircraft constraints (caging and braking) on the aircraft structural dynamics response, and flutter stability, were also variables to be tested.

## Approach

In accordance with the normal practices at the National Aeronautics and Space Administration (NASA) Dryden Flight Research Center (DFRC) (Edwards, California), a buildup approach of risk was performed for flight testing. Three aircraft fuel loadings were cleared for the closed-door envelope in the order of increasing predicted risk: light with reserve tanks 2 and 3 empty, heavy with reserve tanks 2 and 3 empty, and heavy with reserve tanks 2 and 3 full. The last configuration had the only analytical flutter prediction to occur above sea level, so relatively comfortable margins exist. Also, as is typical with transport-type aircraft, the onset of predicted flutter would be gradual and not explosive. Initially, the TA was constrained firmly to the aircraft fuselage bulkhead (caged and braked), as it would be outside of telescope viewing operations, and was finally released to a floating stabilized condition that would occur while observing the far reaches of universal space and time. Figure 1 shows the flutter test points for the closed-door flight configuration displayed over the SOFIA flight envelopes (outboard wing reserve tanks 2 and 3 empty, or full fuel).
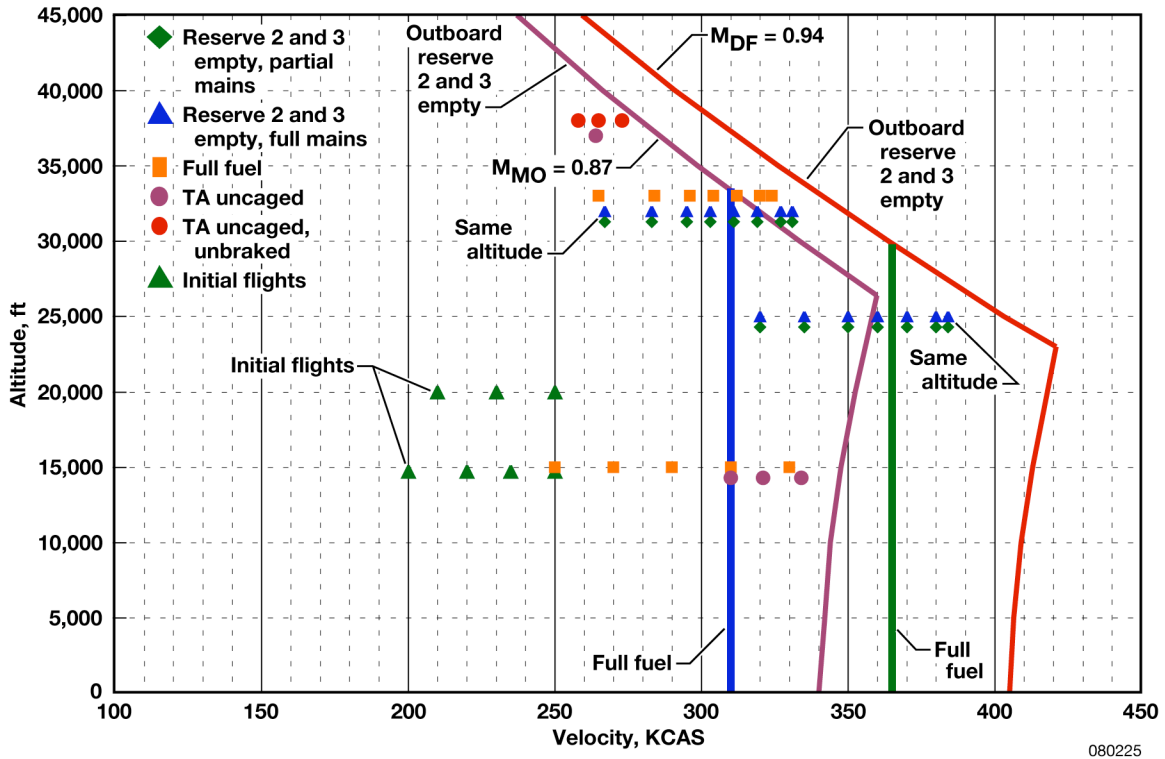
Figure 1. SOFIA closed-door flight test points.

Excitement of the aircraft structural dynamic modes used pilot yoke and rudder raps (to excite pitch, roll, and yaw) at steady level flight test points, followed by test points of increasing levels of dynamic pressure to define the boundaries of the flight envelope. The responses from accelerometers distributed throughout the aircraft were monitored at all times, even outside of the test points, since random gusts or turbulence can also excite these modes. Accelerometer traces were displayed on electronic strip charts using the interactive display system software and were visually assessed for diverging oscillations (immediate indication of impending flutter instability) or relatively large accelerations (excessive vibration). The most critical accelerometers were located on structure involved with the predicted flutter mechanism modes (wing first bending and torsion antisymmetric, aft fuselage torsion, and nacelle lateral bending) and other exterior surfaces exposed to unsteady aerodynamics, such as the new, and large, telescope upper rigid door (URD).

Power structural density plots were taken of the accelerometer responses that were sorted by algorithms to differentiate the predicted flutter mechanism modes by phase and location. Then, modal peaks were selected using the guidance of FE model predictions based on the particular fuel-loading configuration. The peaks were curve-fit to obtain modal frequency and damping, which were then input into a Zimmerman algorithm to predict (with successive test point trends) a flutter instability dynamic pressure, or an equivalent velocity-altitude, to avoid in flight. Modal structural damping coefficient trends were also plotted as another means of estimating stability by avoiding flight below a minimal value of 0.03.

All short-term excitement (raps, gusts) damped out quick enough. The Zimmerman flutter predictions were only credible when within approximately 20 percent of actual flutter; so for these tests, only the full-fuel case, or worst-case, predictions were reliable. Some events

occurred when upstream aircraft speed brakes or inboard engine wakes (at higher angles of attack) would vibrate the horizontal tail tips to a concerned, but not critical, level. The effect of uncaging and unbraking the TA had no effect on aircraft flutter stability in flight, which agreed with FE model predictions.

## Status

As a follow-on to closed-door flight flutter testing, preparation for a series of open-door flights to occur early in 2009 is currently under way. This preparation involves the addition of accelerometers to the URD, aperture, lower flexible door, TA cavity walls, and the actual TA. Estimates are being made of the open-door acoustical effects that may affect aircraft and TA structural dynamic responses as well as aircraft flutter stability.

## Contacts

Roger Truax, DFRC, Code RS, (661) 276-2230
Starr Ginn, DFRC, Code RS, (661) 276-3434

# F-15B QUIET SPIKE™ AEROSERVOELASTIC FLIGHT TEST DATA ANALYSIS

## Summary

System identification or mathematical modeling is utilized in the aerospace community for development of simulation models for robust control law design. These models are often described as linear, time-invariant processes. Nevertheless, it is well-known that the underlying process is often nonlinear. The reason for utilizing a linear approach has been due to the lack of a proper set of tools for the identification of nonlinear systems. Over the past several decades, the controls and biomedical communities have made great advances in developing tools for the identification of nonlinear systems. These approaches are robust and readily applicable to aerospace systems.

## Objective

The objectives of this study are to demonstrate via analysis of F-15B (McDonnell Douglas Corporation, St. Louis, Missouri, now The Boeing Company, Chicago, Illinois) Quiet Spike™ (Gulfstream Aerospace Corporation, Savannah, Georgia) aeroservoelastic flight test data for several flight conditions that:

- Linear models are inefficient for modeling aeroservoelastic data.
- Nonlinear identification provides a parsimonious model description whilst providing a high-percent fit for cross-validated data.
- The model structure and parameters vary as the flight condition is altered.

## Results

Equations (1) through (3) depict the model structure computed using the bootstrap method for the F-15B Quiet Spike™ data and represent flight conditions at Mach 0.85, 0.95, and 1.40, respectively.

At Mach 0.85, altitude 40,000 ft (12,192 m):

$$
\begin{aligned}
z(n) = & \hat{\theta}_1 z(n-1) + \hat{\theta}_2 z(n-2) + \hat{\theta}_3 z(n-3) + \hat{\theta}_4 z^2(n-4) + \hat{\theta}_5 \varepsilon(n-1) \\
& + \hat{\theta}_6 \varepsilon(n-2) + \hat{\theta}_7 \varepsilon(n-3) + \hat{\theta}_8 z(n-4)\varepsilon(n-4) + \hat{\theta}_9 \varepsilon^2(n-4) + \varepsilon(n)
\end{aligned}
\tag{1}
$$

At Mach 0.95, altitude 40,000 ft (12,192 m):

$$
\begin{aligned}
z(n) = & \hat{\gamma}_1 z(n-1) + \hat{\gamma}_2 z(n-2) + \hat{\gamma}_3 z(n-3) + \hat{\gamma}_4 z(n-3)z(n-4) \\
& + \hat{\gamma}_5 z^2(n-4) + \hat{\gamma}_6 \varepsilon(n-1) + \hat{\gamma}_7 \varepsilon(n-2) + \hat{\gamma}_8 \varepsilon(n-3) \\
& + \hat{\gamma}_9 z(n-3)\varepsilon(n-4) + \hat{\gamma}_{10} z(n-4)\varepsilon(n-3) + \hat{\gamma}_{11} \varepsilon(n-3)\varepsilon(n-4) \\
& + \hat{\gamma}_{12} z(n-4)\varepsilon(n-4) + \hat{\gamma}_{13} \varepsilon^2(n-4) + \varepsilon(n)
\end{aligned}
\tag{2}
$$

At Mach 1.40, altitude 40,000 ft (12,192 m):

$$
\begin{aligned}
z(n) = & \hat{\beta}_1 z(n-1) + \hat{\beta}_2 z(n-2) + \hat{\beta}_3 z(n-3) + \hat{\beta}_4 z(n-1)z(n-4) \\
& + \hat{\beta}_5 \varepsilon(n-1) + \hat{\beta}_6 \varepsilon(n-2) + \hat{\beta}_7 \varepsilon(n-3) + \hat{\beta}_8 z(n-1)\varepsilon(n-4) \\
& + \hat{\beta}_9 z(n-4)\varepsilon(n-1) + \hat{\beta}_{10} \varepsilon(n-1)\varepsilon(n-4) + \varepsilon(n)
\end{aligned}
\tag{3}
$$

The computed model structures are represented by a combination of linear and nonlinear lagged output terms and contain 9, 13, and 10 terms for Mach 0.85, 0.95, and 1.40,

respectively. Hence, the bootstrap technique successfully produced a parsimonious model description from the full set of 45 candidate terms.

For AutoRegressive (AR) (linear) model identification using minimum description length (MDL) to compute structure, the estimated models were of order $n_z$ = 42, 44, and 46 for Mach 0.85, 0.95 and 1.40, respectively. These models are not shown since they are simply a dynamic expansion of the output up to an arbitrarily large AR model of $n_z$ = 50.

Figure 1 shows the predicted output for the cross-validation data sets for the identified structures [eqs. (1)–(3)]. Each panel displays the full time history of the predicted output of the linear and nonlinear models superimposed on top of the measured output. For Mach 0.85 the predicted output of the linear and nonlinear models account for over 91 percent and 95 percent of the measured outputs variance, respectively. For Mach 0.95 the predicted output of the linear and nonlinear models account for over 92 percent and 97 percent of the measured outputs variance, respectively. For Mach 1.40 the predicted output of the linear and nonlinear models account for over 91 percent and 96 percent of the measured outputs variance, respectively.
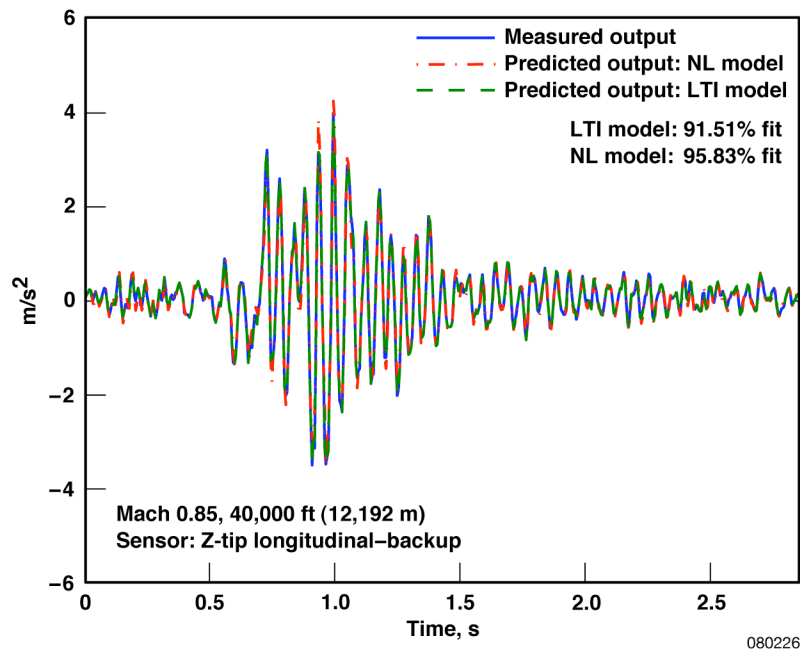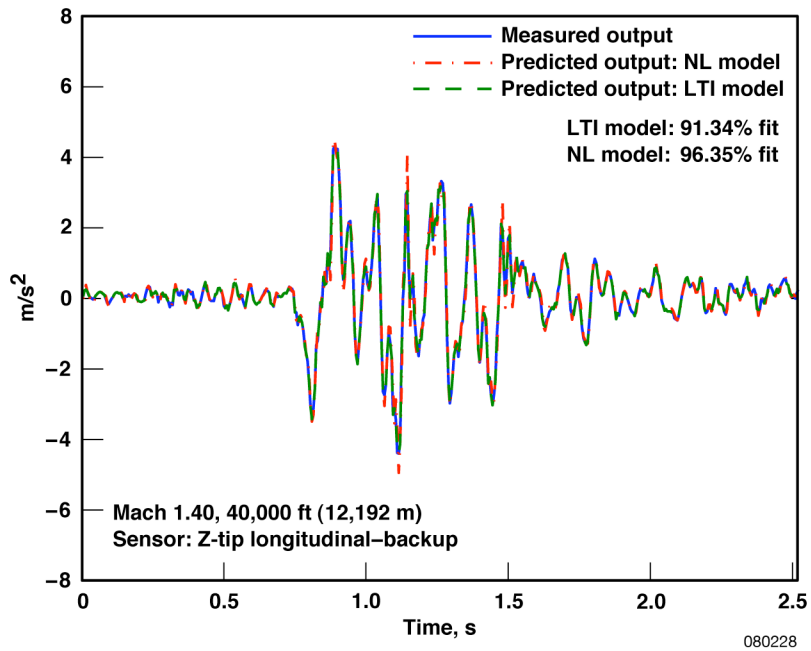


(a). Mach 0.85.

Figure 1. Cross-validation data: predicted linear and nonlinear model accelerometer response of z-tip longitudinal sensor superimposed on top of measured accelerometer output.
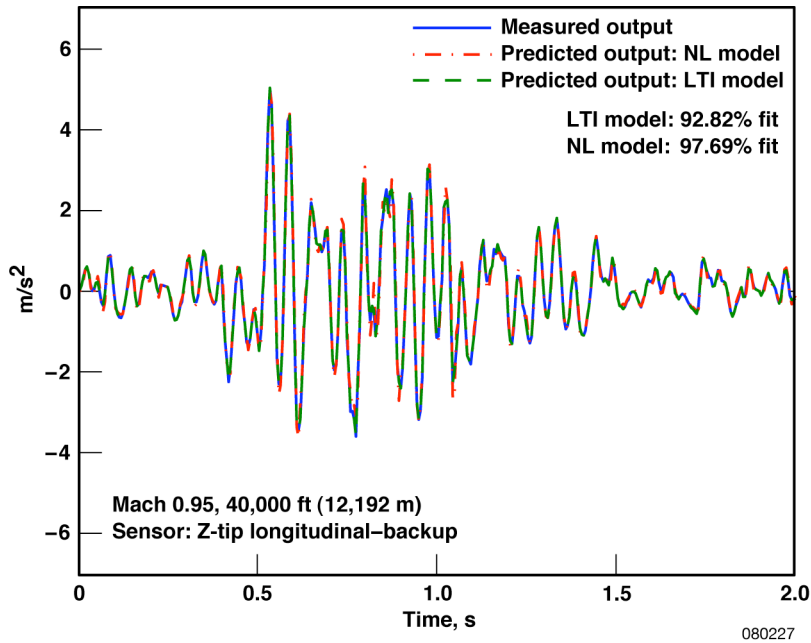
(b). Mach 0.95.



(c). Mach 1.40.

Figure 1. Concluded.

The results demonstrate that although the AR models contain many more terms to explain the underlying process, they still offer a lower percent fit compared to the nonlinear model at the cost of model complexity (higher order), which often leads to more complex control synthesis. The nonlinear models contain only a few terms and were capable of explaining a larger percent of the output variance. For these data sets the results show linear models are inefficient for

accurate modeling of aeroservoelastic data. These results show a nonlinear identification approach offers a parsimonious system description whilst providing a high-percent fit for cross-validated data.

## Status

Results show that linear models are inefficient for modeling aeroservoelastic data, and nonlinear identification provides a parsimonious model description whilst providing a high-percent fit for cross-validated data. Moreover, the results demonstrate that model structure and parameters vary as the flight condition varies. These results may have practical significance for the analysis of aircraft dynamics during envelope expansion and could lead to more efficient control strategies. In addition, this technique could allow greater insight into the functionality of various systems dynamics by providing a quantitative model that is easily interpretable.

## Contact

Dr. Sunil L. Kukreja, DFRC, Code RS, (661) 276-2788

# UAVSAR PLATFORM PRECISION AUTOPILOT FLIGHT RESULTS

## Summary

A platform precision autopilot (PPA) has been developed to enable an aircraft to repeatedly fly nearly the same trajectory hours, days, or weeks later. This capability allows accurate earth deformation measurements through precise repeat-pass interferometry, which is a key element for the success of the National Aeronautics and Space Administration (NASA) Unmanned Aerial Vehicle Synthetic Aperture Radar (UAVSAR) program. The PPA uses a novel approach to interface with a NASA Gulfstream III (G-III) jet aircraft built by Gufstream Aerospace Corporation (Savannah, Georgia), shown in figure 1, by imitating the output of an instrument landing system (ILS) approach. This technique minimizes modifications to the baseline G-III jet and retains the safety features of the autopilot of the aircraft. The PPA finished flight testing in early 2008.

ED07-0042-05

Figure 1. NASA G-III aircraft with synthetic aperture radar pod from NASA Jet Propulsion Laboratory.

## Objective

The primary PPA objective is to make repeat-pass flights within a 5-m (16.4 ft) radius tube over a 200-km (108-nmi) course in conditions of calm to light turbulence for over 90 percent of the time. To generate the best images from the synthetic aperture radar developed by the NASA Jet Propulsion Laboratory (JPL) (Pasadena, California), operating on a steady platform is important. Hence, as a secondary objective, the PPA has to minimize motion of the G-III aircraft during data collection runs.

## Approach

The PPA uses a Kalman filter to generate a real-time navigation solution with aircraft attitude and velocity measurements from the G-III systems and position measurements from a differential global positioning system (DGPS) unit located in the UAVSAR pod. The real-time position solution is used to compute commands that drive two modified ILS testers to produce modulated radio frequency (RF) signals. These RF signals are fed to the aircraft navigation receiver, which then directs the G-III autopilot to fly a simulated constant-altitude ILS approach to meet the PPA requirements for the UAVSAR. After linear and nonlinear simulations of the PPA were performed, flight testing of the system began in early 2007. Cycle 1 flights were designed to evaluate the models of the G-III aircraft and associated systems including the navigation receiver, flight director, and factory G-III autopilot. Cycle 2 flights were designed to

map out the flight envelope and determine the flight conditions in which the PPA requirements are met.

## Results

The 5-m radius tube requirement was met for the majority of flight conditions. Figure 2 shows the results from the cycle 2 evaluation flights. The circles at each flight condition represent the 5-m radius tube. Generally, there was adequate performance to keep the G-III aircraft inside (or within 1 m) of the tube boundary more than 90 percent of the time for each flight segment. In addition, the Euler rates and angles were all within the desired range during each flight segment for more than 90 percent of the time at each flight condition.
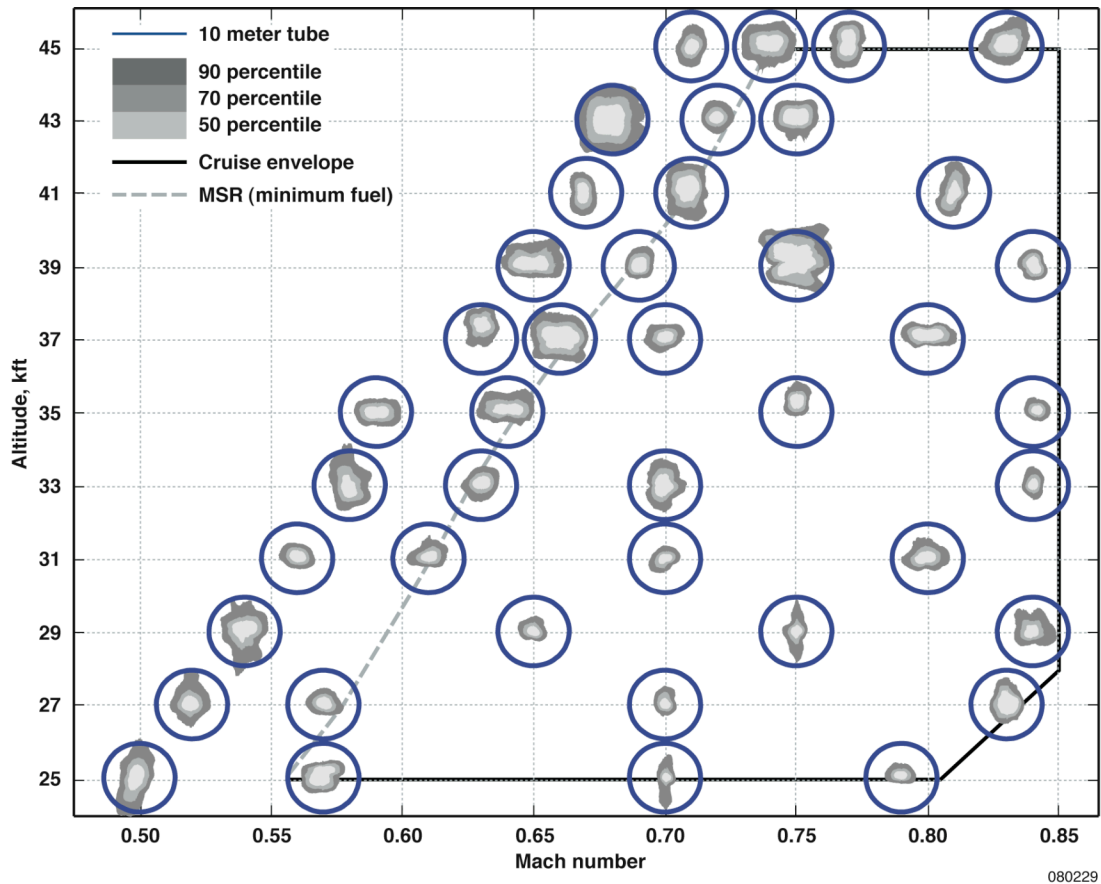


Figure 2. Flight envelope with contours encompassing 90 percent of flight time at each flight condition.

## Status

The PPA completed flight testing in January 2008. The precision autopilot demonstrated the capability to provide a stable platform that can repeatedly fly a predefined trajectory within the tolerances prescribed (5-m radius tube) over a 200-km track. The PPA is currently operating on the NASA G-III aircraft in UAVSAR flights throughout California. Future plans for the PPA involve deployment over Greenland to aid in ice sheet measurements and integration into the Stratospheric Observatory for Infrared Astronomy (SOFIA) program.

**Contacts**
James Lee, DFRC, Code RC, (661) 276-3385
Victor Lin, DFRC, Code RC, (661) 276-5451
Brian Strovers, DFRC, Code RC, (661) 276-5415

# NASA TECH BRIEFS, SPINOFFS, AND PATENTS

### *NASA Tech Briefs* Articles

"Leslie Molzahn, Operations Engineer, Dryden Flight Research Center, Edwards, CA," *NASA Tech Briefs* Vol. 31 No. 5, Who's Who at NASA, May 2007.

"Automated Aerial Refueling Hitches a Ride On AFF," *NASA Tech Briefs* Vol. 31 No. 8, Mechanics/Machinery, August 2007.

"Improved Heat-Stress Algorithm," *NASA Tech Briefs* Vol. 31 No. 8, Information Sciences, August 2007.

"The Altair/Predator B: An Earth Science Aircraft for the 21st Century," *Defense Tech Briefs*, August 2007.

*NASA Tech Briefs* Insider Blog (http://www.techbriefs.com), May 8, 2007, Current Attractions: Leslie Molzahn of NASA's Dryden Flight Research Center.

*NASA Tech Briefs* Insider Blog (http://www.techbriefs.com), August 13, 2007, Current Attractions, Subject: NASA DFRC partners with General Atomics Aeronautical Systems, Inc.

*NASA Tech Briefs* Insider Blog (http://www.techbriefs.com), August 30, 2007, NASA News, Subject: NASA Ikhana Predator B.

### NASA *Spinoff* 2007

"Hybrid Modeling Improves Health and Performance Monitoring," NASA *Spinoff* 2007, Computer Technology.

"Hypersonic Composites Resist Extreme Heat and Stress," NASA *Spinoff* 2007, Industrial Productivity and Manufacturing Technology.

### NASA DFRC Patents

"Compression of a Data Stream by Selection Among a Set of Compression Tools," Patent No. 7,180,943 issued February 20, 2007 for inventors Arild Bertelrud and Russell Franz.

"Sensor-Based Management System for Secure Inventories," Patent Application No. 11/556,054 (Attorney Docket No. DRC006006) filed September 2, 2006 by applicants Vincent Kinsey and Ralph Anton.

"Method for Real-Time Structure Shape-Sensing," Patent Application No. 11/567,118 (Attorney Docket No. DRC006024) filed December 5, 2006 by applicants William L. Ko and William Lance Richards.

"Method for Reducing the Refresh Rate of Fiber Bragg Grating Sensors," Patent Application No. 11/682,969 (Attorney Docket No. DRC006045) filed March 7, 2007 by applicant Allen R. Parker, Jr.

"Cable Tensiometer for Aircraft," Patent Application No. 11/849,843 (Attorney Docket No. DRC007041) filed September 4, 2007 by applicant Mark Nunnelee.

# REPORT DOCUMENTATION PAGE

*Form Approved*
*OMB No. 0704-0188*

The public reporting burden for this collection of information is estimated to average 1 hour per response, including the time for reviewing instructions, searching existing data sources, gathering and maintaining the data needed, and completing and reviewing the collection of information. Send comments regarding this burden estimate or any other aspect of this collection of information, including suggestions for reducing this burden, to Department of Defense, Washington Headquarters Services, Directorate for Information Operations and Reports (0704-0188), 1215 Jefferson Davis Highway, Suite 1204, Arlington, VA 22202-4302. Respondents should be aware that notwithstanding any other provision of law, no person shall be subject to any penalty for failing to comply with a collection of information if it does not display a currently valid OMB control number.
**PLEASE DO NOT RETURN YOUR FORM TO THE ABOVE ADDRESS.**

| 1. REPORT DATE *(DD-MM-YYYY)* | 2. REPORT TYPE | 3. DATES COVERED *(From - To)* |
|---|---|---|
| 01-09-2008 | Technical Memorandum | |

**4. TITLE AND SUBTITLE**
2007 Research & Engineering Annual Report

**5a. CONTRACT NUMBER**

**5b. GRANT NUMBER**

**5c. PROGRAM ELEMENT NUMBER**

**6. AUTHOR(S)**
Stoliker, Patrick; Bowers, Albion; and Cruciani, Everlyn

**5d. PROJECT NUMBER**

**5e. TASK NUMBER**

**5f. WORK UNIT NUMBER**

**7. PERFORMING ORGANIZATION NAME(S) AND ADDRESS(ES)**
NASA Dryden Flight Research Center
P.O. Box 273
Edwards, California 93523-0273

**8. PERFORMING ORGANIZATION REPORT NUMBER**
H-2849

**9. SPONSORING/MONITORING AGENCY NAME(S) AND ADDRESS(ES)**
National Aeronautics and Space Administration
Washington, DC 20546-0001

**10. SPONSORING/MONITOR'S ACRONYM(S)**
NASA

**11. SPONSORING/MONITORING REPORT NUMBER**
NASA/TM-2008-214638

**12. DISTRIBUTION/AVAILABILITY STATEMENT**
Unclassified -- Unlimited
Subject Category 99          Availability: NASA CASI (301) 621-0390          Distribution: Standard

**13. SUPPLEMENTARY NOTES**
Stoliker, Bowers, and Cruciani, NASA Dryden Flight Research Center. An electronic version can be found at http://dtrs.dfrc.nasa.gov or http://ntrs.nasa.gov/search.jsp.

**14. ABSTRACT**
Selected research and technology activities at NASA Dryden Flight Research Center are summarized. These activities exemplify the Center's varied and productive research efforts.

**15. SUBJECT TERMS**
Aerodynamics, Flight, Flight controls, Flight systems, Flight test, Instrumentation, Propulsion, Structural dynamics, Structures

| 16. SECURITY CLASSIFICATION OF: | | | 17. LIMITATION OF ABSTRACT | 18. NUMBER OF PAGES | 19b. NAME OF RESPONSIBLE PERSON |
|---|---|---|---|---|---|
| **a. REPORT** | **b. ABSTRACT** | **c. THIS PAGE** | | | STI Help Desk (email: help@sti.nasa.gov) |
| | | | | | **19b. TELEPHONE NUMBER** *(Include area code)* |
| U | U | U | UU | 107 | (301) 621-0390 |

**Standard Form 298** (Rev. 8-98)
Prescribed by ANSI Std. Z39-18